

1 **RESEARCH ARTICLE**

2 **Transcriptomic Analyses Throughout Chili Pepper Fruit Development Reveal**  
3 **Novel Insights into Domestication Process**

4 Octavio Martínez<sup>a,1</sup>, Magda L. Arce-Rodríguez<sup>b</sup>, Fernando Hernández-Godínez<sup>a</sup>, Christian  
5 Escoto-Sandoval<sup>a</sup>, Felipe Cervantes-Hernández<sup>a</sup>, Corina Hayano-Kanashiro<sup>c</sup>, José J. Ordaz-  
6 Ortiz<sup>a</sup>, M. Humberto Reyes-Valdés<sup>d</sup>, Fernando G. Razo-Mendivil<sup>c</sup>, Ana Garcés-Claver<sup>e</sup>, Neftalí  
7 Ochoa-Alejo<sup>b,2</sup>.

8

9 <sup>a</sup> Unidad de Genómica Avanzada (Langebio), Centro de Investigación y de Estudios Avanzados  
10 del Instituto Politécnico Nacional (Cinvestav), 36824, Irapuato, Guanajuato, México.

11 <sup>b</sup> Departamento de Ingeniería Genética, Centro de Investigación y de Estudios Avanzados del  
12 Instituto Politécnico Nacional, Unidad Irapuato, 36824, Irapuato, Guanajuato, México.

13 <sup>c</sup> Departamento de Investigaciones Científicas y Tecnológicas de la Universidad de Sonora,  
14 Universidad de Sonora, 83000, Hermosillo, México.

15 <sup>d</sup> Department of Plant Breeding, Universidad Autónoma Agraria Antonio Narro, Saltillo,  
16 Coahuila, México.

17 <sup>e</sup> Unidad de Hortofruticultura, Centro de Investigación y Tecnología Agroalimentaria de Aragón,  
18 Instituto Agroalimentario de Aragón - IA2 (CITA-Universidad de Zaragoza), 50059, Zaragoza,  
19 Spain.

20

21 <sup>1,2</sup> Address correspondence to [octavio.martinez@cinvestav.mx](mailto:octavio.martinez@cinvestav.mx) and [neftali.ochoa@cinvestav.mx](mailto:neftali.ochoa@cinvestav.mx).

22

23 The authors responsible for distribution of materials integral to the findings presented in this  
24 article in accordance with the policy described in the Instructions for Authors  
25 ([www.plantcell.org](http://www.plantcell.org)) are: Octavio Martínez ([octavio.martinez@cinvestav.mx](mailto:octavio.martinez@cinvestav.mx)) and Neftalí Ochoa-  
26 Alejo ([neftali.ochoa@cinvestav.mx](mailto:neftali.ochoa@cinvestav.mx)).

27

28 **Short title:** Chili fruit transcriptome and domestication

29

30 **ABSTRACT**

31

32 **Chili pepper (*Capsicum* spp.) is both an important crop and a model for domestication**  
33 **studies. Here we performed a time course experiment to estimate standardized gene**  
34 **expression profiles across fruit development for six domesticated and four wild chili pepper**  
35 **ancestors. We sampled the transcriptome every 10 days, from flower to fruit at 60 Days**  
36 **After Anthesis (DAA), and found that the mean standardized expression profile for**  
37 **domesticated and wild accessions significantly differed. The mean standardized expression**  
38 **was higher and peaked earlier for domesticated vs. wild genotypes, particularly for genes**  
39 **involved in the cell cycle that ultimately control fruit size. We postulate that these gene**  
40 **expression changes are driven by selection pressures during domestication and show a**  
41 **robust network of cell cycle genes with a time-shift in expression which explains some of**  
42 **the differences between domesticated and wild phenotypes.**

43

44 **Key words:** *Capsicum annuum* L., chili pepper, domestication, fruit development, gene  
45 expression profile, RNA-Seq, transcriptome

46

47 **INTRODUCTION**

48

49 Chili peppers of genus *Capsicum* and Solanaceae family are native to the American continent. Of  
50 the approximately 30 chili pepper species, five have been domesticated: *C. annuum* L., *C.*  
51 *frutescens* L., *C. baccatum* L., *C. chinense* Jacq. and *C. pubescens* Ruiz & Pav. (Pickersgill,  
52 1971). Among these species, *C. annuum* is the most important worldwide as a vegetable and  
53 spice crop, and production of this type of pepper has been steadily increasing both in terms of  
54 area harvested and yield (Jarret et al., 2019). In addition to its economic importance, chili  
55 peppers are a source of antioxidants such as flavonoids, phenolic acids, carotenoids and vitamins  
56 (Badia et al., 2017; Cervantes-Hernández et al., 2019), as well as a plant model to study the  
57 genetic and biochemical basis for synthesis of these compounds (Gómez-García and Ochoa-  
58 Alejo, 2013; Gómez-García and Ochoa-Alejo, 2016; Martínez-López et al., 2014).  
59 Capsaicinoids, which are synthesized only in *Capsicum* species, impart pungency to chili

60 peppers and are a focus of active research (Arce-Rodríguez and Ochoa-Alejo, 2017; Tanaka et  
61 al., 2017; Fayos et al., 2019).

62 Chili peppers were domesticated from an ancestral variety, *Capsicum annuum* L. var.  
63 *glabriusculum*, locally known as “piquín” or “chiltepín” (Hayano-Kanashiro et al., 2016) in  
64 northeastern Mexico and/or central-east Mexico (Kraft et al., 2014). The oldest chili pepper  
65 macroremains date to around the time of first cultivation or domestication in the mid-Holocene,  
66 9,000-7,000 BP (Kraft et al., 2014; McClung de Tapia, 1992). The exact time of chili pepper  
67 domestication is a subject of debate (Pickersgill, 2016), as starch microfossils of domesticated  
68 *Capsicum* dating from 6,000 BP have been found at seven sites (Perry et al., 2007), and there is  
69 evidence indicating that the fruit size of domesticated genotypes has increased considerably in  
70 the last 1,500-1,000 years BP (Pickersgill, 2016). Larger fruit size in domesticated compared  
71 with wild ancestors is part of the “domestication syndrome” (Doebley et al., 2006).

72 Domestication, which involves breeding and selection of wild ancestral forms to modify  
73 phenotypes for human use, is not only a key achievement of modern civilization (Zeder, 2015),  
74 but also provides a unique opportunity to identify the genetic basis of adaptation (Ross-Ibarra et  
75 al., 2007). Examples of studies of plant domestication include maize (Doebley et al., 1990; Tian  
76 et al., 2009; Studer et al., 2011; Hufford et al., 2012), common bean (Bellucci et al., 2014; Singh  
77 et al., 2018), tomato (Lippman and Tanksley, 2001; Müller et al., 2016; Sauvage et al., 2017;  
78 Razifard et al., 2020) and *Capsicum* (Hernández-Verdugo et al., 2001; Paran and Van Der  
79 Knaap, 2007; Carvalho et al., 2014; Taitano et al., 2019).

80 The *Capsicum* genome (~3.5 Gb) has been sequenced and annotated (Qin et al., 2014;  
81 Kim et al., 2014); currently there are 9 genomic assemblies available in the NCBI  
82 (<https://www.ncbi.nlm.nih.gov/genome/?term=Capsicum>) and further sequencing of different  
83 genotypes has been reported (Ahn et al., 2016; Hulse-Kemp et al., 2018). In particular, Qin et al.  
84 (2014) provided insights to evaluate the adaptive landscape of cultivated peppers (Albert and  
85 Chang, 2014) and reported a set of 511 genes that have a strong genomic domestication  
86 footprint.

87 To study the divergence caused by domestication in gene expression profiles during chili  
88 pepper fruit development, we examined fruit transcriptomes of six domesticated and four wild  
89 accessions by RNA-Seq every 10 days from anthesis until fruiting at 60 DAA. Our data show  
90 that there are significant differences in the mean expression profiles of domesticated and wild

91 accessions that affected a set of interrelated biological processes, particularly the cell cycle. We  
92 postulate that such differences in expression profiles could partially explain the large difference  
93 in fruit size between domesticated and wild chili pepper varieties.

94

95

96 **RESULTS**

97

98 We constructed and analyzed RNA-Seq libraries from developing fruits at seven time points (0,  
99 10, 20, 30, 40, 50 and 60 DAA) from 10 accessions (6 Domesticated (D) and 4 Wild (W)). Table  
100 1 shows the key, names and accession type.

101

102 **Table 1.** Chili pepper accessions used in this study

| <b>Domesticated (D)</b>   |                          | <b>Wild (W)</b> |                      |
|---|--------------------------|-----------------|----------------------|
| <b>Key</b>  | <b>Name</b>              | <b>Key</b>      | <b>Name</b>          |
| AS  | Ancho San Luis           | CO              | Piquín Coahuila      |
| CW  | California Wonder        | QU              | Piquín Querétaro *   |
| CM  | Criollo de Morelos 334 * | SR              | Piquín Sonora Red    |
| JE  | Jalapeño Espinalteco     | SY              | Piquín Sonora Yellow |
| ST  | Serrano Tampiqueño       |                 |                      |
| ZU  | Zunla *                  |                 |                      |
| * - Genome available for CM (Kim et al., 2014), QU and ZU (Qin et al., 2014). |                          |                 |                      |

103

104 A total of 22,427 genes, representing approximately 64% of the genes annotated in the  
105 *Capsicum* genome, were consistently expressed during fruit development. Data normalization is  
106 a crucial step in gene expression studies (Wu et al., 2019). For our analyses we used the  
107 Standardized Expression Profile (SEP), which is a 7-dimensional vector formed by the estimated  
108 means of expression at each time point (0, 10, 20, 30, 40, 50 and 60 DAA) that has a mean and  
109 standard deviation of 0 and 1, respectively (see Methods). The use of SEPs allows statistical  
110 comparisons between genes, or groups of genes, to be made independently of the relative gene

111 expression of each gene. For each gene within each accession, we estimated SEPs and analyzed  
112 differences between D and W genotypes.

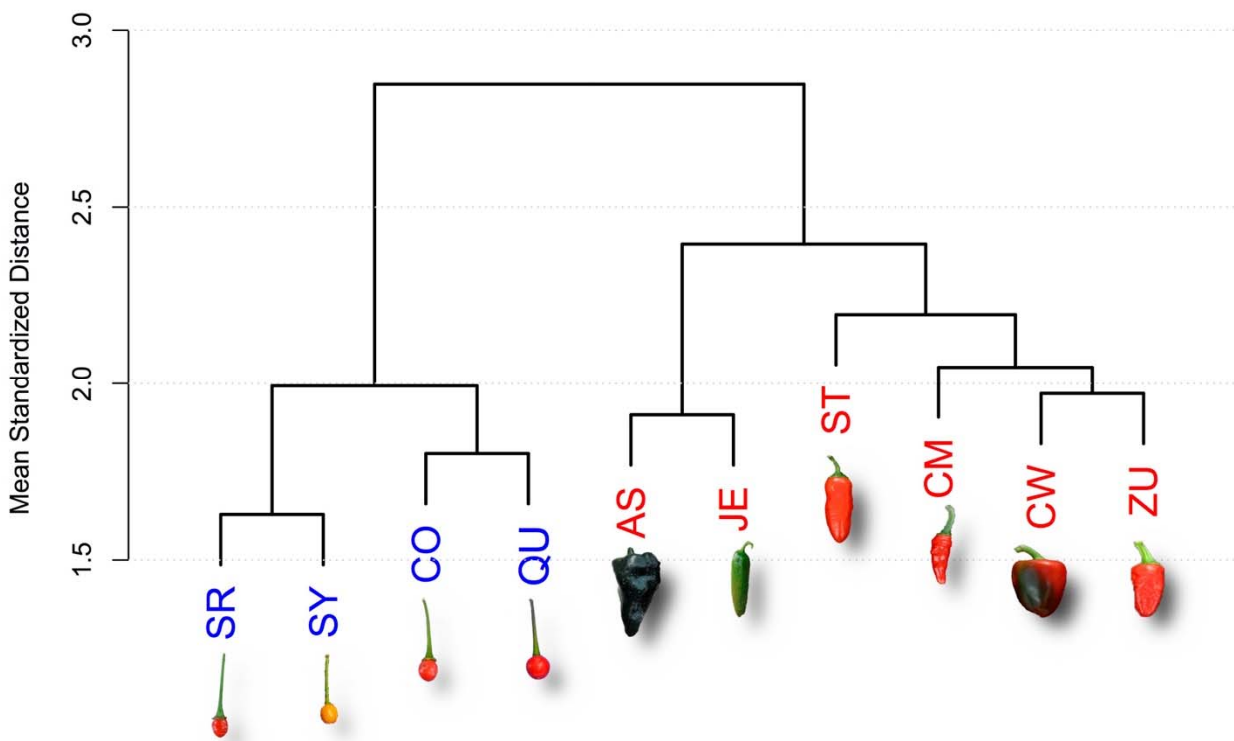
113

### 114 **Domesticated (D) and Wild (W) Accessions Have Different Mean SEPs**

115

116 To study similarities in gene expression profiles between accessions, we calculated the mean  
117 Euclidean distances between SEPs for all 22,427 genes expressed during fruit development to  
118 generate a dendrogram (Figure 1).

119 The D and W accessions form two clearly segregated groups with a mean normalized  
120 distance of 2.85 on the Y-axis (Figure 1). The four W accessions (in blue) form a cluster at a  
121 mean distance of 2, whereas the six D accessions form a cluster at a mean normalized distance of  
122 approximately 2.4 (Figure 1, and Supplemental S-3).



123

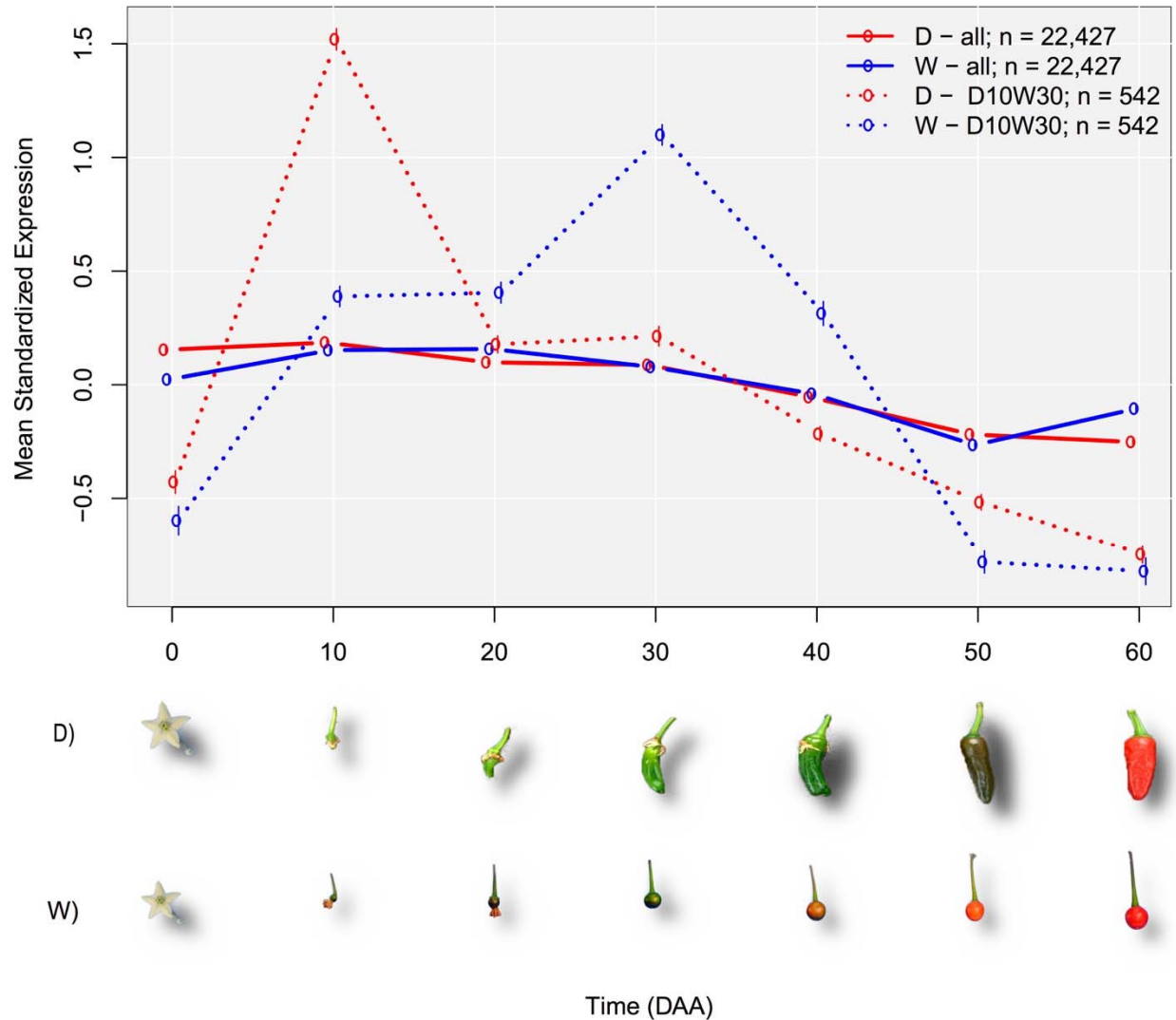
124 **Figure 1.** Dendrogram for Domesticated (D, red) and Wild (W, blue) Accessions.

125 The dendrogram was obtained from the Euclidean distances between the full set of 22,427 SEPs  
126 of genes expressed during fruit development. Representative miniature photographs illustrate the  
127 fruits of the corresponding accessions. See Table 1 for accession names. Photographs of fruits  
128 are not at the same scale.

129 To perform statistical analyses of a gene, or sets of genes, we considered contrasts  
130 between two groups of accessions, 6 D (AS, CW, JE, ST and ZU in Table 1) and 4 W (CO, QU,  
131 SR and SY in Table 1). In all cases, the null hypothesis was that at each time point the mean  
132 expression of the D and W groups was equal, whereas the alternative was that these parameters  
133 differed. Variation within the D and W groups was considered as a statistical error (unexplained  
134 variation) and a t-test was used to obtain Confidence Intervals (CI) for the means and to evaluate  
135 significance at each of the 7 time points sampled. We determined the mean SEPs for different  
136 gene groups in the D and W accessions (Figure 2).

137 The mean for the D and W groups differed significantly (continuous line in Figure 2). At  
138 the mature flower state (0 DAA), the standardized mean expression for D was much higher than  
139 for W, implying that the average transcription activity in this state is substantially larger for the  
140 D genotypes. In the interval between 0 and 10 DAA, the mean standardized expression  
141 increased for both groups, although the rate of increase was higher for D. At 10 DAA, the mean  
142 expression for D reached a peak value, but for W the increase continued, although at a slower  
143 rate, to peak at 20 DAA. From the peak at 10 DAA, the mean expression for D decreased, at  
144 different rates, and was lower at all subsequent time points. The lowest value was seen at 60  
145 DAA. In contrast, decreases in the mean expression for W began later, occurring from 20 up to  
146 50 DAA, and reached a minimum of -0.27, which is smaller than the minimum for the D group, -  
147 0.25, seen at 60 DAA. The more relevant differences in the mean expression profiles between D  
148 and W were seen during the intervals 10 to 20 and 50 to 60 DAA, when the trend was inverted  
149 such that D was decreasing while W was increasing. On the other hand, less marked differences  
150 between D and W were seen between 30 and 50 DAA when the mean standardized expression  
151 decreased nearly in parallel for both groups. The average of the time at which the maximum  
152 expression was reached in each group was five days earlier for D than W. All observed  
153 differences were significant (see Supplemental S-4).

154



155

156 **Figure 2.** Mean SEP (Standardized Expression Profile) for Groups of Genes in Domesticated (D)  
157 and Wild (W) Accessions.

158 Continuous colored lines (red and blue for domesticated (D) and Wild (W) respectively), link the  
159 means of standardized gene expression at each time point for the complete set of expressed genes  
160 (n=22,427). Dashed lines link the means of standardized gene expression at each time point for  
161 the n=542 genes that presented the maximum expression at 10 DAA in D while the maximum  
162 expression was reached at 30 DAA in W. These 542 genes form the group “D10W30” (see text).  
163 Representative miniature photographs illustrate the approximate fruit development of D and W  
164 accessions at each time point. Photographs of fruits are not at the same scale.

165



166 Differences in SEP of individual genes varied between D and W. A total of 463 genes,  
167 representing approximately 2.06% of the total, show significant differences between D and W  
168 with a False Discovery Rate (FDR) threshold of 0.05, which for the individual tests corresponds  
169 to a  $P$  value  $< 0.000002$ . The differences in expression profiles between D and W were well  
170 defined and significant; the peak of mean expression for D occurred at 10 DAA, while the peak  
171 for W occurred later, at 30 DAA. The average time of maximum expression was 11.06 DAA for  
172 D and 28.33 DAA for W, or a difference of -17.27 DAA. Of the 463 selected genes, 36 (36/463  
173  $\approx 0.08$  or 8%) are transcription factors (TFs). This percentage is higher than that for TFs  
174 annotated in the *Capsicum* genome (1,859/34,986  $\approx 0.05$  or 5%). A list and description of the  
175 463 selected genes and details of statistical analyses are presented in the Supplemental SG and S-  
176 4, respectively.

177 We established that the main differences in SEPs between D and W were due to a set of  
178 542 genes which presented the expression peak at 10 DAA in D, while the expression peak was  
179 at 30 DAA in the W accessions, naming such groups of genes as D10W30 (dashed line in Figure  
180 2).

181 The results of this experiment showed differences in expression profiles between D and  
182 W at the level of whole gene sets, groups of particular genes, and individual genes (see  
183 Supplemental S-4). Taking these findings together, we can thus conclude that there are relevant  
184 differences in expression profiles between domesticated and wild varieties of chili peppers  
185 during fruit development.

186 We also found that gene expression diversity, expressed as the coefficient of variation of  
187 gene expression, is significantly ( $P = 0.002$ ) smaller in D than W accessions, corroborating the  
188 findings presented by Liu et al. (2019) for different species of plants and animals.

189

## 190 **Differences in Expression of Genes Related to Cell Reproduction Appear Earlier and are** 191 **Larger in Domesticated than Wild Genotypes**

192

193 Based on the evidence that mean SEPs differ between the D and W accessions, we investigated  
194 differences in expression profiles in groups of genes related to particular biological processes.  
195 We first examined the mean SEPs of a group of 1,125 genes associated with cell reproduction  
196 (Supplemental S-4.1).

197 The mean expression value for 235 genes that are directly annotated in the cell cycle—but  
198 not in other cell reproduction processes—was significantly higher and occurred earlier for D  
199 compared to W, as evidenced by the peak of 0.3 standardized units at 10 DAA for D and 0.2  
200 standardized units 30 DAA for W (Supplemental S-4.1). Similarly, the mean expression for 69  
201 kinesins or kinesin-related proteins among the 1,125 genes associated with cell reproduction  
202 exhibited a differential expression peak at 10 DAA for D accessions, but for W accessions the  
203 peak was later at 30 DAA (Supplemental S-4.1) .

204 Thus, changes in expression of genes associated with cell reproduction were significantly  
205 larger and occurred earlier for D relative to W accessions, not only for the full set of genes, but  
206 also for particular bioprocesses and gene families (Supplemental S-4, S-5 and S-6).

207

### 208 **Biological Processes Enriched in Genes That Are Expressed Earlier in Domesticated** 209 **Genotypes**

210

211 The results presented before indicate that SEPs in D and W accessions undoubtedly differ  
212 (Figure 2), and genes for which expression peaks at 10 DAA for D but at 30 DAA for W  
213 (denoted here as ‘D10W30’) play an important role in cell reproduction. To validate and expand  
214 our study, we considered the D10W30 expression pattern in a Gene Ontology enrichment  
215 analysis (for details see Supplemental S-4.2, S-5 and SG).

216 A total of 86 biological processes (BPs) were significantly enriched (FDR=0.05;  
217  $P < 0.0015$ ) in the D10W30 set, with a median odds ratio of 9.5. As such, these genes were much  
218 more abundant in these BPs than would be expected by chance. Apart from the abovementioned  
219 BPs related to cell reproduction, 43 of the enriched BPs, or 50% of the total, are involved in  
220 either positive or negative regulation of various biological processes. Of these, 4 (5%) are related  
221 to cellular component organization or biogenesis, 3 are associated with cellular component  
222 assembly, and another 3 play roles in organelle organization or fission. The general bioprocess  
223 “cellular process” (GO:0009987) is also highly enriched in the D10W30 gene set, with an odds  
224 estimate of 2.25 and a highly significant  $P$ -value of  $2.76 \times 10^{-8}$ .

225 These results show that genes having the pattern D10W30 are over-represented in  
226 important BPs, which in turn implies that expression of such BPs occurs earlier and at higher  
227 levels in D compared to W genotypes.

228           Interesting examples of D10W30 genes involved in cell reproduction are a high mobility  
229 group B protein 6 (XP\_016555757.1), a MYB-related protein 3R-1 (XP\_016537977.1) and the  
230 kinetochore protein NDC80 (XP\_016539151.1); see Supplemental S-4.2 for SEP plots. The gene  
231 encoding the “high mobility group B protein 6”, is a WRKY transcription factor involved in the  
232 nucleosome/chromatin assembly that was annotated in 12 of the 86 abovementioned BPs,  
233 particularly cell reproduction BP. The gene encoding the transcription factor “MYB-related  
234 protein 3R-1” was included in 6 of the 86 enriched BPs and is mainly related to cellular,  
235 chromosome and organelle organization. The “kinetochore protein NDC80” is part of the  
236 multiprotein kinetochore complexes that couple eukaryotic chromosomes to the mitotic spindle  
237 to ensure proper chromosome segregation. NDC80 is part of the outer kinetochore and forms a  
238 heterotetramer with proteins NUF2, SPC25 and SPC24 (Santaguida and Musacchio, 2009;  
239 D’Archivio and Wickstead, 2017). Interestingly, the genes encoding NUF2 and SPC25 also  
240 exhibit the D10W30 expression pattern. NDC80 is conspicuously present in 74 of the 86  
241 enriched BPs.

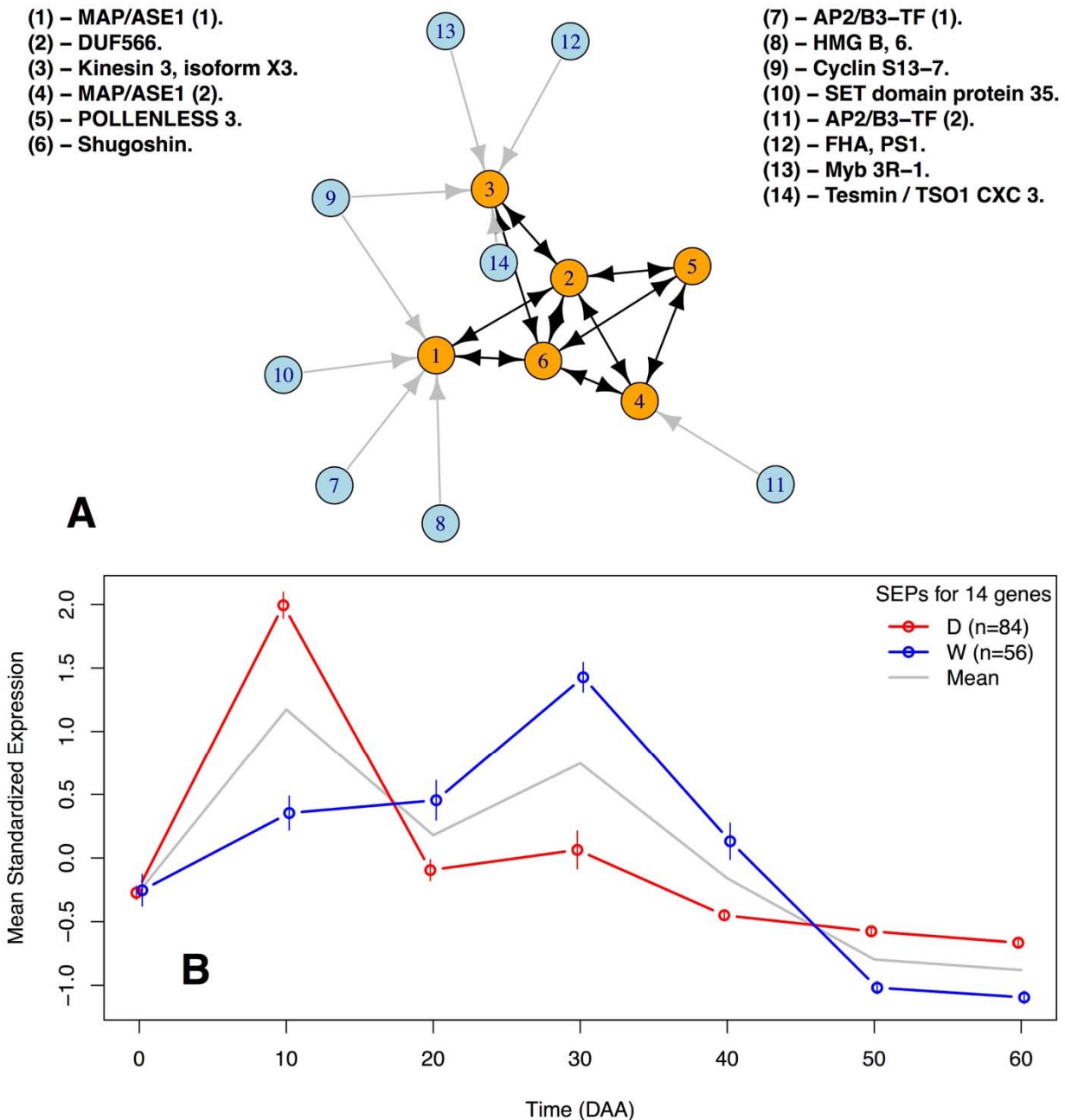
242

### 243 **A Network of Cell Cycle Genes with D10W30 Expression Pattern**

244

245 The availability of genome-wide gene expression technologies, as RNA-Seq, make it possible to  
246 identify gene interactions and represent them as gene networks (Filkov et al., 2005). In  
247 functional genomics it is axiomatic that genes with highly similar expression profiles are likely  
248 to be regulated via the same mechanisms, and this hypothesis is the basis for the discovery of  
249 regulatory networks (Allocco et al., 2004). To show the concerted co-variation through time of  
250 cell cycle genes expression during fruit development, we estimated a gene network comprising  
251 six structural genes and eight TF, candidates to be regulating three of the six structural genes.  
252 Figure 3 presents the estimated gene network, while Table 2 gives the descriptions of the genes  
253 involved.

254



255

256 **Figure 3.** Gene Network of D10W30 Cell Cycle Genes in D and W Accessions.

257 A - Graphic representation of the network. Orange circles represent structural genes while blue

258 ones represent TF candidates to be regulating the genes (see Table 2 and Supplemental S-9). B -

259 Mean standardized expression of the genes in the network in D and W accessions.

260

261

**Table 2.** Identifiers and descriptions for genes in the network of Figure 3A

| Figure 3A legend              | Protein id     | Description  | Ortholog  |
|-------------------------------|----------------|--|-----------|
| (1) - MAP/ASE1 (1).           | XP_016564755.1 | 65-kDa microtubule-associated protein 3            | AT5G51600 |
| (2) - DUF566.                 | XP_016538322.1 | ENDOSPERM DEFECTIVE 1 (DUF566)                     | AT2G44190 |
| (3) - Kinesin 3, Isoform X3.  | XP_016541615.1 | Kinesin 3 isoform X3                               | AT4G21270 |
| (4) - MAP/ASE 1 (2).          | XP_016575449.1 | 65-kDa microtubule-associated protein 3 isoform X1 | AT5G51600 |
| (5) - POLENLESS 3.            | XP_016577799.1 | Protein POLLENLESS 3                               | AT4G20900 |
| (6) - Shugoshin.              | XP_016548908.1 | Shugoshin-1; chromosome segregation                | AT3G44960 |
| (7) - AP2/B3-TF (1).          | XP_016568750.1 | AP2/B3-like TF family protein                      | AT5G42700 |
| (8) - HGM B, 6.               | XP_016555757.1 | High mobility group B protein 6                    | AT4G11080 |
| (9) - Cyclin S13-7.           | XP_016543946.1 | G2/mitotic-specific cyclin S13-7                   | AT3G11520 |
| (10) - SET domain protein 35. | XP_016547461.1 | SET domain; methyltransferase activity.            | AT1G26760 |
| (11) - AP2/B3-TF (2).         | XP_016575946.1 | AP2/B3-like TF family protein                      | AT5G58280 |
| (12) - FHA, PS1.              | XP_016574880.1 | FHA domain-containing protein PS1                  | AT1G34355 |
| (13) - Myb 3R-1.              | XP_016537977.1 | Myb-related protein 3R-1                           | AT4G32730 |
| (14) Tesmin / TSO1 CX3 3.     | XP_016565918.1 | Protein tesmin/TSO1 CXC 3                          | AT3G22780 |

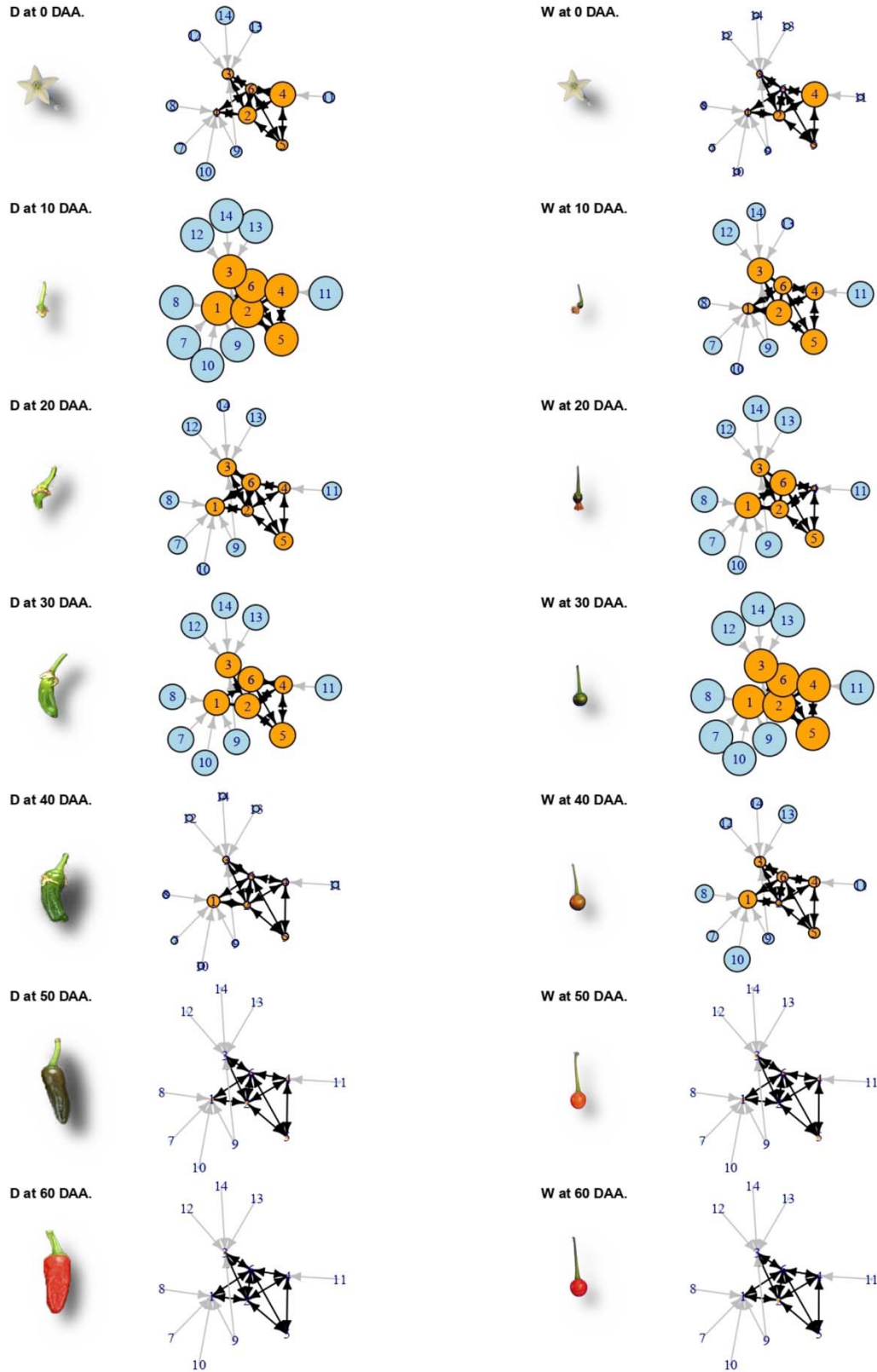
262

263 Figure 3A presents the network formed by 14 D10W30 genes, in which orange circles  
 264 represent 6 structural genes involved in cell cycle, and blue circles represent TF genes candidates  
 265 to be regulating 3 of the structural genes (see Figure 3A legend and Table 2 for gene  
 266 descriptions). Arrows between structural genes are drawn for genes with highly significant ( $P <$   
 267  $0.0001$ ) positive Pearson's correlation coefficients ( $r > 0.96$ ) between mean SEPs within the D  
 268 and W accessions, while Pearson's correlation coefficients of the same gene pairs between D and  
 269 W accessions were small ( $r < 0.4$ ) and not significant ( $P > 0.5$ ). The origin and robustness of the  
 270 network presented in Figure 3 A can be appreciated by observing Figure 3 B, that presents the  
 271 mean SEPs for the 14 genes involved, which represent  $n=84$  independent SEPs estimated from  
 272 the 6 D accessions (red line;  $84/6=14$  genes) and  $n=56$  independent SEPs estimated from the 4 W  
 273 accessions (blue line;  $56/4=14$  genes). In Figure 3 B the 95% CI for the mean standardized  
 274 expression of the genes -vertical lines at each time point, show that these 14 genes are highly  
 275 correlated within D and W accessions, but have a very low correlation between the D and W  
 276 groups. For details see Supplemental S-7 and S-8.

277 For a better appreciation of the changes that occur in the individual standardized  
 278 expression of the genes included in the network of Figure 3, Figure 4 presents a grid in time and

279 accessions groups, but in this case the sizes of the circles representing genes vary in proportion to  
280 their individual standardized expression through time (rows, from 0 to 60 DAA) and sets of  
281 accessions (columns, D in the left hand side and W in the right hand side). Representative  
282 miniature photographs show the approximate fruit development stage for D and W accessions.

283 In Figure 4 we appreciate that individual gene expression is highly coordinated through  
284 time, but largely differs between D and W groups of accessions. At 10 DAA in the D accessions  
285 (second row, left hand side), all 14 genes have reached their maximum expression (largest circle  
286 sizes), while such expression levels are only reached 20 days later, at 30 DAA for the W  
287 accessions (fourth row, right hand side). Thus the main cell cycle genes are well behind in  
288 maximum expression time in the W compared with the D accessions. Also, expression changes  
289 occur faster in D compared with W accessions, a fact that can be verified observing Figure 3 B,  
290 where the slope of the line linking the 0 and 10 DAA is more pronounced than the corresponding  
291 change to reach the maximum from 20 to 30 DAA in the W accessions. Departing from  
292 comparable standardized expression at the mature flower (0 DAA), individual expression rapidly  
293 diverges between D and W groups to finally converge again to basal expression levels at 50 and  
294 60 DAA. The concerted but highly divergent expression of cell cycle genes demonstrates that  
295 domestication has tailored this process to differ between D and W genotypes, explaining in part  
296 the large differences in fruit size between these groups.



297

298 **Figure 4.** Change in Time (Rows) and Groups of Accessions (Columns) of the Network in  
299 Figure 3A.

300 Gene expression is proportional to circle size. Photographs of fruits are not at the same scale.

301

302



## 303 **DISCUSSION**

304

305 Building on our previously described method to estimate the dynamics of the chili pepper  
306 transcriptome (Martínez-López et al., 2014), as well as our time course experiment (Spies and  
307 Ciaudo, 2015) and statistical analysis methods, in this study we generated whole gene expression  
308 profiles (SEPs) across the full course of fruit development to examine differential gene  
309 expression patterns between domesticated (D) and wild (W) varieties of chili peppers (Figure 1).

310

### 311 **Domestication Produced Modified Gene Expression Profiles in Chili Pepper Fruit**

312

313 Domestication, as studied initially by Darwin (Darwin, 1868), is currently defined as a  
314 distinctive coevolutionary and mutualistic relationship between domesticator and domesticate,  
315 and marked a key transition in human history (Zeder, 2015). Here we propose that the  
316 differences observed between gene expression profiles in sets of domesticated (D) and wild (W)  
317 accessions (Figure 2) can be attributed to domestication.

318 Gene expression is an intrinsically noisy process (Swain et al., 2002); however, our  
319 experimental design systematically took into account variations between sets of fruits by  
320 examining two replicates of each accession at each time point, as well as variation within the  
321 target groups (D and W) by examining 6 and 4 genotypes for each group, respectively. Thus, the  
322 differences observed between D and W gene expression profiles can be attributed to differences  
323 in the selection history of the two groups, i.e., to domestication. The effect of domestication on  
324 gene expression patterns is also corroborated by the fact that the D and W accessions belong to  
325 well-segregated clusters in the dendrogram presented in Figure 1. Although the distance between  
326 the D and W groups is approximately 2.85, the maximum distance within the groups is only 2.4,  
327 again demonstrating that gene expression patterns during fruit development were modified by  
328 domestication.

329 Selection during domestication can alter molecular footprints at the genomic level. For  
330 example, in *Capsicum* Qin et al. (2014) identified 115 genomic regions containing 511 genes that  
331 show strong selective sweep signals due to domestication. The same method of searching for  
332 selective sweep signals identified candidate genes not only in plants, such as maize (Tian et al.,  
333 2009), sunflower (Chapman et al., 2008), soybean (Li et al., 2013) and Asian rice (Huang et al.,

334 2012), but also in domesticated animals such as dogs (Pollinger et al., 2005) and cattle  
335 (Rothhammer et al., 2013). Ross-Ibarra et al. (2007) reviewed methods to identify the genes  
336 responsible for adaptation to domestication and classified them in terms of the phenotype-  
337 genotype hierarchy as “top-down”, in which the method starts with a phenotype to identify  
338 candidate genes, and as “bottom-up”, in which genetic analyses are used to identify adaptive  
339 genes. Bioinformatics tools are then used to connect the selected genes to a phenotype. Our  
340 approach in this study can be considered as a hybrid between “top-down” and “bottom-up”  
341 methods in that we began with a molecular phenotype, i.e., a standardized gene expression  
342 profile (SEP), which showed that there are significant differences between D and W groups of  
343 accessions, and then examined the biological relevance of these findings.

344 Differences in gene expression between crops and their wild ancestors were reported in  
345 tomato (Müller et al., 2016; Dai et al., 2017), which, like *Capsicum*, belongs to the Solanaceae  
346 family, common bean (Bellucci et al., 2014; Singh et al., 2018), carrot (Rong et al., 2014), ramie  
347 (Liu et al., 2014) and cotton (Chaudhary et al., 2008). For animals, similar comparisons were  
348 done for turkey (Monson et al., 2016), trout (Christie et al., 2016) and other species (Albert et al.,  
349 2012). All of these studies reported sets of differentially expressed genes between the  
350 domesticated and wild forms, but only for tomato did the study authors use a time course  
351 experiment to evaluate deceleration of the circadian clock (Müller et al., 2016). On the other  
352 hand, a decrease in gene expression diversity in domesticated forms of a set of animals and  
353 plants was reported by Liu et al. (2019). Analysis of our data confirmed that gene expression is  
354 significantly less diverse in domesticated chili peppers compared to that seen for wild accessions.

355

### 356 **Biological Relevance of the Differences Between Gene Expression Profiles**

357

358 Normalization of gene expression profiles of a gene, or sets of genes, discussed here as mean  
359 SEPs (see RESULTS), implies that the mean over time of the profile equals zero, and the  
360 standard deviation equals one. This transformation allows direct and unbiased comparisons of  
361 expression profiles in the D and W groups of accessions, with a statistical evaluation performed  
362 at each time point (Figure 2 and Supplemental S-2 to S-4).

363 It is important to note that the differences in mean SEPs between D and W are produced  
364 by a set of genes that were likely affected by the domestication process (Figure 2). However, the

365 large majority (21,666/22,427; 96.6%) of expressed genes did not exhibit significant differences  
366 in the mean expression profile (Supplemental S-4), implying that a large part of the  
367 transcriptome during fruit development was not affected by domestication.

368 In chili pepper, as in tomato, the first ten days after anthesis (DAA) are characterized by a  
369 period of very active cell division when the number of cell layers across the pericarp double,  
370 compared with that at anthesis, and this number is maintained through the end of development  
371 (Azzi et al., 2015). Fruit growth then proceeds into the cell expansion phase and continues until  
372 ~40 DAA, progressing to full ripening at ~50 DAA before entering senescence at ~60 DAA  
373 (Martínez-López et al., 2014). During the period of cell expansion, from ~10~40 DAA, the  
374 dominant process is cell endoreduplication (Bourdon et al., 2010; Chevalier et al., 2011; Azzi et  
375 al., 2015). In *Capsicum*, pericarp thickness has a high positive correlation with the degree of  
376 polysomaty (Ogawa et al., 2010), which implies that accessions that have a thick pericarp have  
377 higher endoreduplication compared to accessions having a thin pericarp. This relationship has  
378 been corroborated through the induction of different ploidy levels (Ogawa et al., 2012).

379 The time lag observed for the peak of mean standardized expression between D and W  
380 accessions across the entire set of expressed genes (Figure 2) implies that domestication caused a  
381 shift in time and intensity of gene expression, favoring an earlier and higher expression  
382 maximum in D. Considering 463 genes that had the largest differences in expression profiles  
383 between D and W confirmed that the peak of expression for D occurs at 10 DAA compared to 20  
384 DAA for W, and the peak expression value is significantly higher for D than for W. A similar  
385 expression pattern is seen for a gene encoding a G2/mitotic-specific cyclin, which is essential for  
386 control of the cell cycle at the G2/mitosis transition (Supplemental S-4). The transcript of this  
387 gene accumulated steadily during G2 and abruptly declined at mitosis. In *Arabidopsis*, which  
388 exhibits a similar trend in expression, members of the cyclin family are thought to be part of a  
389 developmental mechanism that coordinates the switch between proliferation and  
390 endoreduplication (Vanneste et al., 2011).

391 Here we found the peak gene expression for D at 10 DAA, a time when cell division is  
392 very active (Azzi et al., 2015). Furthermore, domesticated accessions bear substantially larger  
393 fruits than wild accessions (Paran and Van Der Knaap, 2007), and this larger fruit size is  
394 primarily achieved by increases in cell numbers (Guo and Simmons, 2011). As such, we grouped  
395 a set of 1,125 genes associated with cell reproduction by including genes annotated in 9

396 bioprocesses and examined the gene expression profiles (Supplemental S-5). Genes annotated for  
397 the cell cycle presented with an earlier increase and higher mean expression in D relative to W  
398 (Supplemental S-5). Given that both cell number and cell size, which are respectively determined  
399 by cell division and cell expansion (Gonzalez et al., 2007), contribute to fruit size, it is  
400 compelling that in the D accessions the cell division expression profile peaked earlier and higher  
401 than the W genotypes. This finding is consistent with that seen for tomato, in which cell division  
402 genes strongly influence fruit yield (Ariizumi et al., 2013).

403 The mean expression of the genes related to the cell cycle presented with a profile  
404 characterized by a large peak expression at 10 DAA for D, whereas W accessions had a smaller  
405 peak that occurred later at 30 DAA. We isolated a set of 542 genes that presented this pattern,  
406 which we termed “D10W30”. GO enrichment analyses produced a set of 86 biological processes  
407 (BPs) that were highly enriched among the D10W30 genes (Supplemental S-5 and SG). Besides  
408 4 cell reproduction BPs, this set included 43 BPs associated with regulation of different cell  
409 processes including negative regulation of cellular process, and protein modification and  
410 transferase activity. Interestingly, such negative regulation has been associated with fruit  
411 development and ripening (Giovannoni, 2004). Other selected BPs include 4 that are related to  
412 cellular component organization, which has been linked to accumulation of soluble sugars and  
413 organic acids in fruits (Ma et al., 2019) and 3 that are related to cellular component assembly and  
414 also showed differential expression in a proteomic study of *Capsicum* (Guo et al., 2017).  
415 Another 3 in this set were identified with organelle fission or organization and 2 were related to  
416 microtubule-based process or movement, which are clearly associated with mitosis and have  
417 been linked to floral development in the genus *Aquilegia* (Voelckel et al., 2010) and autophagy  
418 BP that allows remodeling of intracellular structures during cell differentiation (Mizushima and  
419 Komatsu, 2011). In *Arabidopsis* this BP has been linked with the complete proteolysis of stromal  
420 proteins (Lee et al., 2013); see Supplemental S-5, S-6 and SG for details.

421 We plotted the expression profiles of genes that follow the D10W30 pattern, i.e.,  
422 expression peaks on 10 DAA and 30 DAA for D and W accessions, respectively (Figure 2).  
423 Interesting examples this expression pattern are genes encoding: (i) the high mobility group B  
424 protein 6 (HMG B, 6), which belongs to a group of chromosomal proteins that regulate DNA-  
425 dependent processes and display a highly dynamic nuclear localization (Launholt et al., 2006);  
426 (ii) transcription factor ‘MYB-related protein 3R-1’, that in *Arabidopsis* synergistically maintain

427 G2/M-specific genes repressed in post-mitotic cells and restricts the time window of mitotic gene  
428 expression in proliferating cells that has a role in determining organ size (Kobayashi et al.,  
429 2015); and (iii) the kinetochore protein NDC80, which is an essential component of the  
430 kinetochore complex that mediates chromosome segregation and spindle checkpoint activity to  
431 ensure proper cell division. In *Arabidopsis* the NDC80 mutant *mun-1* has a reduced cell division  
432 rate, aneuploidy and defects in chromosome segregation (Shin et al., 2018). See Figure 3 and  
433 Supplemental S-4.2.

434 The D10W30 set includes genes coding for “microtubule-associated protein  
435 TORTIFOLIA1”, and the “protein TPX2”, which have genomic fingerprints for domestication in  
436 *Capsicum* (Qin et al., 2014). TORTIFOLIA1 (TOR1) is a plant-specific microtubule-associated  
437 protein (MAP) that regulates cortical microtubule orientation and the direction of organ growth  
438 (Yao et al., 2008). TOR1 also determines microtubule organization by modulating microtubule  
439 severing (Wightman et al., 2013) and participates in organ elongation (Buschmann et al., 2004).  
440 On the other hand, TPX2 performs multiple roles in microtubule organization (Petrovská et al.,  
441 2013), such as regulating prospindle assembly before nuclear envelope breakdown (Vos et al.,  
442 2008) and is linked to fruit development in European pear (Nashima et al., 2013). Of the 300  
443 domestication genes reported by Qin et al. (2014) and expressed during fruit development, 59  
444 (~20%) also showed significant ( $P < 0.05$ ) differences between D and W accessions in this  
445 study.

446 An example of the coordinated time lag existent between D and W accessions is  
447 presented in Figures 3 and 4. The 14 genes involved in this network are pivotal for the cell cycle  
448 process, and thus functionally related, but also present a highly coordinated gene expression  
449 profile within D and W accessions, which markedly differs between these two groups by having  
450 the D10W30 expression pattern (Supplemental S-7, S-8 and S-9). It is important to assess the  
451 robustness of the links inferred between the genes in this network (Figure 3). With this aim we  
452 must take into account the fact that such links were inferred from ten fully independent datasets,  
453 i.e., the ones corresponding to each one of the 10 accessions. Then, if we assume that the  
454 selection of a gene to be part of the network has an error probability “ $e$ ”, then the probability of  
455 selecting erroneously a gene to be part of the networks repeatedly in the ten accessions is  $e^{-10}$ .  
456 Thus, even if the individual error probability is large, for example  $e = 0.1$ , the probability of

457 having committed such error repeatedly in the ten accessions is vanishingly small; for  $e = 0.1$   
458 this equals  $10^{-10}$ , or one in ten billions.

459         Of the genes involved in the network of Figure 3A, two of them, (1) and (4) in the figure  
460 legend, encode two versions of the microtubule-associated protein 3. The *Arabidopsis*  
461 orthologous of these genes, *PLEIADE/AtMAP65-3*, has been shown to have physical and genetic  
462 interactions with the Transport Protein Particle II (TRAPP II), required to coordinate cytokinesis  
463 with the nuclear division cycle (Steiner et al., 2016). Gene (2) in Figure 3A, labeled as DUF566  
464 in the legend, contains the InterPro domain IPR007573 and corresponds with the *Arabidopsis*  
465 orthologous AT2G44190 (Table 2), which codes for the *endosperm-defective1 (ede1)* gene; that  
466 encodes a microtubule-associated protein essential for microtubule function during the mitotic  
467 and cytokinetic stages that generate the endosperm and embryo, and thus is essential for seed  
468 formation (Pignocchi et al., 2009). Gene (3) in Figure 3, encodes a kinesin 3 which *Arabidopsis*  
469 ortholog, AT4G21270, encodes the *ATK1* gene, that has been demonstrated to be required for  
470 spindle morphogenesis (Chen et al., 2002). Consistently, the large majority of chili pepper  
471 kinesins follow the D10W30 expression pattern (Supplemental S-4.1). Gene labeled as “(5) –  
472 *POLLENLESS 3*” in the legend of Figure 3A, contains a tetratricopeptide repeat (TPR), and its  
473 closest *Arabidopsis* ortholog, AT4G20900, encodes the *TDMI* gene, which has been previously  
474 shown to be essential for meiotic termination (Cifuentes et al., 2016). Structural gene (6) in  
475 Figure 3A encodes shugoshin, a conserved kinetochore protein that prevents dissociation of  
476 cohesin from centromeres during mitosis (McGuinness et al., 2005). The closest *Arabidopsis*  
477 ortholog locus of this chili pepper sequence, AT3G44960, encodes 5 splicing variants of  
478 shugoshin, one of which has been reported to protect centromeric cohesion during meiosis  
479 (Kitajima et al., 2004); see also Supplemental S-9. It is intriguing that three of the chili pepper  
480 genes, the ones labeled as numbers (3), (5) and (6) in the legend of Figure 3A, have as closest  
481 orthologs in *Arabidopsis* genes reported primarily in meiosis (Chen et al., 2002), (Cifuentes et  
482 al., 2016) and (Kitajima et al., 2004), respectively, while the expression patterns of these  
483 *Capsicum* genes clearly correspond to genes involved in mitosis. This fact could be due to the  
484 large functional divergence between *Capsicum* and *Arabidopsis* genomes, which diverged from a  
485 common ancestor more than 150 million years before present (Qin et al., 2014).

486         On the other hand, the 8 TF candidates to be regulating the expression of the three  
487 structural genes in the network of Figure 3A (blue circles in Figure 3A; structural genes labeled

488 as (1), (3) and (4) in the figure legend), those where assigned to the corresponding structural  
489 genes by a method that has been proved to successfully recover TF regulating the *AT3* gene in  
490 *Capsicum* (Arce-Rodríguez and Ochoa-Alejo, 2017; Zhu, et al., 2019; Sun et al., 2019); see  
491 METHODS and Supplemental S-8.

492 In summary, the functional network presented in Figures 3 and 4, demonstrates that  
493 domestication has produced a time lag in the expression of core cell cycle genes, anticipating for  
494 approximately 20 days the maximum expression of those genes and producing a higher  
495 standardized expression at the early fruit developing stage (10 DAA) in D when compared with  
496 W accessions.

497 Comparing gene expression profiles, rather than focusing on the differential expression of  
498 single genes at a given time, gives a better perspective on the complex interplay occurring in the  
499 transcriptome over time. Here, we demonstrated that a set of genes exhibits significant  
500 differences in expression profiles between D and W accessions during the development of chili  
501 pepper fruit. Genes in this set are associated with processes that involve cell regulation, cycle,  
502 localization, motility and assembly, as well as with autophagy and organelle organization. In  
503 particular, differences in time and intensity of gene expression of genes are related to cell  
504 reproduction, and provide an explanation at a molecular level of differences in fruit size between  
505 D and W accessions, which is the main morphological difference between these two genotype  
506 groups (Pickersgill, 2007).

507

508

## 509 **METHODS**

510

### 511 **Statistical Design**

512

513 RNA-Seq was performed as a factorial experiment with time (seven levels, 0, 10, 20, 30, 40, 50  
514 and 60 DAA) and accession (10 accessions, 6 domesticated and 4 wild; see Table 1) as factors.  
515 The RNA-Seq library was the experimental unit, and two replicates of every combination of time  
516 per accession were independently replicated two times, for a total of  $7 \times 10 \times 2 = 140$  RNA-Seq  
517 libraries. After quality control, the raw reads were mapped to the *Capsicum* genome (CM334  
518 v1.6) to obtain reliable counts for 22,427 genes. The relative expression of these genes is  
519 considered here as the output variable (see below).

520

### 521 **Plant Materials and Cultivation**

522

523 Seeds of 10 *Capsicum annuum* accessions (Table 1) were surface sterilized with a 70% ethanol  
524 solution for 10 s before treatment with a 10% hypochlorite solution for 10 s and six rinses with  
525 distilled water. Wild accession seeds were similarly treated, after an initial treatment with 50%  
526 sulfuric acid solution to break seed dormancy. All accession seeds were germinated in plastic  
527 trays containing a mixture of three parts peat moss, one part perlite, one part vermiculite, one  
528 part sludge and two parts forest soil in a growth chamber, with 16 h light (photon flux of  $70$   
529  $\mu\text{mol m}^{-2} \text{s}^{-1}$ ) at  $28^\circ\text{C}$  and 66% relative humidity. Three-week-old chili pepper plants were  
530 transplanted individually into plastic 5 L pots containing the same soil mixture described above.  
531 During transplantation, 15 g of a mycorrhizae fungal and beneficial bacteria mixture were added  
532 to optimize root growth and development. Plants were fertilized with Long Ashton solution  
533 every two weeks. Flowers and fruits at 0, 10, 20, 30, 40, 50 and 60 DAA were collected and  
534 immediately frozen in liquid nitrogen, and stored at  $-80^\circ\text{C}$ .

535

### 536 **RNA-Seq Library Construction and Processing**

537

538 Total RNA was extracted from flowers and whole chili pepper fruits at different developmental  
539 stages using a NucleoSpin<sup>TM</sup> RNA Plant kit (MACHEREY-NAGEL) according to the



540 manufacturer's instructions. RNA was extracted from two biological samples comprising either  
541 flowers or fruits from 2-6 different plants. RNA quality was verified by determining the RNA  
542 Integrity Number (RIN) for each sample (Supplemental S-1).

543 Samples of total RNA were shipped to Novogene (<https://en.novogene.com/>) for library  
544 construction, sequencing and mapping to a reference genome. At Novogene, libraries were  
545 prepared and sequenced using the Illumina NovaSeq platform to obtain at least 20 million raw  
546 paired-end reads of 150 bp per sample. These reads were subjected to quality control and then  
547 mapped to the *Capsicum* reference genome CM334 v1.6 (<http://peppergenome.snu.ac.kr/>).  
548 Novogene provided the matrix of raw counts per library for each of the 35,883 *Capsicum* genes.  
549 These genes were identified by a protein product (when known), and annotated with Gene  
550 Ontology (GO) and Kyoto Encyclopedia of Genes and Genomes (KEGG) terms. In total, 140  
551 libraries were processed (7 times x 10 accessions x 2 replicates of each combination of time x  
552 accession), yielding 2,298.8 million reads that mapped to the genome. The number of reads  
553 mapped to the genome had a minimum of 10.3, a median of 16.3, a mean of 16.4 and a  
554 maximum of 23.9 millions of reads per library. See Supplemental S-1 and SG.

555

### 556 **Estimation and Analyses of Standardized Expression Profiles (SEPs)**

557

558 To avoid inclusion of genes that had very low or inconsistent expression patterns, only those  
559 genes having a raw count >0 in at least two of the replicates per accession were selected for  
560 analysis. After this filtering, 22,427 genes remained for analyses, and of these ~62.5% were  
561 identified in the *Capsicum* genome. See Supplemental SG.

562 All results were maintained in an in-site MySQL (<https://www.mysql.com/>) relational  
563 database, and were analyzed with R version 3.4.4 (R Core Team, 2013). For each of the 10  
564 accessions, we used the R package edgeR version 3.20.9 (Robinson et al., 2010) to obtain *P*  
565 values for each gene in the 6 contrasts between neighbor time intervals, i.e., 0-10, 10-20, 20-30,  
566 30-40, 40-50 and 50-60 DAA. Following the method presented in Martínez-López et al. (2014),  
567 the gene expression tendency at each interval was classified as decreasing, steady or increasing,  
568 with adjustment of the Type I error to 0.01. For each gene within each accession, the mean  
569 standardized expression was calculated and the resulting 7-dimensional vector constituted the  
570 Standardized Expression Profile (SEP) in downstream analyses. There were 10 SEPs for each of

571 the 22,427 genes consistently expressed during fruit development, with one for each of the  
572 accessions, and these SEPs were classified into the groups of interest: domesticated (D) with 6  
573 elements, and wild (W) with 4 elements. To evaluate the difference between D and W SEPs, we  
574 calculated Euclidean distances between and within the groups and tested the hypothesis of  
575 equality of distances between and within SEPs with a t-test. Using a FDR (Benjamini and  
576 Hochberg, 1995) of 1% (0.01 in Q value) genes were classified as having an equal or distinct  
577 SEP in the D and W groups. For individual genes or groups of genes, we calculated the 95% CI  
578 for the means at each of the 7 time points sampled as well as the *P* value for the t-test of mean  
579 equality. A set of R functions was programmed to data-mine the results, and a binary file  
580 containing all data and functions is available upon request. Statistical procedures are described in  
581 detail in Supplemental S-2 to S-4.

582

### 583 **Network Estimation**

584

585 We begin the network estimation with the 25 genes with expression profile D10W30 annotated  
586 with the cell cycle biological process in the 10 accessions. For all the  $25 \times (25-1)/2 = 300$   
587 different pairs formed by these 25 genes, we calculated Euclidean distance between their mean  
588 SEPs, selecting the pairs with a distance less than 1 standardized units. This stringent criterion  
589 selected only 10 gene pairs (3.3% of the total, and shown as edges between orange circles in  
590 Figure 3A), which include the 6 structural genes (orange circles in Figure 3A). The SEPs of these  
591 10 gene pairs linked with black double headed arrows have a large ( $r > 0.96$ ) and highly  
592 significant ( $P < 0.0001$ ) mean Pearson's correlation within the D or W genotypes. In contrast, the  
593 corresponding mean correlation between D and W accessions was small ( $r < 0.4$ ) and not  
594 significant ( $P > 0.5$ ), demonstrating that while these genes have a highly concordant expression  
595 within the D and W groups, the expression profiles are very different between those groups  
596 (Figure 3B and Supplemental S-7). Finally, the selection of the 8 TF candidates to be regulating  
597 the expression of the structural genes in the network of Figure 3A was performed employing an  
598 algorithm which select TFs with a highly concordant expression profile between TFs and each  
599 target gene (see Supplemental S-8 for details).

600

### 601 **ACCESSION NUMBERS**

602

603 In process; All sequencing data will be delivered to the NCBI GEO data repository

604 (<https://www.ncbi.nlm.nih.gov/geo/>).

605

## 606 **SUPPLEMENTAL INFORMATION**

607

608 Supplemental (Supplemental.pdf) - Sections of this document are referred to in the text as ‘S-#’

609 where ‘#’ is the number of the corresponding section.

610

611 SG (SG.xlsx) - Supplemental Excel file with four sheets including information about genes and

612 analyses of bioprocesses (BPs).

613

## 614 **FUNDING**

615 This research was funded by the Consejo Nacional de Ciencia y Tecnología, México (Conacyt

616 project 1570).

617

## 618 **AUTHOR CONTRIBUTIONS**

619 Conceptualization, O.M and N.O-A; Methodology O.M, N.O-A and C.E-S; Formal Analysis,

620 O.M, M.H.R-V and C.E-S; Investigation, M.L.A-R, F.H-G, F.C-H, C.H-K, F.G.R-M and C.E-S;

621 Resources C.H-K, A.G-C and M.H.R-V; Data Curation O.M, C.E-S, M.L.A-R and F.C-H;

622 Writing – Original Draft O.M, N.O-A and M.L.A-R; Writing – Review & Editing, O.M, N.O-A,

623 J.J.O-O and C.E-S; Visualization O.M and C.E-S; Supervision O.M, N.O-A and M.L.A-R;

624 Project Administration N.O-A; Funding Acquisition N.O-A, O.M, C.H-K, J.J.O-O, M.H.R-V

625 and A.G-C.

626

## 627 **ACKNOWLEDGMENTS**

628 F.C-H, C.E-S and F.G.R-M acknowledge Conacyt scholarships for PhD studies (numbers

629 707294, 630487 and 261122 respectively). We thank Dr. Victor Olalde-Portugal and M. Sc.

630 Rosalinda Serrato-Flores in providing chili pepper seed germination and plant growth materials.

631 The authors would like to thank Virgilio Alegría-Germán, Antonio Contreras, Dolores Ramírez,

632 Juan B. Teran-Fraijo and María dS Fraijo-Encinas for helping us to collect the wild chili in

633 Sonora. We also acknowledge Clara Borja-Castillo, Pamela Morín-Pérez, Jesús Gámez-  
634 Fernández, Alejandra Gómez-Elizarráz, José M. Villasuso-Aguiñaga, Elías López-Olvera, Sofía  
635 Martínez-Martínez, Isaac Aguirre-Manríquez, Jesús Caudillo-Corona, Frida Figueroa-Gómez  
636 and Valeria Gallardo-Onesto for help in sampling collection and processing. No conflict of  
637 interest declared.

638

639

## SUPPLEMENTAL

### “Transcriptomic Analyses Throughout Chili Pepper Fruit Development Reveal Novel Insights into Domestication Process”

OCTAVIO MARTÍNEZ, M. HUMBERTO REYES-VALDÉS, CHRISTIAN ESCOTO-SANDOVAL AND NEFTALÍ OCHOA-ALEJO.

**NOTE:** Sections of this document are cited in the main text of the paper as “S-#”, where ‘#’ corresponds to the section in the table of Contents (below). In an effort to follow the standards of reproducible research (Peng, 2011), all relevant information is stored into a MySQL relational database named ‘SALSA’, and data as well as functions used in the analyses are in an R (R Core Team, 2013) binary object. These files are available upon request.

#### Contents

|   |    |
|---|----|
| S-1. Library sequencing and mapping to reference genome.  | 1  |
| S-2. Standardized Expression Profile (SEP) estimation   | 4  |
| S-3. Testing differences between Domesticated (D) and Wild (W) SEPs   | 9  |
| S-4. Analyses per time of SEPs in D and W accessions  | 10 |
| S-4.1. Differences in Expression of Genes Related to Cell Reproduction Appear Earlier and are Larger in Domesticated than Wild Genotypes  | 16 |
| S-4.2. Biological Processes Enriched in Genes That Are Expressed Earlier in Domesticated Genotypes  | 18 |
| S-5. Gene Ontology (GO) enrichment analyses   | 20 |
| S-6. Genes and Bio Processes (BPs) reported.  | 20 |
| S-7. Network estimation   | 22 |
| S-8. Transcription Factor (TF) imputation   | 23 |
| S-9. Supplementary descriptions and web links for genes in the network  | 25 |
| References  | 28 |
| S-10. Appendix (R output)   | 30 |
| S-11. Analyses of gene with id=580 (FBN); see Figure 8 which presents the plot obtained with the function.                                | 30 |
| S-11.1. Analyses of gene with id= 19147 (B3 domain-containing protein); see Figure 10 which presents the plot obtained with the function. | 31 |
| S-11.2. Analyses of GO biological process “Cell Cycle” having as target the D10W30 set of genes.  | 32 |

#### S-1. LIBRARY SEQUENCING AND MAPPING TO REFERENCE GENOME.

As mentioned in the main text, after extraction we shipped the 170 total RNA samples to [Novogene](#) for quality control, sequencing and mapping to reference genome [CM334 v1.6](#). The 170 samples correspond to 10 accessions (Table 1 in main text) × 7 stages of fruit development (0, 10, 20, 30, 40, 50 and 60 DAA) × 2 independent biological replicates. Here we briefly describe and exemplify the procedures carried out in Novogene.

RNA sequencing was carried out in the Illumina NovaSeq platform, based on mechanism of SBS (sequencing by synthesis), and the sequencing workflow of the project is illustrated in Figure 1a, while Figure 1b shows the pipeline of the analyses and Figure 1c presents the quality control pipeline for the filtering of raw reads.

Original image data file from the Illumina sequencing platform were transformed into sequenced reads (raw reads) by CASAVA base recognition (Base Calling). Raw data are stored in FASTQ (fq) format files, which contain sequences of reads and corresponding base quality. In Figure 1c we see the post-processing of raw reads which consisted in (1) Remove reads with adaptor contamination, (2) Remove reads when uncertain nucleotides constitute more than 10 percent of either read ( $N > 10\%$ ), (3) Remove reads when low quality nucleotides (Base Quality less than 20) constitute more than 50 percent of the read.

Figure 2 presents examples of the results obtained from the library for sample ‘AS00R1’ (Replicate 1 of the time 0 DAA from accession AS); for brevity not all results are shown for this library and there are results for a total of 170 libraries, all of which were visually inspected before further processing. Figure 2a presents the plot of percentage of error rate ( $Y$ -axis) by position along the reads ( $X$ -axis), and in general, a single base error rate should be lower than 1%. Figure 2c shows the reads distribution to the reference genome as percentage of total raw reads, in categories (1) Adaptor related: (reads containing adaptor) / (total raw reads), (2) Containing N: (reads with more than 10% N) / (total raw reads), (3) Low quality: (reads of low quality) / (total raw reads) and (4) Clean reads: (clean reads) / (total raw reads). For all 170 libraries the large majority of reads were in class (4), i.e., clean reads. Figures 2c and 2d refer to mapping the reads in the reference genome and will be commented below.

The algorithm for mapping filtered sequenced reads to the reference genome is shown in Figure 3.

In Figure 3 shows how the program HISAT2 was run with default parameters to map the clean reads to the genome. As examples of the result of the process Figure 2c shows the reads distribution to the reference genome by categories while Figure 2d shows the reads densities in chromosomes, in both cases for a single library, ‘AS00R1’ (Replicate 1 of the time 0 DAA from accession AS).

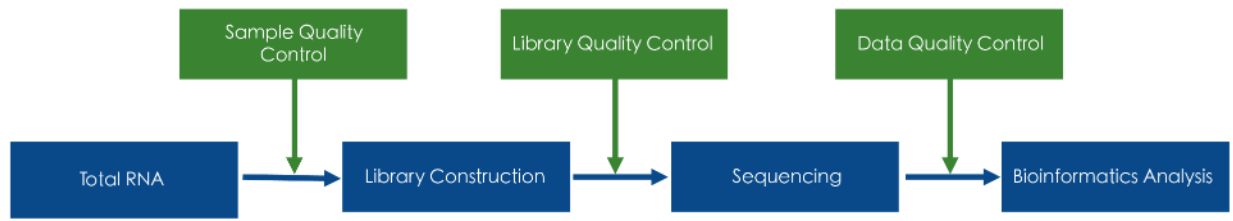
A total of 2298.8 millions of clean reads from the 170 RNA-Seq libraries were mapped to the genome, and the number of clean reads mapped to the genome per library ranges from a minimum of 10.3 millions up to a maximum of 23.9 millions with a mean of 16.4 millions.

To evaluate the accuracy of the results as well as the efficiency of the experimental procedures we can use the matrix of correlation coefficients between gene expression in samples. Figure 4 shows a partial view of that matrix for only 56 of the 170 libraries.

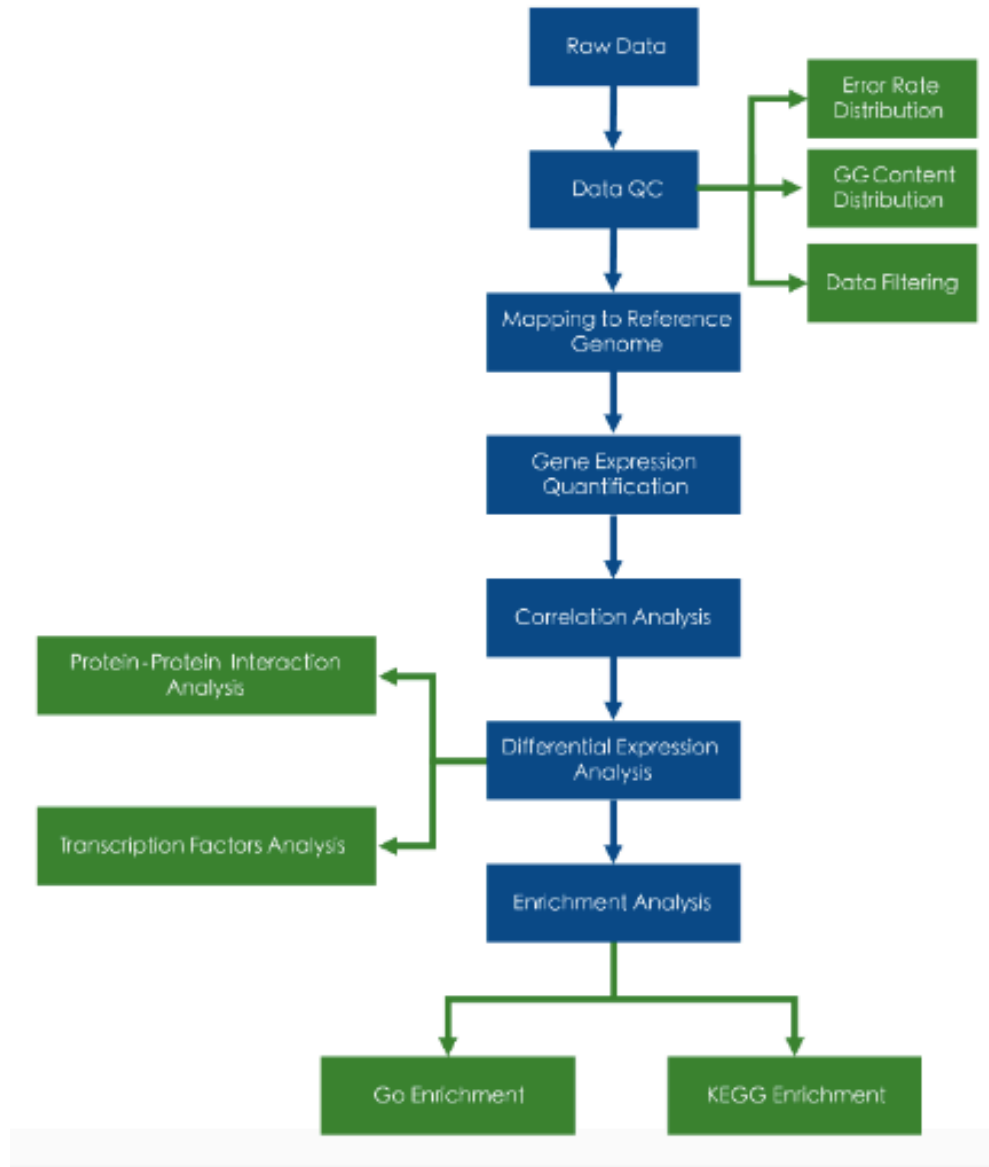
Correlation of the gene expression levels between samples plays an important role to verify reliability and sample selection, which can not only demonstrate the repeatability of the experiment but estimate the differential gene expression analysis as well. The closer the correlation coefficient is to 1, the higher similarity the samples are. Encode suggests that the square of the Pearson correlation coefficient,  $r$ , should be larger than 0.92 (under ideal experiment conditions). Correlation coefficients between samples indicates that the expression pattern is closer. In Figure 4 higher correlation coefficients,  $r$ , are represented by darker color, and replicates of libraries are set adjacent in both axis, while samples are ordered by accession at each axis. The higher correlation ( $r = 1$ ; darkest color) is obviously present between each library with itself, which is shown in the main diagonal of the matrix. In Figure 4 samples are ordered at each axis by genotype (accession) and time (neighboring times are closer), and we can see a pattern of  $4 \times 4$  ‘squares’ corresponding to each one of the 4 accessions, the squares in the main diagonal correspond to correlations between each accession. In general data were highly consistent; in all cases correlations between replicates of the same accession and time were high and there was gradient from higher to lower correlations depending on time.

Novogene results also included all known Gene Ontology [GO](#) and Kyoto Encyclopedia of Genes and Genomes [KEGG](#) annotations of the *Capsicum* genome.

All results from Novogene were downloaded and kept in an in-site [MySQL](#) relational data base called ‘SALSA’.



(A) RNA sequencing workflow



(B) Analysis Pipeline



(c) Raw reads filtering

FIGURE 1. General procedure

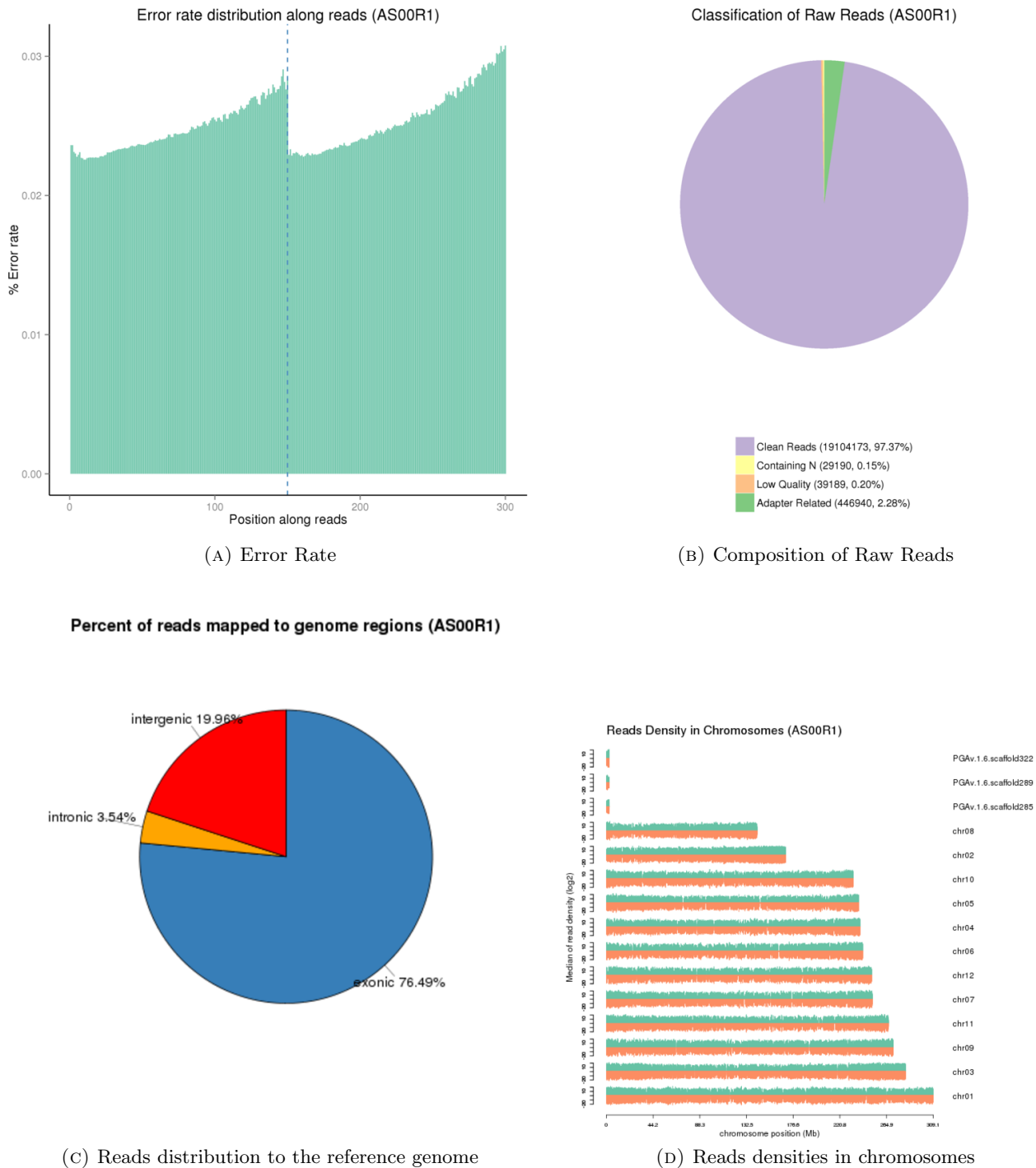


FIGURE 2. Examples for the library obtained from sample 'AS00R1' (Replicate 1 of the time 0 DAA from accession AS).

### S-2. STANDARDIZED EXPRESSION PROFILE (SEP) ESTIMATION

The majority of RNA-Seq studies (Wang et al., 2009) are focus on the direct estimation of differential gene expression. However, in our case we want to estimate the *expression profile*, i.e., the change of the relative gene expression through time. Given that our experiment was an RNA-Seq time-course (Luan and Li, 2003; Iglesias-Martinez et al., 2016) study, the emphasis was to summarize the changes that occur



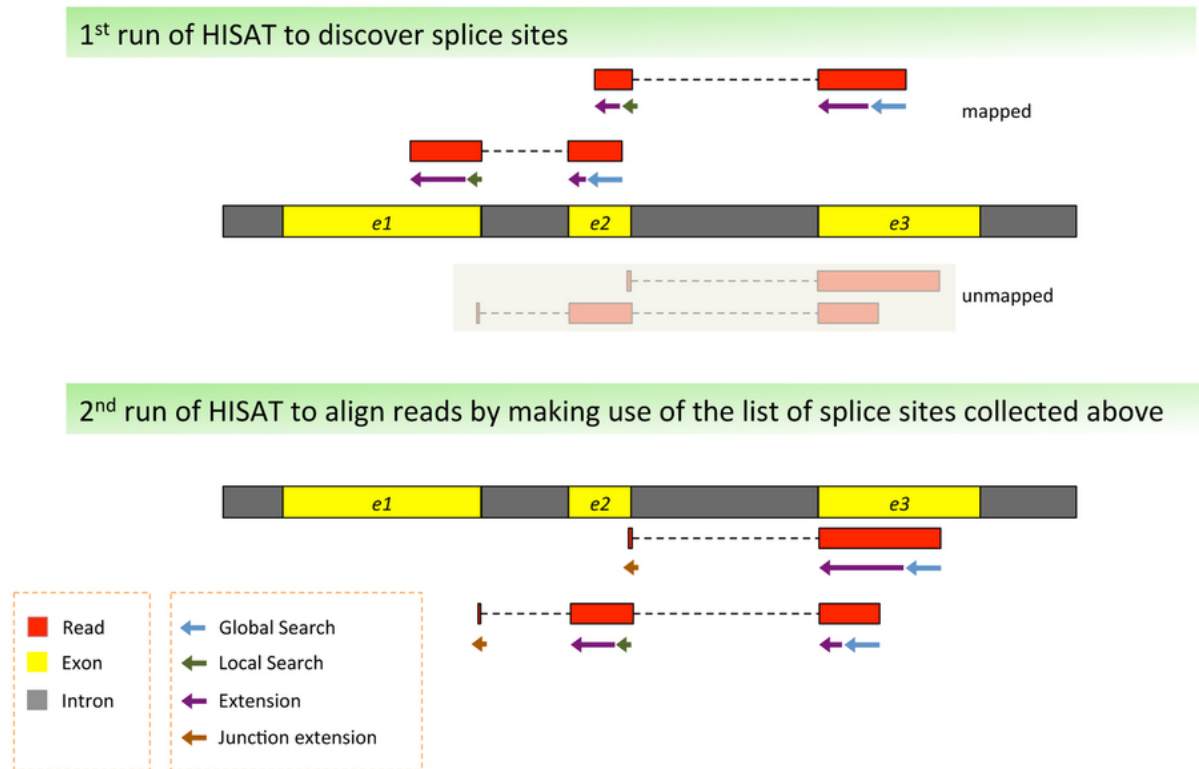


FIGURE 3. Mapping process

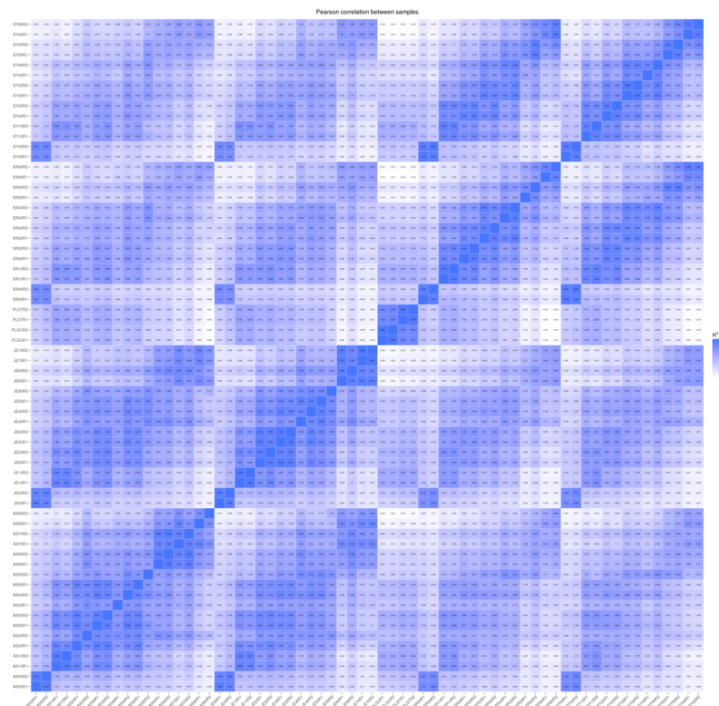


FIGURE 4. Matrix of correlation coefficients between samples (replicates are adjacent).

from one point in time to the next. We sampled seven times during fruit development, say  $t_1, t_2, \dots, t_7$ , corresponding to 0, 10, 20, 30, 40, 50 and 60 DAA, thus the contrasts of interest were between times  $t_i, t_{i+1}$ ;  $i = 1, 2, \dots, 6$ ; i.e., between the six neighboring intervals. Let's denote the true mean gene expression for a given gene within one of the accessions as  $\mu_i$ ;  $i = 1, 2, \dots, 7$ . Then, for each neighbor interval we had three possibilities, say, gene expression decreases from time  $i$  to time  $i + 1$ , denoted as 'D' and expressed by the hypothesis  $\mu_i > \mu_{i+1}$ ; steady gene expression from time  $i$  to time  $i + 1$ , denoted by 'S' and corresponding to  $\mu_i = \mu_{i+1}$  and finally gene expression increases from time  $i$  to time  $i + 1$ , denoted as 'I' corresponding to  $\mu_i < \mu_{i+1}$ . To decide between these alternatives we employed the program edgeR (Robinson et al., 2010) as described below.

It is important to realize that we want to statistically summarize a gene expression profile that exist in the six dimensional space created by the contrasts at neighbor intervals, and thus six tests of hypothesis, one for each one of the neighboring intervals, need to be performed. Given that we test multiple hypotheses (one for each interval), we need to consider the Bonferroni correction (Abdi, 2007) for the probability of calling two expression profiles as statistically different. Thus, to obtain an approximate probability of Error Type I,  $p^*$ , when performing 6 tests, we need to use a  $p^*$  value equal to  $p^* = p^6$ , where  $p$  is the value employed at each one of the 6 individual tests. In our case we fixed  $p^*$  to be equal to 0.01 or 1%. Note that we were not going to directly perform or use hypothesis tests between different gene expression profiles, but only use the expression profile as a reasonable summary of gene expression through time. The basic idea behind this method of estimation was previously published by our group in Martínez-López et al. (2014).

To obtain the  $p^*$  values needed by the method, we run edgeR (Robinson et al., 2010) on the matrix of raw counts of reads for each one of the accessions, performing the tests for each gene in contrasts  $t_i$  vs.  $t_{i+1}$ ,  $i = 1, 2, \dots, 6$ , i.e., for the differences in expression between the 6 pairs of neighboring intervals.

Because at each time interval we had three possibilities for the change of gene expression, as said before, 'D' when  $\mu_i > \mu_{i+1}$ ; 'S' when  $\mu_i = \mu_{i+1}$  and 'I' when  $\mu_i < \mu_{i+1}$ , we call the realization of these profiles 'Ternary Models', because only 3 possibilities were contemplated at each one of the neighboring intervals. Ternary Models can be represented by the six successive results obtained in the intervals; for example, model 'SSSSSS' represent the case where gene expression was steady, i.e., with no significant change during all fruit development, while model 'DDISS' denotes the case where expression decreased from 0 to 10 and 10 to 20 DAA, then increased from 20 to 30 DAA and then stayed steady in the last two intervals, from 40 to 50 and 50 to 60 DAA. Thus, by counting all possibilities we had a total of  $3^6 = 729$  different Ternary Models.

To obtain raw estimated expression profiles we calculate, for each gene within each accession, the mean gene expression of the two biological replicates in FPKM units (Mortazavi et al., 2008)<sup>1</sup>. This gave a vector of seven numbers, say  $\mathbf{m} = (m_1, m_2, \dots, m_7)$ , corresponding to the seven times points where the expression was estimated. The algorithm to obtain the Ternary Model profile from the raw estimated expression profile,  $\mathbf{m}$ , needs also the 6-dimensional model vector

$$\mathbf{M} = (M_1, M_2, \dots, M_6)$$

which contains the letters that denote the change at each one of the 6 intervals; i.e.  $M_i \in \{D, S, I\}$ ;  $i = 1, 2, \dots, 6$ , i.e., the Ternary Model for the gene.

The algorithm to calculate the Ternary Model profile is presented in the next list.

**Algorithm to obtain the Ternary Model profile 'o' from input  $\{\mathbf{m}, \mathbf{M}\}$ .**

- (1) Input  $\mathbf{m}$  and  $\mathbf{M}$ ; initialize a seven numerical vector,  $\mathbf{o} = (o_1, o_2, \dots, o_7)$  with 'NA' in all its elements and also auxiliar variables  $i = 1$ ,  $j = 0$ ,  $k = 0$ ,  $s = m_1$ .
- (2) (main loop): **while**( $i < 6$ ) {

<sup>1</sup>FPKM stands for 'number of Fragments Per Kilobase of transcript sequence per Millions base pairs sequenced'

- **if**( $M_i = S$ )
  - { $s = s + m_{i+1}$ ,  $j = j + 1$ ,  $k = k + 1$  }
  - else**
  - { $t = s/j$ ,  $\mathbf{o}[\min(sub) = \text{'NA': } (k + 1)] = t$ ,  $s = v_{i+1}$ ,  $j = 1$ ,  $k = i$ }
- (3)  $i = i + 1$  } (ends main loop).
- (4) # (Examine last element of  $\mathbf{M}$  and fill element(s) of “ $\mathbf{o}$ ” as needed).
  - **if**( $M_6 = S$ )
    - { $s = s + m_7$ ,  $\mathbf{o}[\min(sub) = \text{'NA': } 7] = s/(j + 1)$ }
    - else**
    - { $t = s/j$ ,  $\mathbf{o}[\min(sub) = \text{'NA': } 6] = t$ ,  $o_7 = v_7$  }
- (5) output  $\mathbf{o}$ .

In the algorithm the elements of the output vector “ $\mathbf{o}$ ”, denoted by “ $\mathbf{o}[\min(sub) = \text{'NA': } x]$ ”, are all elements of the vector that were ‘NA’ from the smallest subindex ( $sub$ ) to  $x$ . The algorithm to calculate the Ternary Model profile obtains a vector,  $\mathbf{o}$ , in which the values of steady intervals (intervals with ‘S’ in the model) are fill with the average of the corresponding values of the elements of  $\mathbf{m}$ . This is so because when there was not statistical significant changes in one or more intervals, the best estimate of the mean expression is given by the average of the corresponding values of  $\mathbf{m}$ .

A pair of numerical examples illustrate this algorithm, which converts a raw estimated expression profile,  $\mathbf{m}$ , into the vector,  $\mathbf{o}$ , which includes the Ternary Model information,  $\mathbf{M}$ .

Firstly, consider the case of the gene with id=3 in accession AS; for this gene we have  $\mathbf{M} = \text{'SSSSSS'}$  (no interval with a significant change) and the rounded numerical values of the raw estimated expression profile are

$$\mathbf{m} = (0.11, 0.05, 0.00, 0.11, 0, 0.12, 0.08)$$

Because none of the changes in expression between neighboring intervals are significant (model is ‘SSSSSS’), all seven values of expression are averaged to obtain each one of the the seven values in  $\mathbf{o}$ , say

$$\mathbf{o} = (0.07, 0.07, 0.07, 0.07, 0.07, 0.07, 0.07)$$

Secondly, consider a gene with a more interesting Ternary Model, say for example gene with id=526 in accession AS, which has  $\mathbf{M} = \text{'DSSISS'}$ . This gene decreases from 0 to 10, stays steady from 10 to 30, increments from 30 to 40 and then remains steady up to 60 DAA. The rounded numerical values of the raw estimated expression profile are

$$\mathbf{m} = (39.75, 17.50, 16.61, 18.56, 25.11, 21.20, 16.77)$$

Applying the algorithm to this vector we obtain

$$\mathbf{o} = (39.75, 17.56, 17.56, 17.56, 21.03, 21.03, 21.03)$$

In this case we have  $o_1 = m_1 = 39.75$  because in the first interval,  $M_1 = \text{'D'}$ , we had a significant decrement from the expression at 0 DAA, 39.75, to the expression at 10 DAA, 17.50, but such decrement was followed by two steady states ( $\mathbf{M} = \text{'DSSISS'}$ ). Now, note that from 10 DAA up to 30 DAA expression was steady, i.e.,  $M_2 = M_3 = \text{'S'}$ , thus the values of  $o_2, o_3$  and  $o_4$  are obtained as the average of the values in  $m_2, m_3$  and  $m_4$ , i.e., the average of 17.50, 16.61 and 18.56 which equals 17.56, thus  $o_2 = o_3 = o_4 = 17.56$ . In interval  $M_4$  (from 30 to 40 DAA) we have a significant increment, from  $m_4 = 18.56$  to  $m_5 = 25.11$ , but such increment was followed by two steady intervals,  $M_5 = M_6 = \text{'S'}$ , and thus values of  $o_5, o_6$  and  $o_7$  are equal to the average of 25.11, 21.20 and 16.77 which is 21.03.

Note that vectors of expression profiles,  $\mathbf{o}$ , are not standardized to have a mean over time of 1 and a standard deviation of 1. Thus the last step to obtain Standardized Expression Profiles (SEPs) is to subtract the mean and divide by the standard deviation all elements of  $\mathbf{o}$ , say to obtain the SEP,  $\mathbf{s}$  from

$\mathbf{o}$  we standardize setting  $n_i = (o_i - \bar{o})/S_{\mathbf{o}}$ , where  $\bar{o}$  is the average of the seven elements of  $\mathbf{o}$  and  $S_{\mathbf{o}}$  is the standard deviation of the elements of  $\mathbf{o}$ .

In the second example (gene with id=526 in accession AS) we have that  $\bar{o} = 22.21$  and  $S_{\mathbf{o}} = 7.93$ , thus the final representation of the Standardized Expression Profile (SEP),  $\mathbf{s}$ , is given by

$$\mathbf{s} = (2.21, -0.59, -0.59, -0.59, -0.15, -0.15, -0.15)$$

which has an average of 0 and a standard deviation of 1, i.e. it is 'standardized'.

In summary, the estimation of a SEP,  $\mathbf{s}$ , proceeds following the steps  $\{\mathbf{M}, \mathbf{m}\} \Rightarrow \mathbf{o} \Rightarrow \mathbf{s}$ , and it takes into consideration the mean gene expression  $\mathbf{m}$ , which for each time is the average resulting from two RNA-Seq libraries as well as the statistical significance between neighboring times, contained in the Ternary Model  $\mathbf{M}$ , adjusting the expression at each time to reflect significant changes by averaging the expression intervals where there is not significance, obtaining the Ternary Model profile,  $\mathbf{o}$ , to finally obtain the SEP,  $\mathbf{s}$ , by standardizing  $\mathbf{o}$ . Even when this procedure could be judged as highly convoluted, it has a great advantage: It allows to compare gene expression profiles throughout time independently of the raw gene expression and it integrates the available statistical evidence for expression change between neighboring times.

Figure 5 shows the plot of the SEP for gene with id=526 in accession AS, presented before as second example.

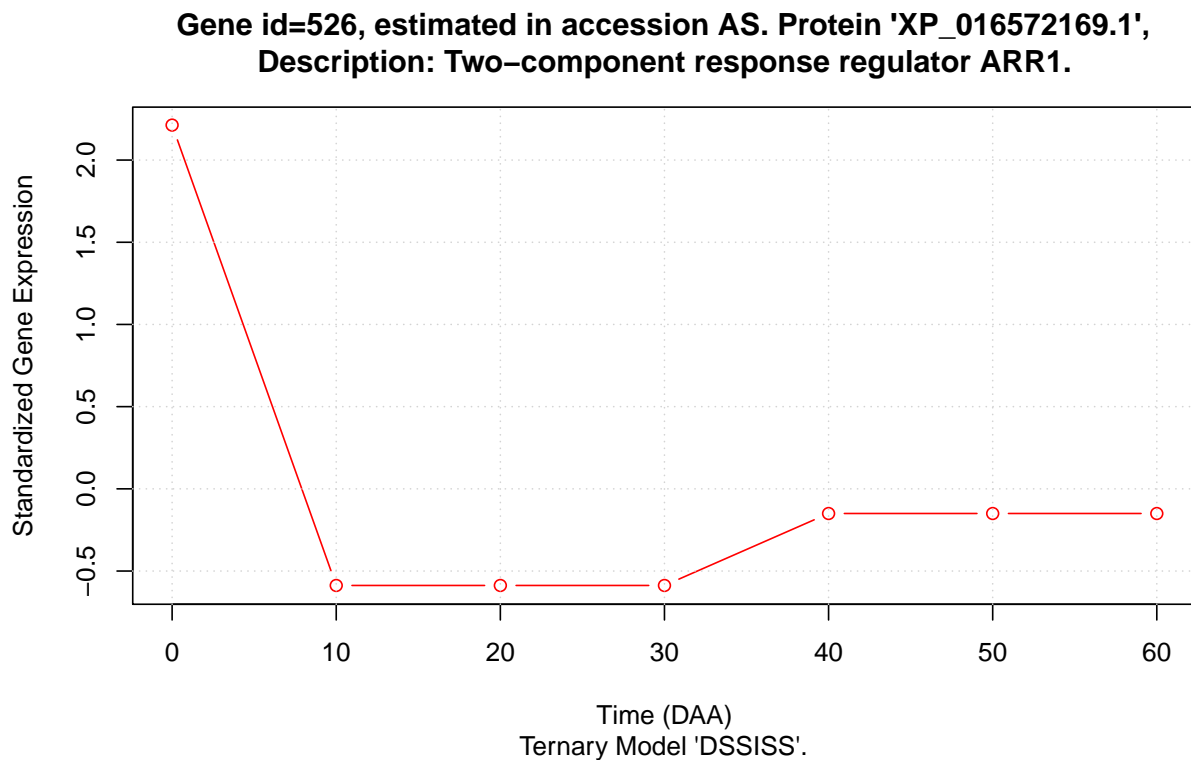


FIGURE 5. Example: Standardized Expression Profile (SEP;  $\mathbf{s}$  vector) for gene with id=526 in accession AS.

In Figure 5 we can appreciate the plot of the SEP used as second example. Additionally to showing the best estimates of standardized changes in expression throughout time, we can see how the SEP model preserves the relative magnitude of expression changes; observing this plot we can immediately notice that the change from 0 to 10 DAA, with a total absolute difference of 2.8 standardized units, is much larger than the change from 30 to 40 DAA, which has a total absolute difference of 0.74 standardized units.

### S-3. TESTING DIFFERENCES BETWEEN DOMESTICATED (D) AND WILD (W) SEPs

The focus of this work was the detection of changes in standardized expression profiles (SEPs) between D and W accessions caused by the domestication process. We studied 10 accessions, 6 D and 4 W (see Table 1 in the main text), and found that a total of 22427, representing approximately 64% of the genes annotated in the *Capsicum* genome (CM334 v1.6) were consistently expressed in all 10 accessions at one or more of the times sampled and in more than one of the two biological replicates per accession.

For each gene we had 10 SEPs, 6 from D and 4 from W accessions, and we want to discriminate with a univariate statistic if there were differences in SEPs when grouping them in the D and W sets. For this we selected the [Euclidean distance](#) between SEPs, defined as

$$d_{a,b} = d(\mathbf{s}^a, \mathbf{s}^b) = \sum_{i=1}^{i=7} (s_i^a - s_i^b)^2$$

where  $\mathbf{s}^a$ ,  $\mathbf{s}^b$  are two different profiles for the same gene. For a given gene we calculated the total of  $10(10-1)/2 = 45$  different distances,  $d_{a,b}$ ;  $a \neq b$ , and classified those distances into two groups, *distances between* D and W accessions and *distances within* one of the groups. The number of distances between D and W is equal to  $6 \times 4 = 24$ , while the remaining  $45 - 24 = 21$  distances happen within the two groups, say  $6(6-1)/2 = 15$  within D accessions and  $4(4-1)/2 = 6$  within W accessions.

For a single gene, our interest was to detect significant differences in SEPs between the D and W accessions, and this can be translated to the statistical hypothesis  $\mathcal{H}_0 : \mu_b = \mu_w$  versus  $\mathcal{H}_a : \mu_b > \mu_w$ , where  $\mu_b$  and  $\mu_w$  are the true means of the distances between and within the D and W groups, respectively. If we accept the null hypothesis  $\mathcal{H}_0$  as true, then we have no evidence of differences between SEPs in the D and W accessions, while if this hypothesis is rejected in favor of  $\mathcal{H}_a : \mu_b > \mu_w$  (note that this alternative implies a one-tail test), we conclude that the mean distance between the two groups is significantly larger than the distance within those groups, and this implies a difference in SEPs between D and W. To perform the statistical test we assayed a randomization test comparing it with the usual parametric one tail t-test, and found that those alternatives were almost equivalent, opting for the second given the high computational cost of the second and the large number of tests (22427) that needed to be performed.

Figure 6 presents the histogram of the  $P$ -values obtained in the 22427 test of the null hypothesis  $\mathcal{H}_0 : \mu_b = \mu_w$  versus  $\mathcal{H}_a : \mu_b > \mu_w$ .

An interesting feature in Figure 6 is that the first bar, including  $P$  values between between 0 and 0.05, includes 4465 cases, approximately 20% of the total. This indicates that the  $P$  distribution of the tests performed is far from being uniform, as expected from randomized tests (Bland, 2013). And because we tested all genes expressed during fruit development, the non-uniformity of the  $P$  distribution for the tests implies that selection had an important role in the modification of SEPs.

Table 1 presents the matrix of average mean distances between 22427 SEPs, corresponding to equal number of genes, in the 10 accessions.

In Table 1 we can see that the minimum of the mean distances, 1.63 (in blue), occurs between SR and SY, two W accessions, while the maximum, 2.40 in red, happens between AS and SR as well as between AS and ST, in both cases a D and W accessions respectively. On the other hand, the mean average distance within D and W accessions (21 values from the matrix) is 2.02, while the mean average distance between D and W accessions (24 values from the matrix) is 2.18; i.e., the D and W accessions form two well segregated groups.

The dendrogram presented in the Figure 1 of the main text was obtained by applying the agglomerative [Ward's](#) algorithm on the distance matrix shown in Table 1. In that figure W accessions are grouped in a single cluster (left hand side), well separated at a mean Euclidean distance  $> 2.8$  from the one formed

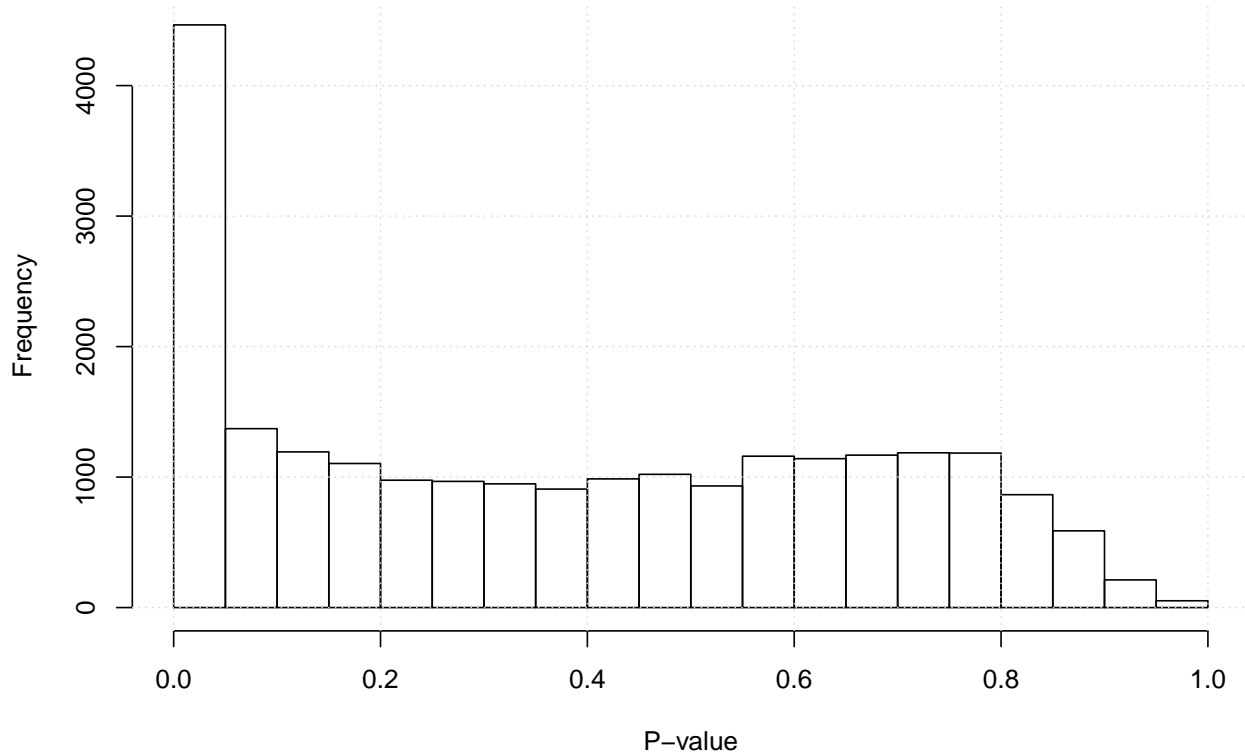


FIGURE 6. Histogram of the  $P$ -values obtained in the 22427 test of the null hypothesis  $\mathcal{H}_0 : \mu_b = \mu_w$  versus  $\mathcal{H}_a : \mu_b > \mu_w$  employing the one-tail t-test.

TABLE 1. Matrix of average mean distances between the SEPs in the 10 accessions.

|        | CM (D) | CO (W) | CW (D) | JE (D) | QU (W) | SR (W) | ST (D) | SY (W) | ZU (D) |
|--------|--------|--------|--------|--------|--------|--------|--------|--------|--------|
| AS (D) | 2.13   | 2.33   | 2.05   | 1.91   | 2.35   | 2.40   | 2.40   | 2.37   | 2.27   |
| CM (D) |        | 1.96   | 2.07   | 2.01   | 1.98   | 1.95   | 2.11   | 1.97   | 1.98   |
| CO (W) |        |        | 2.26   | 2.22   | 1.80   | 1.78   | 2.18   | 1.74   | 1.95   |
| CW (D) |        |        |        | 2.02   | 2.29   | 2.31   | 2.23   | 2.31   | 1.97   |
| JE (D) |        |        |        |        | 2.26   | 2.29   | 2.31   | 2.18   | 2.08   |
| QU (W) |        |        |        |        |        | 1.91   | 2.15   | 2.00   | 2.12   |
| SR (W) |        |        |        |        |        |        | 2.21   | 1.63   | 2.05   |
| ST (D) |        |        |        |        |        |        |        | 2.23   | 2.06   |
| SY (W) |        |        |        |        |        |        |        |        | 2.04   |

by the 6 D accessions (right hand side), this shows that gene expression variability within the W and D groups is smaller than the distance between those groups.

#### S-4. ANALYSES PER TIME OF SEPs IN D AND W ACCESSIONS

For each one of the 22427 genes expressed during fruit development we have 10 SEPs, and in the previous section we have described the univariate test performed on the Euclidean distances to decide if the SEPs in the set of 6 D accessions could be considered different to the 4 ones in the W group. Independently of the fact that SEPs grouped into the D and W could be considered to be equal or not by that test, we can additionally analyze the differences between SEPs in the 7 stages of development (0, 10, 20,  $\dots$ , 60 DAA), grouping a single gene or sets of genes in the D and W sets.

Let's denote as  $\mathbf{s}_n^D$ ,  $\mathbf{s}_n^W$ , the 7-dimensional SEP vectors for genes in an arbitrary set of genes  $\mathbf{n}$ , which cardinality is  $n$ , i.e., the set  $\mathbf{n}$  is constituted by  $n$  different genes ( $|\mathbf{n}| = n$ ).

As an example, define  $\mathbf{n}$  as the set formed with the gene with identifier 580 (a single gene). Then  $\mathbf{s}_n^D$  is constituted by 6 different vectors, each one corresponding to each one of the 6 D accessions, while  $\mathbf{s}_n^W$  is formed by 4 different vectors, each one corresponding to each one of the 4 W accessions. Now, for each stage of development,  $i = 1, 2, \dots, 7$ , we have two sets of independent standardized gene expressions, say,  $d_i = \{s_{ij}\}$ ;  $j = 1, 2, 3, 4, 5, 6$  for D and  $w_i = \{s_{ik}\}$ ;  $k = 1, 2, 3, 4$  where the subindex  $j$  denote accession, D or W, respectively. Note that all elements  $\{s_{ij}\}$ ,  $\{s_{ik}\}$  are fully independent, because each one of them was estimated from a different RNA-Seq library.

For each one of the stages of development, the hypotheses of interest are:  $\mathcal{H}_0 : \mu_{n,i}^D = \mu_{n,i}^W$  versus  $\mathcal{H}_a : \mu_{n,i}^D \neq \mu_{n,i}^W$ , where  $i = 1, 2, \dots, 7$  and  $\mu_{n,i}^D, \mu_{n,i}^W$  represent the true means of standardized expression at developing stages 0, 10,  $\dots$ , 60 DAA, respectively. The number of standardized observations in the sets D and W depend on the number of genes in the set  $\mathbf{n}$ , as before  $|\mathbf{n}| = n$ , thus if  $n = 1$  (a single gene tested), then the number of observations to be included in the two sets to be tested are 6 for D and 4 for W, while in general for any any set of genes  $\mathbf{n}$  with  $n$  genes we will have  $6n$  and  $4n$  observations for D and W, respectively. To perform the tests  $\mu_{n,i}^D = \mu_{n,i}^W$ ;  $i = 1, 2, \dots, 7$  as well as to obtain 95% Confidence Intervals (CIs) for the means of each group at each one of the times we employed the two tail t-test. The procedure to perform the test and plot the results for any arbitrary set of genes was programed in an R function.

On the other hand, it was considered important to evaluate the stage at which the maximum expression of a gene was reached. In this case for each SEP we determine stage (0, 10,  $\dots$ , 60) at which the maximum standardized expression is reach. Denote as  $m_i$  the point of development at which the maximum of the SEP vector  $\mathbf{s}_i = (s_{i1}, s_{i2}, \dots, s_{i7})$  is found. For example, if  $\max(\mathbf{s}_i) = s_{i3}$ , this means that the maximum standardized expression took place at the third stage ( $i = 3$ ), corresponding to 20 DAA, thus the value of  $m_{i3}$  is 20, etc. For any gene or set of genes  $\mathbf{n}$ , we calculated the set of maxima in D and W accessions and tested the hypothesis  $\mathcal{H}_0 : \Psi_{n,i}^D = \Psi_{n,i}^W$  versus  $\mathcal{H}_a : \Psi_{n,i}^D \neq \Psi_{n,i}^W$ , where  $\Psi_{n,i}^D, \Psi_{n,i}^W$  represent the true means of the maximum standardized expression and calculated the corresponding 95% CI.

The functions to analyze and plot the results for an arbitrary set of genes,  $\mathbf{n}$ , where employed to obtain figures 2, 3 and 4 presented in the main text. In these, as in any results from such functions, the corresponding plots show the 95% CI for mean standardized expression as thin lines at each stage of development, while the estimated mean maximum expression is shown by asterisks with their corresponding 95% CIs shown by an horizontal line. To illustrate these kinds of results we present examples for two genes.

Our first example corresponds to the results obtained for the gene with id=580, and plots are presented in figures 7 and 8.

Figure 7 presents SEPs for the *Capsicum* fibrillin (FBN). Fibrillins are nuclear-encoded, plastid proteins associated with chromoplast fibrils and chloroplast plastoglobules (Singh and McNellis, 2011), and in Figure 7 we can appreciate how expression of FBN is highly concordant in all accessions. In that figure the points plotted are slightly displaced in the X axis (DAA) to avoid line and symbols overlapping. In all accessions TMs for FBN had a low standardized expression from 0 up to 40 DAA, where the expression increases rapidly, reaching the maxima at 50 (in 3 accessions; 2 D and 1 W) or 60 (7 accessions; 5 D, 3 W) DAA. The FBN gene does not present a significant difference in distances between D and W accessions, having a  $P$ -value of 0.8 in that test, and exemplifying a case of a gene which was not affected by domestication. On the other hand, Figure 7 presents mean SEPs for the FBN gene. That figure was produced with our function 'TMmean.plot()', which also produced the output presented in Appendix S-11.

In Appendix S-11 we see that the results include tables of means and CI for the means for the standardized expression at each point in time; those CI are plot as thin vertical lines in Figure 8, allowing the visual

**Individual SEPs for gene FBN (fibrillin) per accession.  
(XP\_016560176.1 light-induced protein, chloroplastic)**

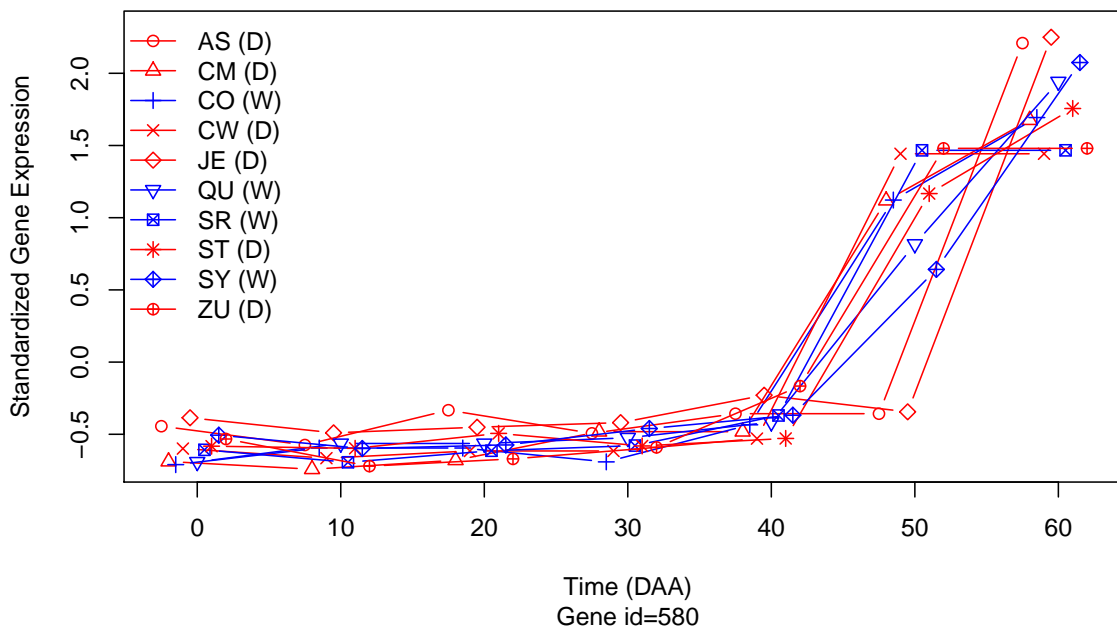


FIGURE 7. SEPs per accession for a gene with highly concordant expression patterns in all 10 accessions. Values per accession were slightly displaced in the Y axis to avoid overlapping.

judgment of the difference between the means in the D (red) and W (blue) sets. For all time points (0, 10, ..., 60 DAA) we see that the CI of D and W overlap, and the lack of a significant difference can be observed in the  $P$ -values for the t-test of means D vs W per time point in Appendix S-11. The second analysis performed is the estimation of means and t-test for the maxima in the D and W groups. Appendix S-11 presents the means and 95% CI for those estimates. The mean for the D group is 56.67 DAA while the mean for the W set is only slightly different, 57.5, with CIs overlap between the two groups. Finally, the lack of significance of the difference in the mean maxima between the two groups is confirmed by the t-test, which gives a value of  $P = 0.8065$ . The function even gives the interpretation of the result in the line: '(Genes are Early in D but the difference is NOT significant at 0.05)'. Figure 8 presents the means of the times where the maximum expression for each set is estimated as asterisks and the corresponding CI as broad horizontal lines. From all the analyses we can conclude that the FBN gene has a highly similar expression pattern in both, D and W accessions. This kind of analysis and plots were used for figures 2, 3 and 4 in the main text with different sets of genes.

Figures 9 and 10 present plots for a gene with highly different SEPs between D and W and Appendix S-11.1 presents the statistical analysis for this case.

The gene with id=19147, a transcription factor identified as 'B3 domain-containing protein At5g42700-like' and with protein identifier XP\_016568750.1, was highly significant ( $P < 4.6 \times 10^{-14}$ ) in the univariate test for differences in SEPs between D and W, and in fact Figure 9 shows that this gene has SEPs which in D accessions have a maximum at 10 DAA, while in W the maximum is present at 30 DAA. This expression pattern indicates that this gene belongs to the group of 'D10W30' genes defined in the main text. Indeed, in Figure 10, which presents the mean SEPs for the gene and the 95% CIs for time of maximum expression over the the X axis, and standardized gene expression over the Y axis, shows that the maxima are different for D and W, while there are significant differences in mean expression at 10,



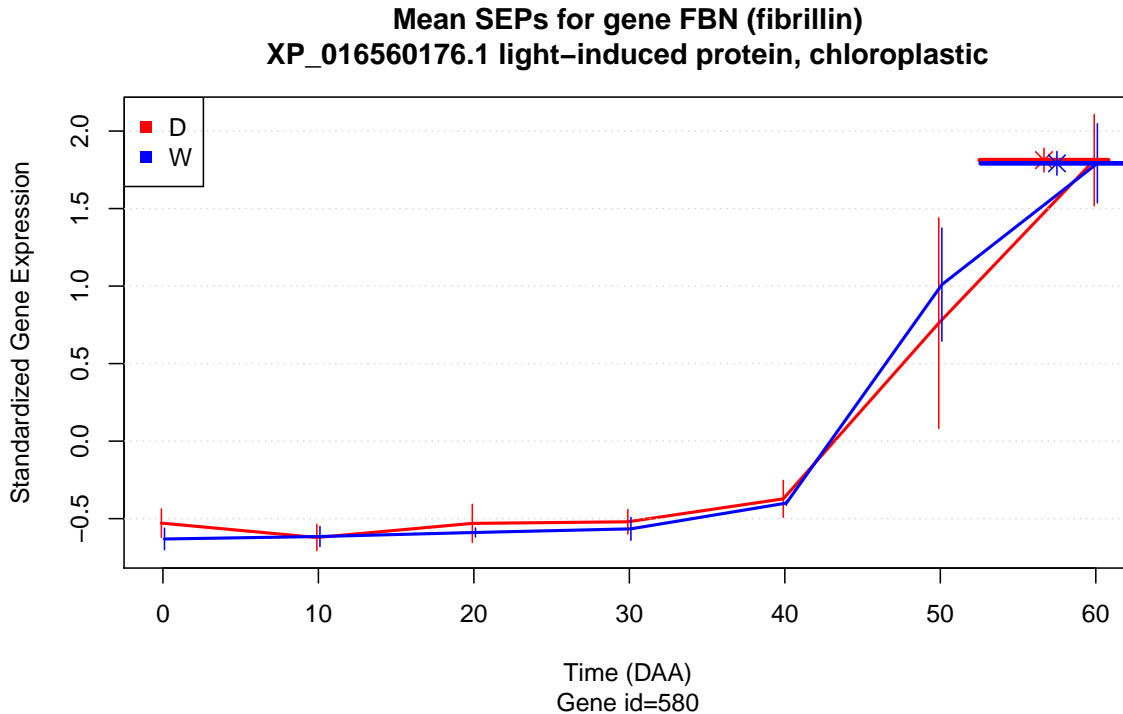


FIGURE 8. Main lines link the mean SEPs and the thin vertical lines give the 95% CI for the respective estimated points. Asterisks point to the estimated time in DAA where the maximum mean expression was estimated while broad lines over the asterisks are the 95% CI for those points.

30, 40, 50 and 60 DAA. Appendix S-11.1 presents the R output with the statistical results obtained in the analyses.

The same plots and statistical analyses presented in figures 8 and 10 and appendices S-11 and S-11.1 for individual genes can be performed for groups of genes, as done to plot figures 2, 3 and 4 in the main text. To perform statistical analyses of a gene, or sets of genes, we considered contrasts between two groups of accessions, 6 D (AS, CW, JE, ST and ZU in Table 1) and 4 W (CO, QU, SR and SY in Table 1 in main text). In all cases, the null hypothesis was that at each time point the mean expression of the D and W groups was equal, whereas the alternative was that these parameters differed. Variation within the D and W groups was considered as a statistical error (unexplained variation) and a t-test was used to obtain Confidence Intervals (CI) for the means and to evaluate significance at each of the 7 time points sampled. We determined the mean SEPs for different gene groups in the D and W accessions (Figure 11).

The mean for the D and W groups differed significantly (Figure 11 A). At the mature flower state (0 DAA), the standardized mean expression for D was much higher than for W, implying that the average transcription activity in this state is substantially larger for the D genotypes. In the interval between 0 and 10 DAA, the mean standardized expression increased for both groups, although the rate of increase was higher for D. At 10 DAA, the mean expression for D reached a peak value, but for W the increase continued, although at a slower rate, to peak at 20 DAA. From the peak at 10 DAA, the mean expression for D decreased, at different rates, and was lower at all subsequent time points. The lowest value was seen at 60 DAA. In contrast, decreases in the mean expression for W began later, occurring from 20 up to 50 DAA, and reached a minimum of -0.27, which is smaller than the minimum for the D group, -0.25, seen at 60 DAA. The more relevant differences between mean expression profiles between D and W were seen during the intervals between 10 and 20 and 50 to 60 DAA, when the trend (i.e., slope of

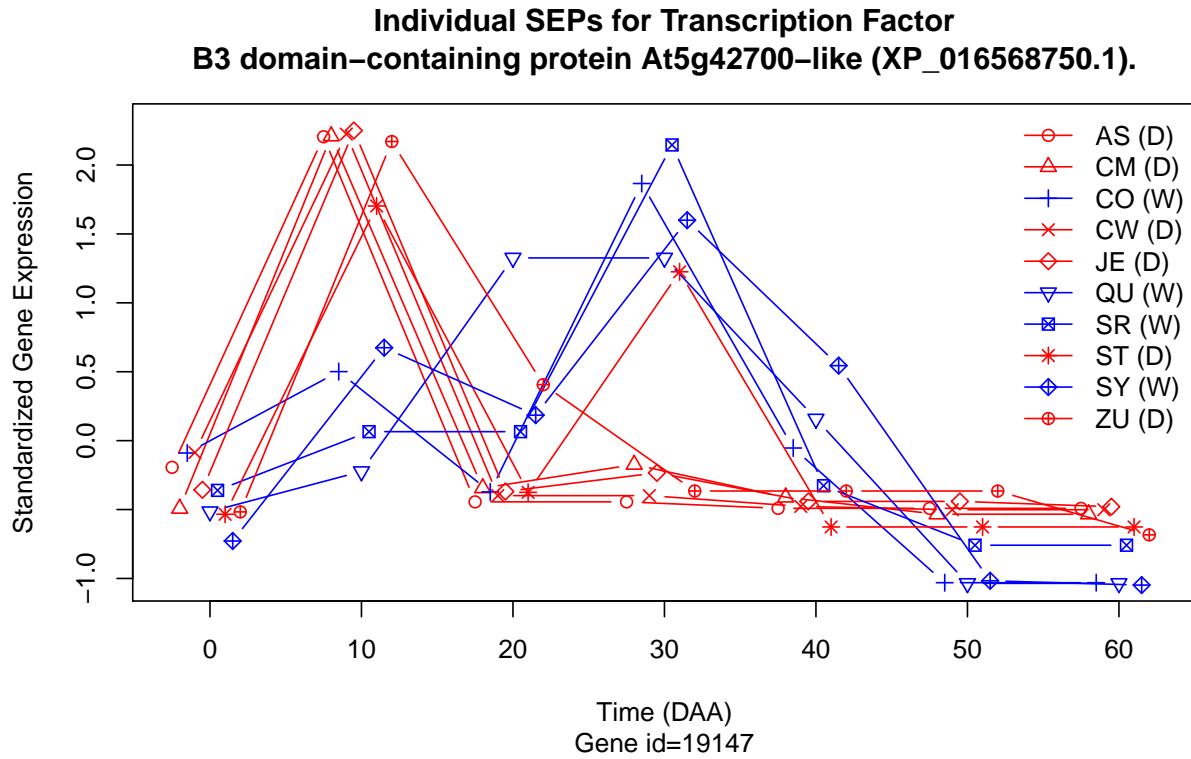


FIGURE 9. SEPs per accession for a gene with highly different expression patterns between D and W. Values in Y axis slightly displaced to avoid overlap.

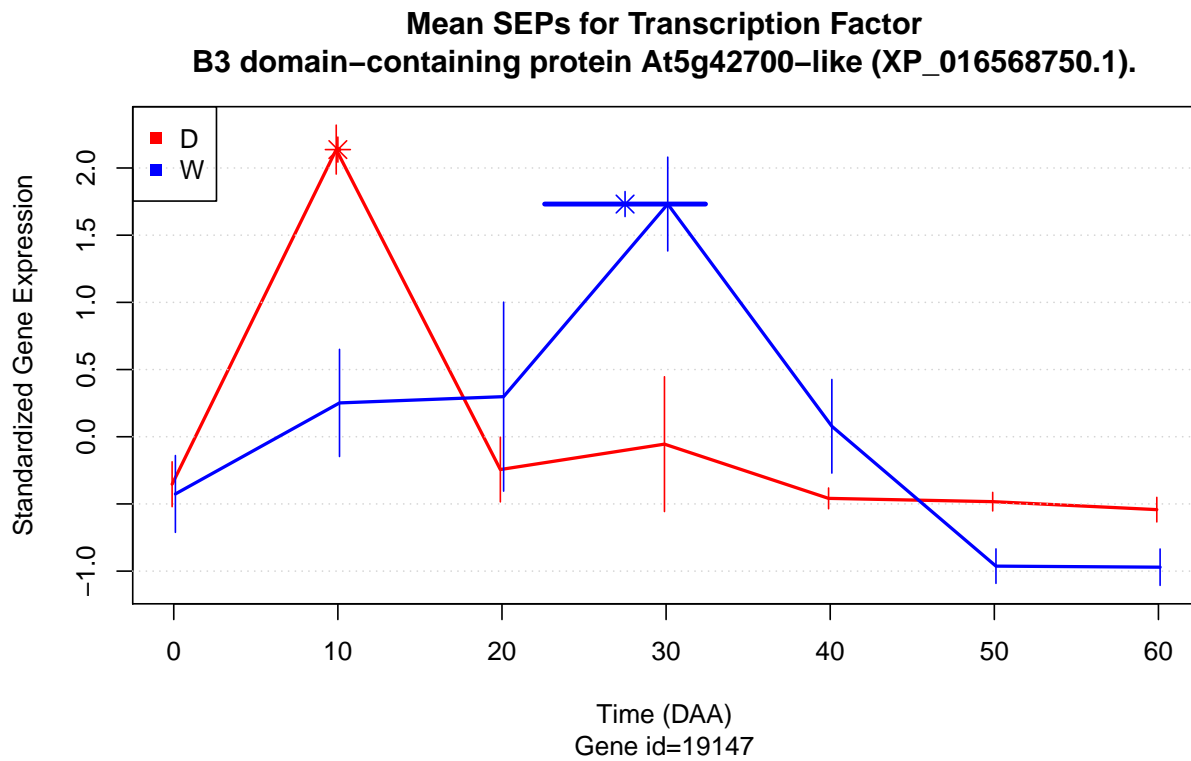
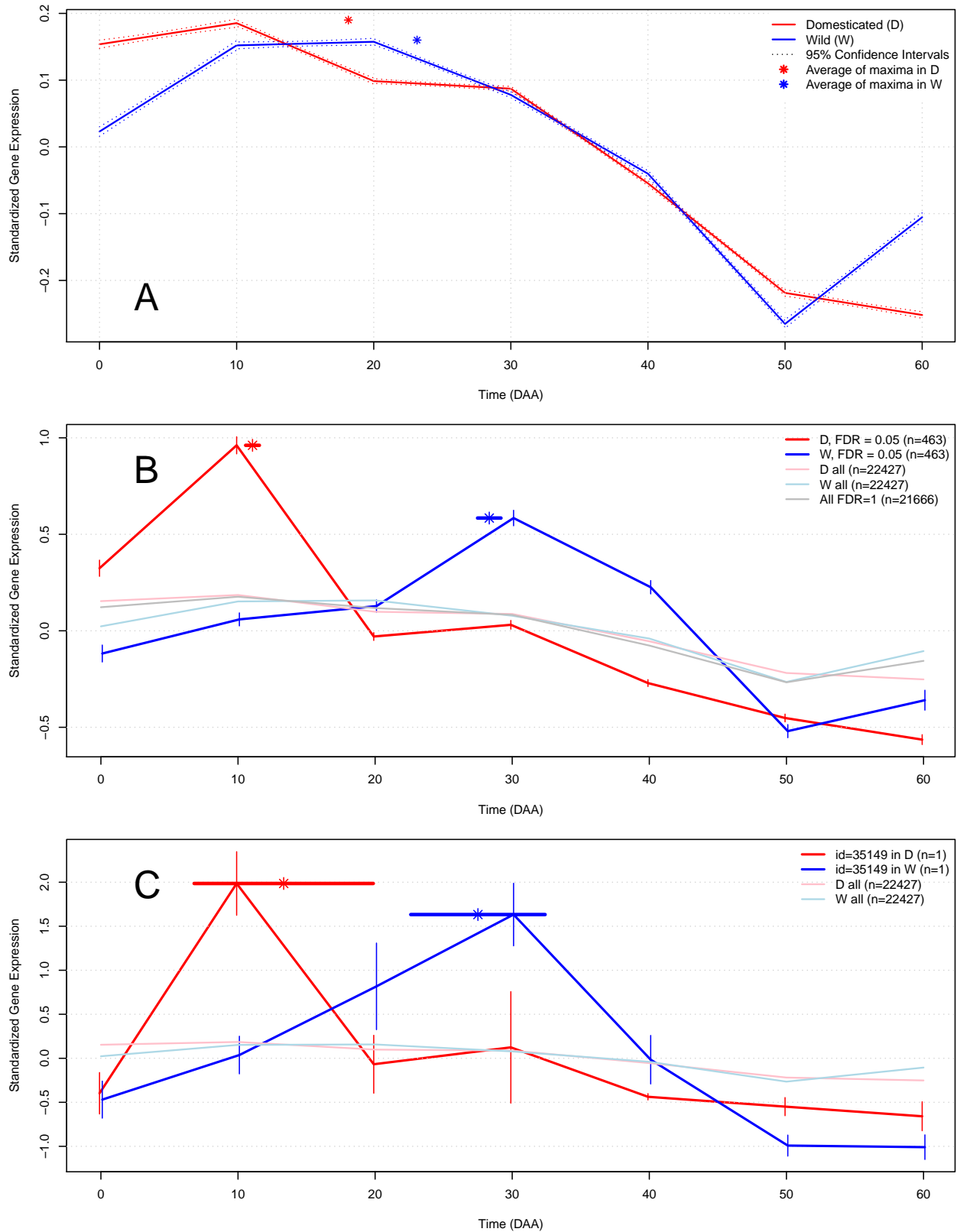


FIGURE 10. Mean SEPs per accession for a gene with highly different expression patterns between D and W.



**FIGURE 11. Mean SEP (Standardized Expression Profile) for groups of genes in Domesticated (D) and Wild (W) accessions.** Continuous colored lines link the means of standardized gene expression at each time point. (A) Complete set of expressed genes (n=22,427). (B) Set of genes having differential expression profiles between D and W (n=463; FDR=0.05). Pale colors indicate the expression profile for all genes, and the gray line represents genes that had no difference in expression between D and W (FDR = 1). (C) Expression profiles for the gene (n=1) encoding the protein “G2/mitotic-specific cyclin S13-7” (XP\_016543946.1). In B and C the thin vertical lines represent the 95% CI for the means. Asterisks indicate the mean time of maximum expression and the horizontal lines over the asterisks represent the 95% CI for the mean at each time point.

the regression models) was inverted such that D was decreasing while W was increasing. On the other hand, less marked differences between D and W were seen between 30 and 50 DAA when the mean standardized expression decreased nearly in parallel for both groups. The average of the time at which the maximum expression was reached in each group (marked by asterisks) was five days earlier for D than W. All observed differences were significant.

Differences in SEP of individual genes varied between D and W. To select the genes having the largest differences between D and W, we applied a statistical test on individual differences and used a False Discovery Rate (FDR) threshold of 0.05, which for these tests produced a  $P$  value  $< 0.000002$ . Using these criteria we selected a set of 463 genes, representing approximately 2.06% of the total (Figure 11 B). The expression profiles of these 463 selected genes differed markedly between D and W, ranging from -0.56 (D at 60 DAA) to 0.96 (D at 10 DAA), which is much larger than the range of variation for the means of all genes (Figure 11 B, pale red and blue lines). The profiles for these genes also completely differed from the average profile of genes that had similar expression profiles in both D and W (grey line, FDR = 1). The differences in expression profiles between D and W were well defined and significant; the peak of mean expression for D occurred at 10 DAA, while the peak for W occurred later, at 30 DAA. The average time of maximum expression (asterisks with corresponding 95% CIs) was 11.06 DAA for D and 28.33 DAA for W, or a difference of -17.27 DAA. Of the 463 selected genes, 36 ( $36/463 \approx 0.08$ ; 8%) are transcription factors (TFs). This percentage is higher than that for TFs annotated in the Capsicum genome ( $1,859/34,986 \approx 0.05$  or 5%). A list and description of the 463 selected genes and details of statistical analyses are presented in the Supplemental SG and SM-4, respectively.

We next focused on the expression profiles in the D and W accessions for a single gene encoding the protein ‘G2/mitotic-specific cyclin S13-7’ (Figure 11 C). For this gene, the 95% confidence intervals (CIs) for the means at each time (thin vertical lines), as well as for the average of the time at which maximum expression was reached for each group (horizontal lines over the asterisks) was longer, since the means were obtained from only one gene ( $n=1$ ) and thus each point is obtained from only individual data for the 6 and 4 accessions for D and W, respectively (see Methods). Nevertheless, the sample size and statistical method employed show that there are significant differences between the D and W profiles for a single gene, given that the 95% CI values do not overlap (Figure 11 C).

The results indicate that the design and results of this experiment showed differences in expression profiles between D and W at the level of whole gene sets (Figure 11 A), groups of particular genes (Figure 11B), and individual genes (Figure 11 C). Taking these findings together, we can thus conclude that there are relevant differences in expression profiles between domesticated and wild varieties of chili peppers.

**S-4.1. Differences in Expression of Genes Related to Cell Reproduction Appear Earlier and are Larger in Domesticated than Wild Genotypes.** Based on the evidence that mean SEP differ between the D and W accessions, we investigated differences in expression profiles in groups of genes related to particular biological processes. We first examined the mean SEPs of a group of 1,125 genes associated with cell reproduction (Figure 12).

We observed that the mean tendency of all 1,125 genes (solid lines) and a subset of 170 genes showed significant ( $P < 0.01$ ) differences in expression profiles between D and W (dashed lines; Figure 12 A). Moreover, significant differences between D and W were observed at all 7 time points for both the entire group and gene subset. For both groups ( $n=1,125$  and  $n=170$ ), the mean expression was higher in D than for W at 0, 10 and 50 DAA. Meanwhile, the intervals from 10 to 20 and 50 to 60 DAA had contrasting tendencies for D and W. For both intervals the mean expression decreased for D, but increased for W. The peak of mean expression occurred earlier for D (at 10 DAA) than for W (at 30 DAA) and the magnitude of expression at the peak was also much larger for D than for W.

The mean expression value for 235 genes that are directly annotated in the cell cycle—but not in other cell reproduction processes— was significantly higher and occurred earlier for D compared to W, as evidenced by the peak of 0.3 standardized units at 10 DAA for D and 0.2 standardized units 30 DAA for

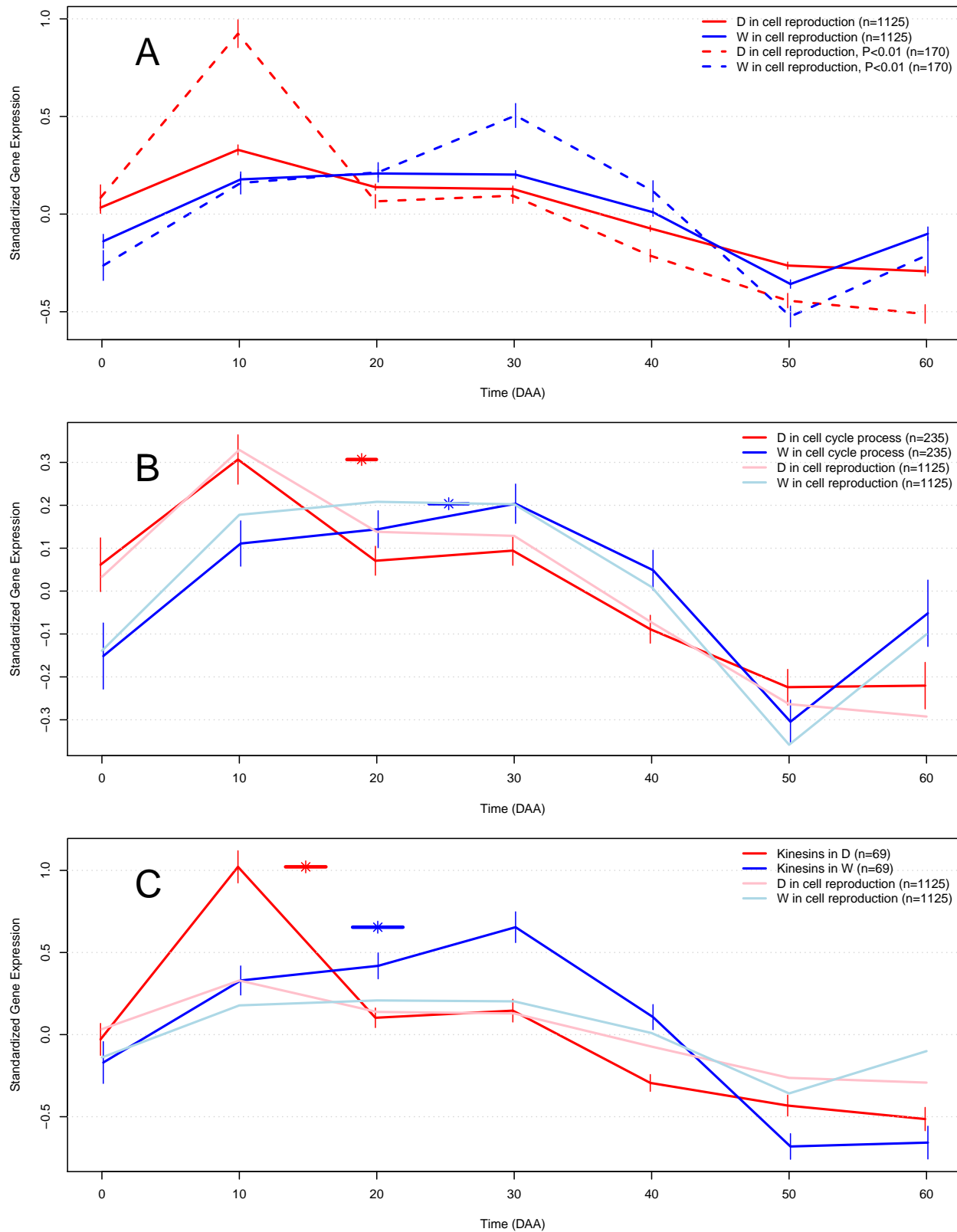


**FIGURE 12. Mean Standardized Expression Profile (SEPs) for groups of genes associated with cell reproduction in Domesticated (D) and Wild (W) accessions.** Vertical lines indicate 95% CI, asterisks denote mean time of maximum expression and horizontal lines over asterisks represent the 95% CI for the parameter. (A) Solid lines show the expression profile for the entire set of 1,125 genes and dashed lines represent expression of a set of 170 genes that had the highest differential expression between the D and W groups ( $P < 0.01$ ). Genes annotated in (B) cell cycle process and (C) Kinesins.

W (Figure 12 B). Similarly, the mean expression for 69 kinesins or kinesin-related proteins among the 1,125 genes associated with cell reproduction exhibited a differential expression peak at 10 DAA for D accessions, but for W accessions the peak was later at 30 DAA (Figure 12 C).

Thus, changes in expression of genes associated with cell reproduction were significantly larger and occurred earlier for D relative to W accessions, not only for the full set of genes, but also for particular bioprocesses and gene families (Figure 12).

**S-4.2. Biological Processes Enriched in Genes That Are Expressed Earlier in Domesticated Genotypes.** The results presented above indicate that SEPs in D and W accessions undoubtedly differ (Figure 11), and genes for which expression peaks at 10 DAA for D but at 30 DAA for W (denoted here as ‘D10W30’) play an important role in cell reproduction (Figure 12). To validate and expand our study, we considered 542 genes having the D10W30 expression pattern in a Gene Ontology enrichment analysis.

A total of 86 biological processes (BPs) were significantly enriched (FDR = 0.05;  $P < 0.0015$ ) in the D10W30 set, with a median odds ratio of 9.5. As such, these genes were much more abundant in these BPs than would be expected by chance. Apart from the abovementioned BPs related to cell reproduction, 43 of the enriched BPs, or 50% of the total, are involved in either positive or negative regulation of various biological processes. Of these, 4 (5%) are related to cellular component organization or biogenesis, 3 are associated with cellular component assembly, and another 3 play roles in organelle organization or fission. The general bioprocess “cellular process” (GO:0009987) is also highly enriched in the D10W30 gene set, with an odds estimate of 2.25 and a highly significant P-value of  $2.76 \times 10^{-8}$ .

These results show that genes having the pattern D10W30 are over-represented in important BPs, which in turn implies that expression of such BPs occurs earlier and at higher levels in D compared to W genotypes.

These results consider the expression patterns of sets of genes grouped by D and W accessions. Next we considered SEPs for single genes (Figure 13). For the three highlighted genes, the mean expression values for D occur at 10 DAA, while for W the means are observed at 30 DAA, consistent with the pattern D10W30. However, the expression patterns for individual accessions (dotted lines) are variable, even when the mean tendency (continuous lines) consistently followed the D10W30 pattern (Figure 13 A to C).

In examining the expression patterns for the gene encoding the “high mobility group B protein 6”, a WRKY transcription factor involved in the nucleosome/chromatin assembly that was annotated in 12 of the 86 abovementioned BPs, particularly cell reproduction BP, there are two outliers among the D10W30 pattern (Figure 13 A). Accession ST (D) had an expression peak at 30 DAA rather than at 10 DAA -even though it had a local maximum at 10 DAA. Accession SY (W) had an expression peak at 40 DAA instead of at 30 DAA. However, the average expression pattern for this gene conforms to the D10W30 pattern and the differences in mean expression between D and W are significant at the two critical points, 10 DAA and 30 DAA.

The gene encoding the transcription factor “MYB-related protein 3R-1” was included in 6 of the 86 enriched BPs and is mainly related to cellular, chromosome and organelle organization. Notably, in comparing Figures 13 A and 13 B, the same accessions, ST (D) and SY (W), are outliers among genes showing the D10W30 pattern, and both had the same tendencies, i.e., high expression at 30 DAA for ST (D) and a late peak at 40 DAA for SY (W). On the other hand, differences in mean expression between D and W were significant at the two critical points 10 DAA and 30 DAA (Figure 13 A, B).

The “kinetochore protein NDC80” is part of multiprotein kinetochore complexes that couple eukaryotic chromosomes to the mitotic spindle to ensure proper chromosome segregation. NDC80 is part of the outer kinetochore and forms a heterotetramer with proteins NUF2, SPC25 and SPC24 (Santaguida and Musacchio, 2009; D’Archivio and Wickstead, 2017). Interestingly, the genes encoding NUF2 and SPC25

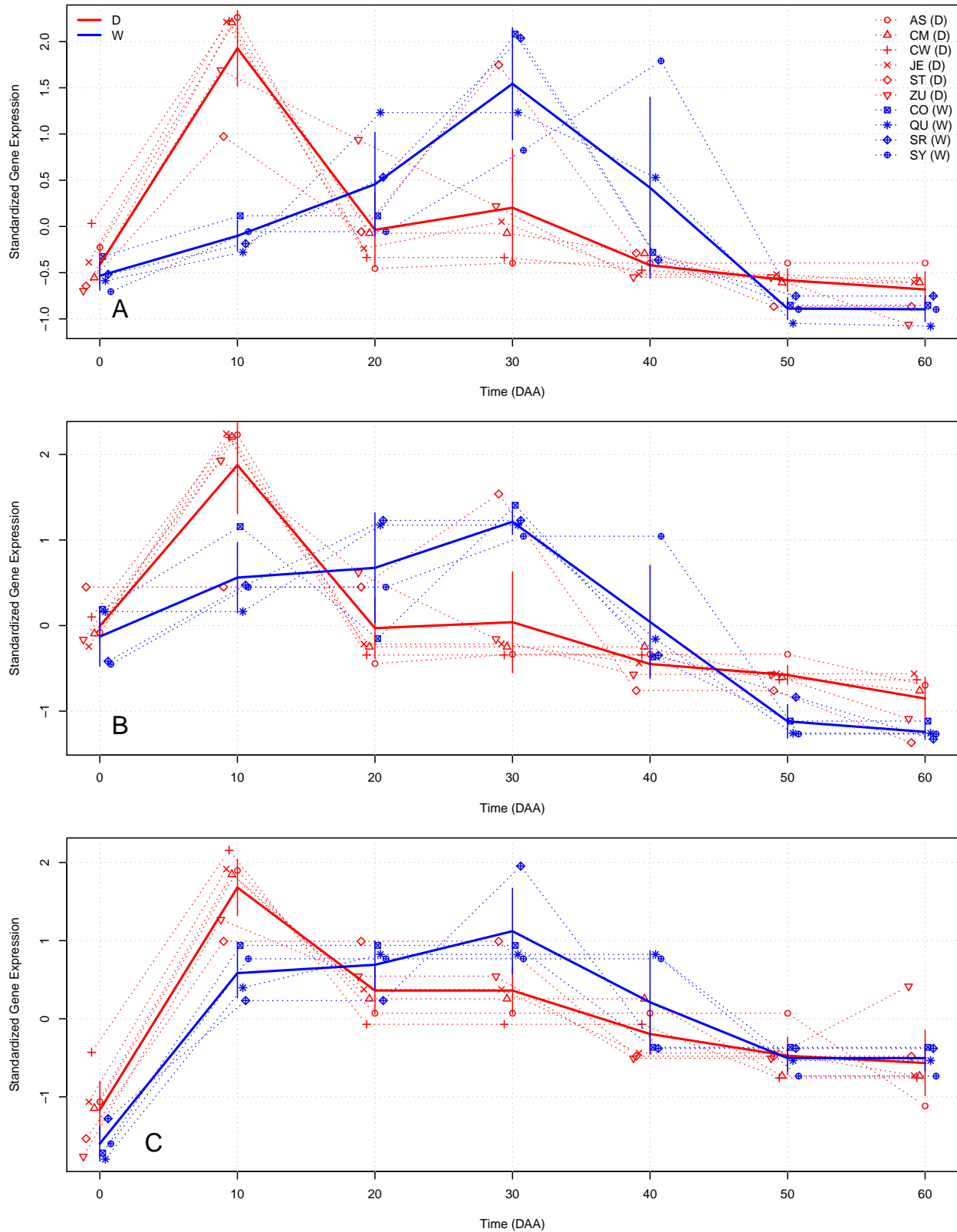


**FIGURE 13. Gene expression patterns for three genes having the D10W30 expression pattern in Domesticated (D) and Wild (W) accessions.** Dashed lines show the SEPs for each accession, and solid lines show mean SEPs per group (D and W). Vertical lines represent 95% CI for mean values at each time. Keys correspond to those shown in Table 1. (A) High mobility group B protein 6 (XP\_016555757.1); (B) MYB-related protein 3R-1 (XP\_016537977.1); (C) Kinetochores protein NDC80 (XP\_016539151.1).

also exhibit the D10W30 expression pattern. NDC80 is conspicuously present in 74 of the 86 enriched BPs (Figure 13 C).

#### S-5. GENE ONTOLOGY (GO) ENRICHMENT ANALYSES

After discovering that mean SEP in the D accessions was different to the one in the W group (Figure 1A in the main text), we confronted the problem of finding the functional meaning of that difference, and for this aim we employed Gene Ontology or ‘GO’ annotations (Ashburner et al., 2000). We isolated the set of genes with a more extreme difference, the  $n = 463$  genes with a False Discovery Rate,  $FDR = 0.05$  (Benjamini and Hochberg, 1995), presented in Figure 1B of the main text, and noticed that this group presented the pattern ‘D10W30’, where the maximum mean expression was at 10 DAA in D, while such maximum occurred at 30 DAA in W (Figure 1B in the main text). Furthermore, we found that a set of 542 genes presented SEPs with D10W30 patterns, and this set was one of the targets for GO enrichment analyses, employing the ‘Biological Process’ GO ontology and motivated by the results in (Lægneid et al., 2003).

To perform GO enrichment analyses we considered the total population of 22427 genes expressed during fruit development of which 12102 are annotated in one or more of the 2547 GO biological processes annotated in chili. We are interested in the property of a gene to belong to a specific GO category, with the aim to establish whether the class of genes with a specific expression pattern, e.g. genes with mean SEPs D10W30, presented an enrichment in the GO Biological Process of interest with respect to the total gene population. Among the different tests that could be used to test association between a target gene set and a functional GO Biological Process (Rivals et al., 2007), we selected the Fisher’s exact test.

We programed a function to summarize the results of the test, and employing different targets performed the analyses of the 2547 GO biological processes, evaluating the  $P$ -value of each result, and transforming it to a  $Q$ -value to have a FDR (Benjamini and Hochberg, 1995) of 5%. To take into account the structure of the GO ontology, which is fundamental to the analyses interpretation (Rhee et al., 2008), we performed a filtering of redundant and highly correlated biological process using a gene network approach.

As an example of the analyses performed, Appendix S-11.2 presents the R output for the ‘Cell Cycle’ biological process having as target the set of 542 genes with D10W30 patterns. In Appendix S-11.2 we can see the output of function ‘BP.analysis.ById’. This function gives the observed and expected  $2 \times 2$  contingency tables as well as the full results of Fisher’s exact test, making easier result’s interpretation.

Sheet ‘Bio Process’ in the excel file “SG.xlsx” of ‘Supplemental Information’ presents the full results of the analyses of the 2547 GO biological processes using as target the set of genes with pattern D10W30.

#### S-6. GENES AND BIO PROCESSES (BPs) REPORTED.

Excel file “SG.xlsx” in ‘Supplemental Information’ includes four sheets with the following results:

**Gene :** Data for the 22427 genes expressed during fruit development (in table “gene” of the SALSA database).

**Gene column definitions :** Column definitions for the “Gene” sheet.

**id:** Numerical identifier in the SALSA database.

**ProtId:** Protein identifier of the gene product (if known, otherwise NULL).

**Prot\_Desc:** Protein short description (if known, otherwise NULL).

**URL:** URL for UniProtKB database using Prot\_Desc (if known, otherwise NULL).

**isTF:** Is the gene product annotated as Transcription Factor? (T if True, F if False).



**D10W30:** Is the SEP of the gene of class ‘D10W30’ [see main text] (TRUE or FALSE).

**BioProc:** Is the gene product annotated in one or more GO Bio Processes (T if True, F if False).

**ZunlaDom:** Is the gene annotated with domestication footprint in Qin et al. (2014)? NULL if it is not annotated as such, otherwise the name of the gene reported by Qin et al. (2014) is given.

**P\_value:** P value for the test of differences of SEPs between domesticated (D) and wild (W) accessions. See main Methods and Supplemental SI-1.3.

**Q\_value:** P\_value transformed to Q\_value using R function `p.adjust()` with method = “fdr” to calculate False Discovery Rate (DFR).

**Gene.id:** Genomic identifier of the gene.

**chromosome:** Chromosome where the gene is located; “NULL” if unknown see “scaffold” below.

**scaffold:** scaffold Scaffold where the gene was located (If Chromosome “NULL”).

**Strand:** Strand coding for the gene (“+” or “-”)

**start:** Genomic coordinate where the gene starts.

**end:** Genomic coordinate where the gene ends.

**length:** Length of the gene in base pairs (bps).

**sequence:** Gene sequence.

**Bio Process :** Data for the 2547 Gene Ontology (GO) biological processes analyzed (in table “ResBioProcess” of the SALSA database).

**Bio Process column definitions :** Column definitions for the “Bio Process” sheet.

**BP.id:** Numerical identifier of the Biological Process in the SALSA database.

**bio.process:** Gene Ontology (GO) Biological Process.

**odds:** Estimated odds in the contingency table.

**P:** P-value of the Fisher’s exact test for the  $2 \times 2$  contingency table.

**AnnTarg:** Number of genes in the process which are annotated in the target.

**NotAnnTarg:** Number of genes in the process which are NOT annotated in the target.

**AnnNotTarg:** Number of genes in the process which are annotated but NOT in the target.

**NotAnnNotTarg:** Number of genes in the process which are NOT annotated and NOT in the target.

**Q:** P value transformed to Q value using R function `p.adjust()` with method = “fdr” to calculate False Discovery Rate (DFR).

Information in the “**Gene**” sheet was obtained from the data send by NovoGene after RNA-Seq sequencing and analyses and corresponds to the annotation in the reference genome [CM334 v1.6](#). On the other hand, information in the “**Bio Process**” sheet was the results of the GO enrichment analyses described here in section S-5.

S-7. NETWORK ESTIMATION

As mentioned in (Allocco et al., 2004),

*“It is axiomatic in functional genomics that genes with similar mRNA expression profiles are likely to be regulated via the same mechanisms. This hypothesis is the basis for almost all attempts to use mRNA expression data from microarray experiments to discover regulatory networks.”*

Ideally we would like to estimate a Gene Regulatory Network (GRN) for the whole chili transcriptome. That aim is practically impossible with the current incomplete knowledge of the interactions between genes in the *Capsicum* transcriptome. However, an attainable and relevant goal within the framework of our study is to estimate robust networks of functionally related genes, as the one presented in Figures 3 and 4 of the main text. Here we detail the method employed to obtain that network.

We have a total of 22,427 genes consistently expressed in all accessions, of which 352 are annotated in the BP ‘Cell Cycle’ and of these 25 belong to the class ‘D10W30’, i.e., these 25 genes present a maximum expression at 10 DAA in the 6 domesticated (D), while the maximum expression is at 30 DAA in the 4 wild (W) accessions. After examining the Euclidean distances between the SEPs of the 25 genes, we selected 6 of them which present a highly consistent SEPs in both, D and W expression. We selected the 6 structural genes presented in the network of Figure 3 and 4 of the main text (represented by orange circles in that figure) by setting a threshold of Euclidean distance  $\leq 1$  between pairs of gene SEPs. Table 2 presents the medians of the Pearson correlation ( $\hat{r}$ ) and  $P$  values for SEPs of the 6 Structural genes included in the network.

TABLE 2. Median Pearson Correlation ( $\hat{r}$ ) and  $P$  values for SEPs of the 6 Structural genes included in the network presented in Figures 3 and 4 of the main text.

|            |                 |          |          |
|------------|-----------------|----------|----------|
|            | Between D and W | Within D | Within W |
| $n$        | 144             | 90       | 36       |
| $\hat{r}$  | 0.37477         | 0.92227  | 0.77658  |
| $P$ -value | 0.40749         | 0.00310  | 0.04001  |
|            | Between         | Within   |          |
| $n$        | 144             | 126      |          |
| $\hat{r}$  | 0.37477         | 0.88496  |          |
| $P$ -value | 0.40749         | 0.00810  |          |

In Table 2 column ‘Between D and W’ presents cases where correlation was estimated for the same gene but taking one D and one W accession, thus correlations are between SEPs in D and W. The number of such pairs of different correlations equals  $6 \text{ D} \times 4 \text{ W} \times 6 \text{ genes}$ ,  $n = 6 \times 4 \times 6 = 144$ . On the other hand, columns ‘Within D’ and ‘Within W’ present cases where correlation was estimated for the same gene but taking different accessions within the same group (D or W, respectively). The number of possible comparisons are  $n = (6 \times (6 - 1))/2 \times 6 = 90$  for the column ‘Within D’ and  $n = (4 \times (4 - 1))/2 \times 6 = 36$  for the column ‘Within W’. In Table 2 we can see that the median of the correlations for SEPs within the D and W groups are high, 0.92227 and 0.77658 and significant ( $P$ -values of 0.00310 and 0.04001), respectively, while the median of the correlation for SEPs between the D and W groups was smaller, 0.37477, and not significant ( $P$ -value of 0.40749). Last rows of Table 2 groups columns ‘Within D’ and ‘Within W’ into a single column, ‘Within’, and from such grouping we obtain the same conclusion than above, i.e., the 6 structural genes have highly and significantly correlated SEPs within but not between accession groups.

Results in Table 2 refer to all possible pairs of the 6 structural genes. However, not all pairs of structural genes are linked (by double headed arrows) in the network of Figures 3 and 4; the genes considered as linked in the network present a value of  $\hat{r} > 0.96$  within D and W groups, with a  $P$ -value  $< 0.0001$ . In

contrast the same pairs of structural genes present a value of  $\hat{r} < 0.40$  between D and W groups, with a non-significant  $P$ -value  $> 0.5$ . Thus the network of structural genes presented in Figures 3 and 4 presents a set of cell cycle genes which are highly coordinated in time within the D and W groups, presenting the expression pattern D10W30.

To corroborate that the expression of the 14 genes included into the network are indeed very well segregated, we performed a Principal Component Analysis (PCA) of the  $14 \times 10 = 140$  7-dimensional SEPs, which tendency by group is presented in Figure 3 B in the main text. In the biplot shown in Figure 14 we see the expression of the 14 genes labeled by their accession of origin and with colors denoting the set of origin (D in red and W in blue), plot in the 2 dimensional space of the first 2 principal components, of which the first ( $Y$  axis) explains 57.7% and the second ( $X$  axis) explains 17.4% of the data variance, thus together the two first principal components explain 75.1% of the total variance. In this figure we can see that the first principal component efficiently segregates the data into two groups, D in the upper and W in the lower parts of the plot, with only a few outliers. Observing the eigenvectors (dark red arrows in the plot, labeled by the time DAA: 0, 10,  $\dots$ , 60) we see that the one at time 0 is almost horizontal, and thus have very small influence in the coordinates transformation. This makes sense, because at 0 DAA both groups (D and W) share the same level of expression, as shown in Figure 3 B in the main text. In contrast all the other 6 eigenvectors, corresponding to times 10, 20,  $\dots$ , 60 DAA, have a strong influence in the segregation of the D and W sets, as previously observed in Figure 3 B in the main text.

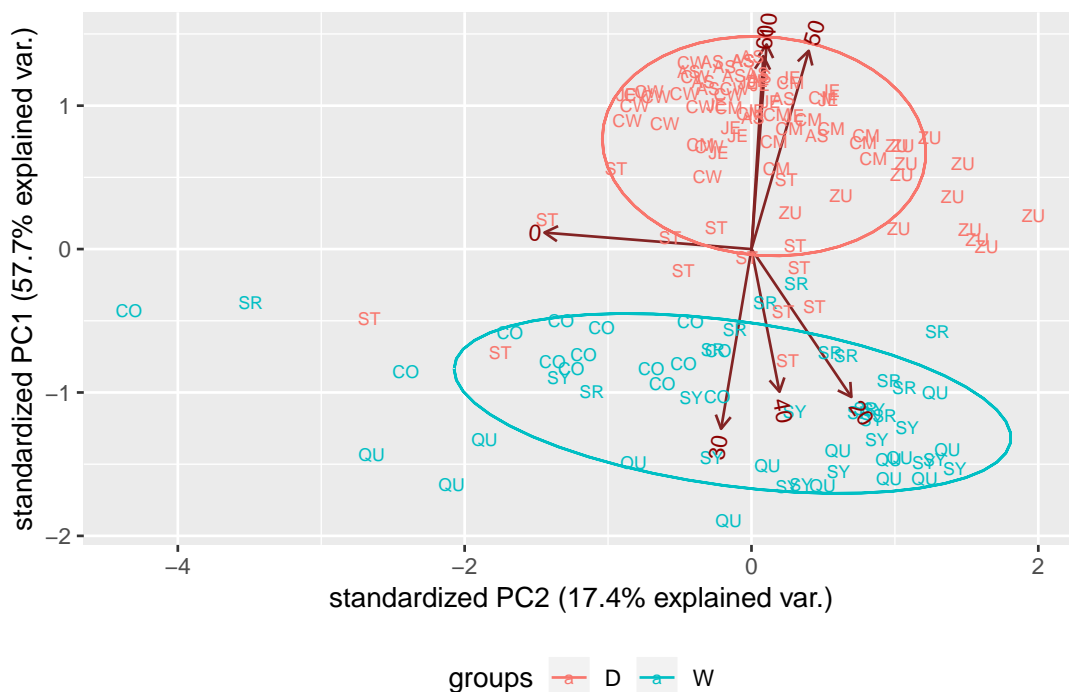


FIGURE 14. PCA analysis of the SEPs for the 14 genes in the network (Figure 2 B).

#### S-8. TRANSCRIPTION FACTOR (TF) IMPUTATION

The authors of Allocco et al. (2004) analyzed 611 microarrays and found that the correlation between expression profiles of two genes must be larger than  $r \approx 0.84$  to have a 50% chance of sharing a common transcription factor binder. Here we assume that a target gene and a TF which is regulating it will share very alike expression patterns (SEPs) and developed an statistical approach to select a set of candidate TFs. This approach was implemented in an R function which performs the following steps:

### Algorithm for TF imputation

- (1) Basic input: `id` - Identifier of the target gene; `min.r` - Threshold for the minimum correlation value,  $r > 0$ ; `min.r0m.a` - Threshold for the minimum ratio of  $r/ma$ , where  $ma$  is the maximum of the absolute difference between the SEPs of the target gene and the SEP of a TF; `acc.set` - The set of accessions where the search will be performed.
- (2) Obtains from the database all SEPs for all TFs in all accessions that belong to `acc.set`.
- (3) Obtains from the database all SEPs for target gene (`id`) in all accessions that belong to `acc.set`.
- (4) For each accession that belong to `acc.set` calculates the correlation,  $r$ , and  $r/ma$  between the SEPs of each TF and the target gene. Keeps only the cases where  $r \geq \text{min.r}$  AND  $r/ma \geq \text{min.r0m.a}$ .
- (5) Obtains a final list of candidate TFs by founding the intersection of all the sets of candidates in each one of the accessions defined int the input (`acc.set`).
- (6) Output the list of TFs candidates (if any) as well as variables to judge the adequacy of each TF candidate.

It is important to consider two facts about the above described method. Firstly, parameters  $r \geq \text{min.r}$  AND  $r/ma \geq \text{min.r0m.a}$  are selected in an ‘*per accession*’ base; i.e., they are compared only with the SEPs of the TFs in the same accession. Assume that a given target gene, `id`, is regulated by the same TF, say, `x`, but that target gene has very different expression pattern in two different accessions. If `id` is regulated by `x` in both accessions, the method will likely report `x` in both accessions at step (4), and thus `x` will be part of the final output in (6). Secondly, and more important, given that the data in all accessions are fully independent, the probability of reporting ‘erroneous’ or ‘spurious’ TFs decreases exponentially with the number of accessions taken into account. This is, if the probability of reporting a spurious TF in any of the  $k$  accessions is  $\varepsilon$ , then the probability that the procedure reports the same spurious transcription factor in  $k$  accessions is  $\varepsilon^k$ , e.g. if  $\varepsilon = 0.5$  and  $k = 6$  we have  $\varepsilon^k = 0.5^6 \approx 0.016$  and if  $k = 10$ ,  $\varepsilon^k = 0.5^{10} \approx 0.001$ , etc. Under the null hypothesis of no true correlation between two arbitrary SEPs, the true value of the correlation parameter,  $\rho$ , is uniformly distributed in the interval  $[-1, 1]$ , and if we restrict ourselves to positive values,  $\rho \geq 0$ , the parameter space is simply  $[0, 1]$ , and by setting a threshold `min.r` =  $1 - \varepsilon$  and employing  $k$  independent accessions in the determination we can effectively fix any desired error probability to be  $(1 - \varepsilon)^k$ . Furthermore, by additionally asking that  $r/ma \geq \text{min.r0m.a}$  we will filter cases where the correlation,  $r$ , is high but at the same time there is an outlier in one of the times, where the maximum of the absolute value,  $ma$ , is large. This additional filter adds stringency to the selection method.

After running the algorithm to estimate the TF candidates for each one of the structural genes, we found the 8 TFs which are shown in Figure 3 A as blue circles and in rows 7 to 14 in Table 2 of the main text. The algorithm was run with parameters `min.r` = 0.5, `min.r0m.a` = 0.9 with the full set of 10 accessions. The next box presents the summaries of auxiliar estimates that help to calculate the robustness of the TF candidates.

|          | <code>r</code> | <code>m.a</code> | <code>r0m.a</code> |
|----------|----------------|------------------|--------------------|
| Min.     | :0.8752        | Min. :0.0924     | Min. : 1.088       |
| 1st Qu.: | 0.9489         | 1st Qu.:0.1923   | 1st Qu.: 1.712     |
| Median   | :0.9807        | Median :0.3072   | Median : 3.211     |
| Mean     | :0.9682        | Mean :0.3747     | Mean : 3.749       |
| 3rd Qu.: | 0.9931         | 3rd Qu.:0.5388   | 3rd Qu.: 5.159     |
| Max.     | :0.9988        | Max. :0.8413     | Max. :10.805       |

The box above summarizes the results for the 8 TFs selected, which are potential regulator of 3 of the structural genes, as shown in Figure 3 A in the main text. The statistics shown are produced from the estimation of  $10 \times (4 + 4 + 1) = 90$  cases, that arise because each one of the 3 TFs was evaluated in 10

accessions, and two of them are potential regulators of 4 structural genes and one of them is potential regulator of 1 gene. By taking the mean of the 90  $r$  values, 0.9682, the realized error probability is estimated as  $(1 - \hat{\varepsilon})^k = (1 - 0.9682)^{10} = 0.0318^{10} \approx 1.06 \times 10^{-15}$ , a vanishing small quantity, thus we can be reasonably sure that the relations found between the structural genes and TFs are, at least for some of the cases, very likely to reflect either, direct or indirect regulation of structural genes by the TF candidates.

The algorithm presented in this section for TF imputation was applied in our data to nominate TF candidates for the AT3 gene, resulting in the selection of only two TF, precisely the ones that have been experimentally validated as regulators of AT3 (Arce-Rodríguez and Ochoa-Alejo, 2017; Zhu et al., 2019; Sun et al., 2019). The fact that our approach recovers experimentally validated TFs demonstrates that this approach retrieves strong TFs candidates.

## S-9. SUPPLEMENTARY DESCRIPTIONS AND WEB LINKS FOR GENES IN THE NETWORK

### Descriptions

Items in this list give a short description and references for genes in the network of Figures 3 A and 4 and Table 2 in the main text. In each case the *Capsicum* protein identifier from Table 3 is followed by the putative *Arabidopsis* ortholog between parenthesis. Order in this list is the same than the one presented in Table 2 of the main text as well as in the rows of tables 3 and 4 presented below.

- (1) XP\_016564755.1 (AT5G51600) 65-kDa microtubule-associated protein 3 (MAP65/ASE1). Members of the AtMAP65 family –to which AT5G51600 belongs, link membrane and microtubule dynamics during plant cytokinesis, the part of the cell division process during which the cytoplasm of a single cell divides into two daughter cells. It appears that these proteins are required to coordinate cytokinesis with the nuclear division cycle, and some MAP65 family members are known to be targets of cell cycle-regulated kinases (Steiner et al., 2016).
- (2) XP\_016538322.1 (AT2G44190) QWRF motif-containing protein 6 (DUF566). It has been demonstrated that ENDOSPERM DEFECTIVE1 (EDE1), a mutant of the AT2G44190 gene, is expressed in the endosperm and embryo of developing seeds, and its expression is tightly regulated during cell cycle progression (Pignocchi et al., 2009). Furthermore, the authors show that EDE1 protein accumulates in nuclear caps in premitotic cells, colocalizes along microtubules of the spindle and phragmoplast, and binds microtubules in vitro. The aforementioned paper concludes that this gene codes for a microtubule-associated protein (DUF566), essential for seed development in *Arabidopsis*.
- (3) XP\_016541615.1 (AT4G21270) Kinesin 3 isoform X3 (kinesin 1). The spindle is critical for chromosome segregation, and kinesins play crucial roles in spindle structure; in particular the *Arabidopsis* ATK1 gene (AT4G21270) is required for spindle morphogenesis in male meiosis (Chen et al., 2002). Even when XP\_016541615.1 is identified as kinesin 3 (row 3 in Table 3), it is more alike with the kinesin 1 of *Arabidopsis* (alignments obtained by blastx in Appendix S-11.1) and thus it is identified with AT4G21270 in Table 4.
- (4) XP\_016575449.1 (AT5G51600); see item (1) in this list and (Steiner et al., 2016).
- (5) XP\_016577799.1 (AT4G20900) Protein POLLENLESS 3 (TPR). Members of the tetratricopeptide repeat (TPR) superfamily had been found in cell cycle clusters during apple fruit development (Janssen et al., 2008) and it had been demonstrated that their expression is highly regulated in early developing that fruit (Soria-Guerra et al., 2011).
- (6) XP\_016548908.1 (AT3G44960) Shugoshin. Shugoshin protects the sister chromatid cohesion complex (cohesin) for proper chromosome segregation in mitosis, until kinetochores are properly captured by the spindle microtubules (Kitajima et al., 2006)

- (7) XP\_016568750.1 (AT5G42700) B3 domain protein (AP2/B3-like transcriptional factor family protein) The plant-specific B3 superfamily includes families, such as the auxin response factor (ARF) family and the LAV family, as well as less well understood families, such as RAV and REM. There are indications that the B3 domain evolved on the plant lineage before multicellularity (Swaminathan et al., 2008), and, for example, the over-expression of an *Arabidopsis* B3 TF, ABS2/NGAL1 leads to the loss of flower petals (Shao et al., 2012).
- (8) XP\_016555757.1 (AT4G11080) High mobility group B protein 6 (HMG). The high mobility group B protein 6, belongs to the HMG (high mobility group) box proteins, which is a group of chromosomal proteins that are involved in the regulation of DNA-dependent processes such as transcription, replication, recombination, and DNA repair (Johns, 2012).
- (9) XP\_016543946.1 (AT3G11520) G2/mitotic-specific cyclin S13-7 (CYCLIN B1;3) is a regulatory protein involved in mitosis and, importantly, it is first activated in the cytoplasm and that centrosomes may function as sites of integration for the proteins that trigger mitosis (Jackman et al., 2003).
- (10) XP\_016547461.1 (AT1G26760) B3 domain-containing protein (SET domain protein 35). AT1G26760 received high scores for plastids localization (Schwacke et al., 2007), and has been also reported in maintaining H3K4 methylation (Liu and Gong, 2011).
- (11) XP\_016575946.1 (AT5G58280) B3 domain-containing protein At5g58280; AP2/B3-like transcriptional factor family protein. This gene has been reported to be differentially expressed in the flower and seed in *Brassica rapa*, castor bean, cocoa, soybean, and maize (Peng and Weselake, 2013), with tissues of preferential expression of the orthologous B3 gene pairs in *Arabidopsis* and rice.
- (12) XP\_016574880.1 (AT1G34355) FHA domain-containing protein PS1; forkhead-associated (FHA) domain-containing protein. An insertional mutation of AT1G34355, the AtPS1 gene has been characterized and found to lead to the production of diploid pollen grains (d'Erfurth et al., 2008).
- (13) XP\_016537977.1 (AT4G32730) Myb-related protein 3R-1 (Homeodomain-like protein). In plants, this class of Myb proteins are believed to regulate the transcription of G2/M phase-specific genes; in particular MYB3R1 act as transcriptional activator and positively regulate cytokinesis. In addition, MYB3R1 may play an important role during fruit development by regulating G2/M-specific genes (Haga et al., 2011).
- (14) XP\_016565918.1 (AT3G22780). Protein tesmin/TSO1 CXC 3; Tesmin/TSO1-like CXC domain-containing protein. TSO1 is a protein that modulates cytokinesis and cell expansion in *Arabidopsis* (Hauser et al., 2000).

TABLE 3. NCBI links and descriptions of genes in Figure 3 A and Table 2 in the main text.

| Row | id    | Prot. Id (link)                | Short Protein Description                            |
|-----|-------|--------------------------------|--|
| 1   | 673   | <a href="#">XP_016564755.1</a> | 65-kDa microtubule-associated protein 3              |
| 2   | 6090  | <a href="#">XP_016538322.1</a> | QWRF motif-containing protein 6                      |
| 3   | 15446 | <a href="#">XP_016541615.1</a> | kinesin 3 isoform X3                                 |
| 4   | 19658 | <a href="#">XP_016575449.1</a> | 65-kDa microtubule-associated protein 3 isoform X1   |
| 5   | 19813 | <a href="#">XP_016577799.1</a> | protein POLLENLESS 3                                 |
| 6   | 24546 | <a href="#">XP_016548908.1</a> | shugoshin-1; meiotic chromosome segregation          |
| 7   | 19147 | <a href="#">XP_016568750.1</a> | B3 domain Prot. At5g42700                            |
| 8   | 24186 | <a href="#">XP_016555757.1</a> | high mobility group B protein 6                      |
| 9   | 35149 | <a href="#">XP_016543946.1</a> | G2/mitotic-specific cyclin S13-7                     |
| 10  | 5824  | <a href="#">XP_016547461.1</a> | SET domain; methyltransferase activity; LOC107847605 |
| 11  | 11410 | <a href="#">XP_016575946.1</a> | B3 domain-containing protein At5g58280               |
| 12  | 12656 | <a href="#">XP_016574880.1</a> | FHA domain-containing protein PS1                    |
| 13  | 13605 | <a href="#">XP_016537977.1</a> | Myb-related protein 3R-1                             |
| 14  | 7175  | <a href="#">XP_016565918.1</a> | protein tesmin/TSO1 CXC 3                            |

TABLE 4. Putative *Arabidopsis* orthologous of genes in Figure 3 A and Table 2 in the main text.

| Row | id    | NCBI id                        | TAIR id                   | Short Protein Description.                          |
|-----|-------|--------------------------------|---------------------------|---|
| 1   | 673   | <a href="#">NP_199973.1</a>    | <a href="#">AT5G51600</a> | Microtubule associated protein (MAP65/ASE1).        |
| 2   | 6090  | <a href="#">NP_181947.1</a>    | <a href="#">AT2G44190</a> | ENDOSPERM DEFECTIVE protein (DUF566).               |
| 3   | 15446 | <a href="#">NP_193859.1</a>    | <a href="#">AT4G21270</a> | Kinesin 1   |
| 4   | 19658 | <a href="#">NP_199973.1</a>    | <a href="#">AT5G51600</a> | Microtubule associated protein (MAP65/ASE1).        |
| 5   | 19813 | <a href="#">NP_001328331.1</a> | <a href="#">AT4G20900</a> | Tetratricopeptide repeat (TPR)-like superfamily.    |
| 6   | 24546 | <a href="#">NP_001319686.1</a> | <a href="#">AT3G44960</a> | Shugoshin   |
| 7   | 19147 | <a href="#">NP_001318733.1</a> | <a href="#">AT5G42700</a> | AP2/B3-like transcriptional factor family protein   |
| 8   | 24186 | <a href="#">NP_192846.1</a>    | <a href="#">AT4G11080</a> | HMG (high mobility group) box protein               |
| 9   | 35149 | <a href="#">NP_187759.2</a>    | <a href="#">AT3G11520</a> | CYCLIN B1;3   |
| 10  | 5824  | <a href="#">NP_173998.2</a>    | <a href="#">AT1G26760</a> | SET domain protein 35                               |
| 11  | 11410 | <a href="#">NP_001330080.1</a> | <a href="#">AT5G58280</a> | AP2/B3-like transcriptional factor family protein   |
| 12  | 12656 | <a href="#">NP_001320842.1</a> | <a href="#">AT1G34355</a> | forkhead-associated (FHA) domain-containing protein |
| 13  | 13605 | <a href="#">NP_001328944.1</a> | <a href="#">AT4G32730</a> | Homeodomain-like protein                            |
| 14  | 7175  | <a href="#">NP_566718.2</a>    | <a href="#">AT3G22780</a> | Tesmin/TSO1-like CXC domain-containing protein      |

REFERENCES

- Abdi H (2007) Bonferroni and šidák corrections for multiple comparisons. *Encyclopedia of measurement and statistics*, 3, 103–107.
- Allocco DJ, Kohane IS, and Butte AJ (2004) Quantifying the relationship between co-expression, co-regulation and gene function. *BMC bioinformatics*, 5, 1–10.
- Arce-Rodríguez ML and Ochoa-Alejo N (2017) An r2r3-myb transcription factor regulates capsaicinoid biosynthesis. *Plant physiology*, 174, 1359–1370.
- Ashburner M, Ball CA, Blake JA, Botstein D, Butler H, Cherry JM, Davis AP, Dolinski K, Dwight SS, Eppig JT, et al. (2000) Gene ontology: tool for the unification of biology. *Nature genetics*, 25, 25–29.
- Benjamini Y and Hochberg Y (1995) Controlling the false discovery rate: a practical and powerful approach to multiple testing. *Journal of the royal statistical society. Series B (Methodological)*, pp. 289–300.
- Bland M (2013) Do baseline P-values follow a uniform distribution in randomised trials? *PloS one*, 8, e76010.
- Chen C, Marcus A, Li W, Hu Y, Calzada JPV, Grossniklaus U, Cyr RJ, and Ma H (2002) The arabidopsis atk1 gene is required for spindle morphogenesis in male meiosis. *Development*, 129, 2401–2409.
- D’Archivio S and Wickstead B (2017) Trypanosome outer kinetochore proteins suggest conservation of chromosome segregation machinery across eukaryotes. *Journal of Cell Biology*, 216, 379–391.
- d’Erfurth I, Jolivet S, Froger N, Catrice O, Novatchkova M, Simon M, Jenczewski E, and Mercier R (2008) Mutations in atps1 (arabidopsis thaliana parallel spindle 1) lead to the production of diploid pollen grains. *PLoS Genet*, 4, e1000274.
- Haga N, Kobayashi K, Suzuki T, Maeo K, Kubo M, Ohtani M, Mitsuda N, Demura T, Nakamura K, Jürgens G, et al. (2011) Mutations in myb3r1 and myb3r4 cause pleiotropic developmental defects and preferential down-regulation of multiple g2/m-specific genes in arabidopsis. *Plant Physiology*, 157, 706–717.
- Hauser BA, He JQ, Park SO, and Gasser CS (2000) Tso1 is a novel protein that modulates cytokinesis and cell expansion in arabidopsis. *Development*, 127, 2219–2226.
- Iglesias-Martinez LF, Kolch W, and Santra T (2016) Bgrmi: A method for inferring gene regulatory networks from time-course gene expression data and its application in breast cancer research. *Scientific Reports*, 6.
- Jackman M, Lindon C, Nigg EA, and Pines J (2003) Active cyclin b1-cdk1 first appears on centrosomes in prophase. *Nature cell biology*, 5, 143–148.
- Janssen BJ, Thodey K, Schaffer RJ, Alba R, Balakrishnan L, Bishop R, Bowen JH, Crowhurst RN, Gleave AP, Ledger S, et al. (2008) Global gene expression analysis of apple fruit development from the floral bud to ripe fruit. *BMC Plant Biology*, 8, 16.
- Johns E (2012) *The Chromosomal Proteins*. Elsevier.
- Kitajima TS, Sakuno T, Ishiguro Ki, Iemura Si, Natsume T, Kawashima SA, and Watanabe Y (2006) Shugoshin collaborates with protein phosphatase 2a to protect cohesin. *Nature*, 441, 46–52.
- Læg Reid A, Hvidsten TR, Midelfart H, Komorowski J, and Sandvik AK (2003) Predicting gene ontology biological process from temporal gene expression patterns. *Genome research*, 13, 965–979.
- Liu Q and Gong Z (2011) The coupling of epigenome replication with dna replication. *Current opinion in plant biology*, 14, 187–194.



- Luan Y and Li H (2003) Clustering of time-course gene expression data using a mixed-effects model with b-splines. *Bioinformatics*, 19, 474–482.
- Martínez-López LA, Ochoa-Alejo N, and Martínez O (2014) Dynamics of the chili pepper transcriptome during fruit development. *BMC genomics*, 15, 143.
- Mortazavi A, Williams BA, McCue K, Schaeffer L, and Wold B (2008) Mapping and quantifying mammalian transcriptomes by rna-seq. *Nature methods*, 5, 621.
- Peng FY and Weselake RJ (2013) Genome-wide identification and analysis of the b3 superfamily of transcription factors in brassicaceae and major crop plants. *Theoretical and Applied Genetics*, 126, 1305–1319.
- Peng RD (2011) Reproducible research in computational science. *Science*, 334, 1226–1227.
- Pignocchi C, Minns GE, Nesi N, Koumproglou R, Kitsios G, Benning C, Lloyd CW, Doonan JH, and Hills MJ (2009) Endosperm defective1 is a novel microtubule-associated protein essential for seed development in arabidopsis. *The Plant Cell*, 21, 90–105.
- Qin C, Yu C, Shen Y, Fang X, Chen L, Min J, Cheng J, Zhao S, Xu M, Luo Y, et al. (2014) Whole-genome sequencing of cultivated and wild peppers provides insights into capsicum domestication and specialization. *Proceedings of the National Academy of Sciences*, 111, 5135–5140.
- R Core Team (2013) *R: A language and environment for statistical computing*. R Foundation for Statistical Computing, Vienna, Austria. URL <http://www.r-project.org>.
- Rhee SY, Wood V, Dolinski K, and Draghici S (2008) Use and misuse of the gene ontology annotations. *Nature Reviews Genetics*, 9, 509.
- Rivals I, Personnaz L, Taing L, and Potier MC (2007) Enrichment or depletion of a go category within a class of genes: which test? *Bioinformatics*, 23, 401–407.
- Robinson MD, McCarthy DJ, and Smyth GK (2010) edgeR: a bioconductor package for differential expression analysis of digital gene expression data. *Bioinformatics*, 26, 139–140.
- Santaguida S and Musacchio A (2009) The life and miracles of kinetochores. *The EMBO journal*, 28, 2511–2531.
- Schwacke R, Fischer K, Ketelsen B, Krupinska K, and Krause K (2007) Comparative survey of plastid and mitochondrial targeting properties of transcription factors in arabidopsis and rice. *Molecular Genetics and Genomics*, 277, 631–646.
- Shao J, Liu X, Wang R, Zhang G, and Yu F (2012) The over-expression of an arabidopsis b3 transcription factor, *abs2/ngal1*, leads to the loss of flower petals. *PloS one*, 7, e49861.
- Singh DK and McNellis TW (2011) Fibrillin protein function: the tip of the iceberg? *Trends in plant science*, 16, 432–441.
- Soria-Guerra RE, Rosales-Mendoza S, Gasic K, Wisniewski ME, Band M, and Korban SS (2011) Gene expression is highly regulated in early developing fruit of apple. *Plant Molecular Biology Reporter*, 29, 885.
- Steiner A, Rybak K, Altmann M, McFarlane HE, Klaeger S, Nguyen N, Facher E, Ivakov A, Wanner G, Kuster B, et al. (2016) Cell cycle-regulated pleiade/at map 65-3 links membrane and microtubule dynamics during plant cytokinesis. *The Plant Journal*, 88, 531–541.
- Sun B, Zhu Z, Chen C, Chen G, Cao B, Chen C, and Lei J (2019) Jasmonate-inducible r2r3-myb transcription factor regulates capsaicinoid biosynthesis and stamen development in capsicum. *Journal of agricultural and food chemistry*, 67, 10891–10903.

Swaminathan K, Peterson K, and Jack T (2008) The plant b3 superfamily. *Trends in plant science*, 13, 647–655.

Wang Z, Gerstein M, and Snyder M (2009) RNA-Seq: a revolutionary tool for transcriptomics. *Nature reviews genetics*, 10, 57–63.

Zhu Z, Sun B, Cai W, Zhou X, Mao Y, Chen C, Wei J, Cao B, Chen C, Chen G, et al. (2019) Natural variations in the myb transcription factor myb31 determine the evolution of extremely pungent peppers. *New Phytologist*, 223, 922–938.

#### S-10. APPENDIX (R OUTPUT)

S-11. ANALYSES OF GENE WITH ID=580 (FBN); SEE FIGURE 8 WHICH PRESENTS THE PLOT OBTAINED WITH THE FUNCTION.

---

```
> TMmean.plot(580)
```

```
Means of 10 TMs in 6 D and 4 W accessions
(1 different genes)
```

```
Function call: TMmean.plot 580
```

```
alpha = 0.05 All Confidence Intervals (CI) at 95%.
```

```
Means and CI for Standardized expression per time in D
```

|      | ne.0  | ne.10 | ne.20 | ne.30 | ne.40 | ne.50 | ne.60 |
|------|-------|-------|-------|-------|-------|-------|-------|
| Mean | -0.53 | -0.62 | -0.53 | -0.52 | -0.37 | 0.76  | 1.81  |
| LL   | -0.62 | -0.71 | -0.65 | -0.60 | -0.49 | 0.08  | 1.52  |
| UL   | -0.44 | -0.54 | -0.41 | -0.44 | -0.25 | 1.44  | 2.11  |

```
Means and CI for Standardized expression per time in W
```

|      | ne.0  | ne.10 | ne.20 | ne.30 | ne.40 | ne.50 | ne.60 |
|------|-------|-------|-------|-------|-------|-------|-------|
| Mean | -0.63 | -0.62 | -0.59 | -0.57 | -0.40 | 1.01  | 1.79  |
| LL   | -0.70 | -0.68 | -0.62 | -0.64 | -0.41 | 0.64  | 1.54  |
| UL   | -0.56 | -0.55 | -0.56 | -0.49 | -0.38 | 1.37  | 2.05  |

```
P-values for the t-test of means D vs W per time point:
```

|  | ne.0   | ne.10  | ne.20  | ne.30  | ne.40  | ne.50  | ne.60  |
|--|--------|--------|--------|--------|--------|--------|--------|
|  | 0.1196 | 0.9104 | 0.4017 | 0.4331 | 0.6729 | 0.5471 | 0.9198 |

```
Summary of those P-values:
```

|  | Min.   | 1st Qu. | Median | Mean   | 3rd Qu. | Max.   |
|--|--------|---------|--------|--------|---------|--------|
|  | 0.1196 | 0.4174  | 0.5471 | 0.5721 | 0.7917  | 0.9198 |

```
Estimation of the point in time (DAA)
of maximum Standardized expression in D
```

|  | LCL   | mean  | UCL   |
|--|-------|-------|-------|
|  | 52.53 | 56.67 | 60.80 |

```
Estimation of the point in time (DAA)
```

of maximum Standardized expression in W

LCL mean UCL  
52.6 57.5 62.4

Estimated difference between maxima in D and W: -0.83 DAA

(Genes are Early in D but the difference is NOT significant at 0.05)

T-test for the difference of maxima expression between D and W

Welch Two Sample t-test

data: D.max.perTM and W.max.perTM

t = -0.25482, df = 6.739, p-value = 0.8065

alternative hypothesis: true difference in means is not equal to 0

95 percent confidence interval:

-8.627334 6.960667

sample estimates:

mean of x mean of y

56.66667 57.50000

-----  
**S-11.1. Analyses of gene with id= 19147 (B3 domain-containing protein); see Figure 10 which presents the plot obtained with the function.**

-----  
> TMmean.plot(19147)

Means of 10 TMs in 6 D and 4 W accessions  
(1 different genes)

Function call: TMmean.plot 19147

alpha = 0.05 All Confidence Intervals (CI) at 95%.

Means and CI for Standardized expression per time in D

|      | ne.0  | ne.10 | ne.20 | ne.30 | ne.40 | ne.50 | ne.60 |
|------|-------|-------|-------|-------|-------|-------|-------|
| Mean | -0.35 | 2.14  | -0.24 | -0.06 | -0.46 | -0.48 | -0.54 |
| LL   | -0.52 | 1.95  | -0.48 | -0.56 | -0.54 | -0.55 | -0.63 |
| UL   | -0.19 | 2.32  | 0.00  | 0.45  | -0.38 | -0.41 | -0.45 |

Means and CI for Standardized expression per time in W

|      | ne.0  | ne.10 | ne.20 | ne.30 | ne.40 | ne.50 | ne.60 |
|------|-------|-------|-------|-------|-------|-------|-------|
| Mean | -0.43 | 0.25  | 0.3   | 1.73  | 0.08  | -0.96 | -0.97 |
| LL   | -0.71 | -0.15 | -0.4  | 1.38  | -0.27 | -1.09 | -1.11 |
| UL   | -0.14 | 0.65  | 1.0   | 2.08  | 0.43  | -0.83 | -0.84 |

P-values for the t-test of means D vs W per time point:

|  | ne.0   | ne.10  | ne.20  | ne.30  | ne.40  | ne.50  | ne.60  |
|--|--------|--------|--------|--------|--------|--------|--------|
|  | 0.6861 | 0.0008 | 0.2311 | 0.0005 | 0.0535 | 0.0016 | 0.0026 |

Summary of those P-values:

| Min.      | 1st Qu.   | Median    | Mean      | 3rd Qu.   | Max.      |
|-----------|-----------|-----------|-----------|-----------|-----------|
| 0.0004559 | 0.0012052 | 0.0025650 | 0.1394492 | 0.1423184 | 0.6860762 |

Estimation of the point in time (DAA)  
of maximum Standardized expression in D

| LCL mean | UCL |
|----------|-----|
| 10       | 10  |

Estimation of the point in time (DAA)  
of maximum Standardized expression in W

| LCL mean | UCL  |
|----------|------|
| 22.6     | 27.5 |

Estimated difference between maxima in D and W: -17.5 DAA

(Genes are Early in D )

Note: maxima in D and W are uniform  
(thus no t-test was possible)

---

S-11.2. Analyses of GO biological process “Cell Cycle” having as target the D10W30 set of genes.

---

```
# Running function 'BP.analysis.ById' and printing results
> BP.analysis.ById(D10W30.ids, BP.id=207)
Number of ids in target: 542
In accessions: All
Biological Process: cell cycle
```

Observed matrix:

|         | Target | NotTarget |
|---------|--------|-----------|
| Annot   | 25     | 327       |
| NoAnnot | 282    | 11444     |

Rounded expected values:

|         | Target | NotTarget |
|---------|--------|-----------|
| Annot   | 8.95   | 343.05    |
| NoAnnot | 298.05 | 11427.95  |

Estimated odds ratio from the table:

3.102566

Fisher's Exact Test for Count Data

data: temp.t

p-value = 3.513e-06

alternative hypothesis: true odds ratio is not equal to 1

95 percent confidence interval:

1.944868 4.758091

sample estimates:

odds ratio

3.102053

```
# Running function 'BP.analysis.ById' without printing results
```

```
# (for further analysis of groups of biological processes)
```

```
> temp <- BP.analysis.ById(D10W30.ids, BP.id=207, print.all=FALSE)
```

```
> temp
```

|   | Acc | BP.id | bio.process   | odds     | P            | AnnTarg | NotAnnTarg | AnnNotTarg |
|---|-----|-------|---------------|----------|--------------|---------|------------|------------|
| 1 | All | 207   | cell cycle    | 3.102566 | 3.512919e-06 | 25      | 282        | 327        |
|   |     |       | NotAnnNotTarg |          |              |         |            |            |
| 1 |     |       | 11444         |          |              |         |            |            |

-----

## Parsed Citations

Albert, F.W., Somel, M., Carneiro, M., Aximu-Petri, A., Halbwax, M., Thalmann, O., Blanco-Aguiar, J.A., Plyus-Nina, I.Z., Trut, L., Villafuerte, R., et al. (2012). A comparison of brain gene expression levels in domesticated and wild animals. *PLoS Genet.* 8(9):e1002962. <https://doi.org/10.1371/journal.pgen.1002962>.

Google Scholar: [Author Only](#) [Title Only](#) [Author and Title](#)

Albert, V.A., and Chang, T.H. (2014). Evolution of a hot genome. *Proc. Natl. Acad. Sci. USA* 111: 5069–5070. <https://doi.org/10.1073/pnas.1402378111>.

Google Scholar: [Author Only](#) [Title Only](#) [Author and Title](#)

Allocco, D.J., Kohane, I.S. and Butte, A.J. (2004). Quantifying the relationship between co-expression, co-regulation and gene function. *BMC Bioinformatics.* 5: 1-10. <https://doi.org/10.1186/1471-2105-5-18>.

Google Scholar: [Author Only](#) [Title Only](#) [Author and Title](#)

Ahn, Y.K., Karna, S., Jun, T.H., Yang, E.Y., Lee, H.E., Kim, J.H., and Kim, J.H. (2016). Complete genome sequencing and analysis of *Capsicum annuum* varieties. *Mol. Breed.* 36: 140. <https://doi.org/10.1007/s11032-016-0557-9>.

Google Scholar: [Author Only](#) [Title Only](#) [Author and Title](#)

Arce-Rodríguez, M.L., and Ochoa-Alejo, N. (2017). An R2R3-MYB transcription factor regulates capsaicinoid biosynthesis. *Plant Physiol.* 174: 1359–1370. <https://doi.org/10.1104/pp.17.00506>.

Google Scholar: [Author Only](#) [Title Only](#) [Author and Title](#)

Ariizumi, T., Shinozaki, Y., and Ezura, H. (2013). Genes that influence yield in tomato. *Breed. Sci.* 63: 3–13. <https://doi.org/10.1270/jsbbs.63.3>.

Google Scholar: [Author Only](#) [Title Only](#) [Author and Title](#)

Azzi, L., Deluche, C., Gévaudant, F., Frangne, N., Delmas, F., Hernould, M., and Chevalier, C. (2015). Fruit growth-related genes in tomato. *J. Exp. Bot.* 66: 1075–1086. <https://doi.org/10.1093/jxb/eru527>.

Google Scholar: [Author Only](#) [Title Only](#) [Author and Title](#)

Badia, A.D., Spina, A.A., and Vassalotti, G. (2017). *Capsicum annuum* L.: An overview of biological activities and potential nutraceutical properties in humans and animals. *J. Nutr. Ecol. Food Res.* 4: 167–177. <https://doi.org/10.1166/jnef.2017.1163>.

Google Scholar: [Author Only](#) [Title Only](#) [Author and Title](#)

Bellucci, E., Bitocchi, E., Ferrarini, A., Benazzo, A., Biagetti, E., Klie, S., Minio, A., Rau, D., Rodriguez, M., Panziera, A., et al. (2014). Decreased nucleotide and expression diversity and modified coexpression patterns characterize domestication in the common bean. *Plant Cell* 26: 1901–1912. <https://doi.org/10.1105/tpc.114.124040>.

Google Scholar: [Author Only](#) [Title Only](#) [Author and Title](#)

Benjamini Y and Hochberg Y (1995) Controlling the false discovery rate: a practical and powerful approach to multiple testing. *Journal of the Royal Statistical Society. Series B (Methodological)* 57: 289–300. <https://doi.org/10.1111/j.2517-6161.1995.tb02031.x>.

Google Scholar: [Author Only](#) [Title Only](#) [Author and Title](#)

Bourdon, M., Frangne, N., Mathieu-Rivet, E., Nafati, M., Cheniclet, C., Renaudin, J.P., and Chevalier, C. (2010). Endoreduplication and growth of fleshy fruits. In Lüttge U., Beyschlag W., Büdel B., and Francis D. (Eds.). *Progress in Botany 71. Progress in Botany (Genetics - Physiology - Systematics - Ecology)*, vol 71. Springer, Berlin, Heidelberg. Pp. 101–132. [https://doi.org/10.1007/978-3-642-02167-1\\_4](https://doi.org/10.1007/978-3-642-02167-1_4).

Google Scholar: [Author Only](#) [Title Only](#) [Author and Title](#)

Buschmann, H., Fabri, C.O., Hauptmann, M., Hutzler, P., Laux, T., Lloyd, C.W., and Schöffner, A.R. (2004). Helical growth of the *Arabidopsis* mutant *torifolia1* reveals a plant-specific microtubule-associated protein. *Curr. Biol.* 14: 1515–1521. <https://doi.org/10.1016/j.cub.2004.08.033>.

Google Scholar: [Author Only](#) [Title Only](#) [Author and Title](#)

Carvalho, S.I., Ragassi, C.F., Bianchetti, L. B., Faleiro, F.G., and Cerrados, E. (2014). Morphological and genetic relationships between wild and domesticated forms of peppers (*Capsicum frutescens* L. and *C. chinense* Jacquin ). *Genet. Mol. Res.* 13: 7447–7464. <https://doi.org/10.4238/2014>.

Google Scholar: [Author Only](#) [Title Only](#) [Author and Title](#)

Cervantes-Hernández, F.; Alcalá-González, P.; Martínez, O.; Ordaz-Ortiz, J.J. (2019). Placenta, pericarp, and seeds of Tabasco chili pepper fruits show a contrasting diversity of bioactive metabolites. *Metabolites* 9, 206. <https://doi.org/10.3390/metabo9100206>.

Google Scholar: [Author Only](#) [Title Only](#) [Author and Title](#)

Chapman, M.A., Pashley, C.H., Wenzler, J., Hvala, J., Tang, S., Knapp, S.J., and Burke, J.M. (2008). A genomic scan for selection reveals candidates for genes involved in the evolution of cultivated sunflower (*Helianthus annuus*). *Plant Cell* 20: 2931–2945. <https://doi.org/10.1105/tpc.108.059808>.

Google Scholar: [Author Only](#) [Title Only](#) [Author and Title](#)

Chaudhary, B., Hovav, R., Rapp, R., Verma, N., Udall, J.A., and Wendel, J.F. (2008). Global analysis of gene expression in cotton fibers from wild and domesticated *Gossypium barbadense*. *Evol. & Develop.* 10: 567–582. <https://doi.org/10.1111/j.1525-142X.2008.00272.x>.

Google Scholar: [Author Only](#) [Title Only](#) [Author and Title](#)

Chen, C., Marcus, A., Li, W., Hu, Y., Calzada, J.Ph.V., Grossniklaus, U., Cyr, R.J., and Ma, H. (2002). The Arabidopsis ATK1 gene is required for spindle morphogenesis in male meiosis. *Development* 129: 2401-2409.

Google Scholar: [Author Only Title Only Author and Title](#)

Chevalier, C. (2018). Cell cycle control and fruit development. *Annual Plant Reviews book series*, chapter 12. 32: 269-293. <https://doi.org/10.1002/9781119312994.apr0343>.

Google Scholar: [Author Only Title Only Author and Title](#)

Christie, M.R., Marine, M.L., Fox, S.E., French, R.A., and Blouin, M.S. (2016). A single generation of domestication heritably alters the expression of hundreds of genes. *Nature Comm.* 7: 1–6. <https://doi.org/10.1038/ncomms10676>.

Google Scholar: [Author Only Title Only Author and Title](#)

Cifuentes, M., Jolivet, S., Cromer, L., Harashima, H., Bulankova, P., Renne, C., Crismani, W., Nomura, Y., Nakagami, H., Sugimoto, K. and others (2016). TDM1 regulation determines the number of meiotic divisions. *PLoS Genetics* 12: e1005856. doi:10.1371/journal.pgen.1005856.

Google Scholar: [Author Only Title Only Author and Title](#)

D'Archivio, S., and Wickstead B. (2017). Trypanosome outer kinetochore proteins suggest conservation of chromosome segregation machinery across eukaryotes. *J. Cell Biol.* 216: 379–391. <https://doi.org/10.1083/jcb.201608043>.

Google Scholar: [Author Only Title Only Author and Title](#)

Dai, Q., Geng, L., Lu, M., Jin, W., Nan, X., He, Pa., and Yao, Y. (2017). Comparative transcriptome analysis of the different tissues between the cultivated and wild tomato. *PLoS One* 12:e0172411. <https://doi.org/10.1371/journal.pone.0172411>.

Google Scholar: [Author Only Title Only Author and Title](#)

Darwin, C. (1868). *The variation of animals and plants under domestication*. Cambridge University Press, New York. 486 pp.

Google Scholar: [Author Only Title Only Author and Title](#)

Doebley, JF., Stec, A., Wendel, J., and Edwards, M. (1990). Genetic and morphological analysis of a maize-teosinte F2 population: implications for the origin of maize. *Proc. Natl. Acad. Sci. USA* 87: 9888–9892. <https://doi.org/10.1073/pnas.87.24.9888>.

Google Scholar: [Author Only Title Only Author and Title](#)

Doebley, JF., Gaut, BS., and Smith, BD. (2006). The molecular genetics of crop domestication. *Cell*. 127: 1309-1321. <https://doi.org/10.1016/j.cell.2006.12.006>.

Google Scholar: [Author Only Title Only Author and Title](#)

Fayos, O., Ochoa-Alejo, N., Martínez O., Savirón, M., Orduna, J., Mallor, C., Barbero, G.F., and Garcés-Claver, A (2019). Assessment of capsaicinoid and capsinoid accumulation patterns during fruit development in three chili pepper genotypes (*Capsicum* spp.) carrying *pun1* and *part* alleles related to pungency. *J. Agric. Food Chem.* 67: 12219–12227. <https://doi.org/10.1021/acs.jafc.9b05332>.

Google Scholar: [Author Only Title Only Author and Title](#)

Filkov, V. (2005). Identifying gene regulatory networks from gene expression data In: *Handbook of computational molecular biology*. 1st Ed. Chapman & Hall/CRC Press. Boca Raton. Pp. 101-132.

Google Scholar: [Author Only Title Only Author and Title](#)

Giovannoni, J.J. (2004). Genetic regulation of fruit development and ripening. *Plant Cell* 16: S170–S180. <https://doi.org/10.1105/tpc.019158>.

Google Scholar: [Author Only Title Only Author and Title](#)

Gómez-García, M.R., and Ochoa-Alejo N. (2013). Biochemistry and molecular biology of carotenoid biosynthesis in chili peppers (*Capsicum* spp.). *Int. J. Mol. Sci.* 14: 19025–19053. <https://doi.org/10.3390/ijms140919025>.

Google Scholar: [Author Only Title Only Author and Title](#)

Gómez-García, M.R., and Ochoa-Alejo, N. (2016). Predominant role of the L-galactose pathway in l-ascorbic acid biosynthesis in fruits and leaves of the *Capsicum annum* L. chili pepper. *Brazilian J. Bot.* 39: 157–168. <https://doi.org/10.1007/s40415-015-0232-0>.

Google Scholar: [Author Only Title Only Author and Title](#)

Gonzalez, N., Gévaudant, F., Hernould, M., Chevalier, C., and Mouras, A (2007). The cell cycle-associated protein kinase WEE1 regulates cell size in relation to endoreduplication in developing tomato fruit. *Plant J.* 51: 642–655. <https://doi.org/10.1111/j.1365-313X.2007.03167.x>.

Google Scholar: [Author Only Title Only Author and Title](#)

Guo, J., Wang, P., Cheng, Q., Sun, L., Wang, H., Wang, Y., Kao, L., Li, Y., Qiu, T., Yang, W., et al. (2017). Proteomic analysis reveals strong mitochondrial involvement in cytoplasmic male sterility of pepper (*Capsicum annum* L.). *J. Proteom.* 168: 15–27. <https://doi.org/10.1016/j.jprot.2017.08.013>.

Google Scholar: [Author Only Title Only Author and Title](#)

Guo, M., and Simmons, C.R. (2011). Cell number counts—the *fw2.2* and *CNR* genes and implications for controlling plant fruit and organ size. *Plant Sci.* 181: 1–7. <https://doi.org/10.1016/j.plantsci.2011.03.010>.

Google Scholar: [Author Only Title Only Author and Title](#)

Hayano-Kanashiro C., Gámez-Meza N., and Medina-Juárez L.A (2016). Wild pepper *Capsicum annum* L. var. *glabrusculum*: Taxonomy, plant morphology, distribution, genetic diversity, genome sequencing, and phytochemical compounds. *Crop Sci.* 56: 1–11.

<https://doi.org/10.2135/cropsci2014.11.0789>.

Google Scholar: [Author Only](#) [Title Only](#) [Author and Title](#)

Hernández-Verdugo, S., Luna-Reyes, R., and Oyama, K. (2001). Genetic structure and differentiation of wild and domesticated populations of *Capsicum annuum* (Solanaceae) from Mexico. *Plant System. Evol.* 226: 129–142. doi: 10.1007/s006060170061.

Google Scholar: [Author Only](#) [Title Only](#) [Author and Title](#)

Hufford, M.B., Xu, X., Van Heerwaarden, J., Puhjäärvi, T., Chia, J.M., Cartwright, R.A., Elshire, R.J., Glaubitz, J.C., Guill, K.E., Kaepler, S.M., et al. (2012). Comparative population genomics of maize domestication and improvement. *Nature Genet.* 44: 808–811.

<https://doi.org/10.1038/ng.2309>.

Google Scholar: [Author Only](#) [Title Only](#) [Author and Title](#)

Huang CL, Hung, C.Y., Chiang, Y.C., Hwang, C.C., Hsu, T.W., Huang, C.C., Hung, K.H., Tsai, K.C., Wang, K.H., Osada, N., et al. (2012). Footprints of natural and artificial selection for photoperiod pathway genes in *Oryza*. *Plant J.* 70: 769–782. <https://doi.org/10.1111/j.1365-313X.2012.04915.x>.

Google Scholar: [Author Only](#) [Title Only](#) [Author and Title](#)

Hulse-Kemp, A.M., Maheshwari, S., Stoffel, K., Hill, T.A., Jaffe, D., Williams, S.R., Weisenfeld, N., Ramakrishnan, S., Kumar, V., Shah, P., et al. (2018). Reference quality assembly of the 3.5-Gb genome of *Capsicum annuum* from a single linked-read library. *Horticult. Res.* 5: 1–13. <https://doi.org/10.1038/s41438-017-0011-0>.

Google Scholar: [Author Only](#) [Title Only](#) [Author and Title](#)

Jarret, R.L., Barboza, G.E., da Costa Batista, F.R., Berke, T., Chou, Y.Y., Hulse-Kemp, A., Ochoa-Alejo, N., Tripodi, P., Veres, A., Garcia, C.C., et al. (2019). *Capsicum* -an abbreviated compendium. *J. Am. Soc. Hortic. Sci.* 144: 3–22. <https://doi.org/10.21273/JASHS04446-18>.

Google Scholar: [Author Only](#) [Title Only](#) [Author and Title](#)

Kim, S., Park, M., Yeom, S.I., Kim, Y.M., Lee, J.M., Lee, H.A., Seo, E., Choi, J., Cheong, K., Kim, K.T., et al. (2014). Genome sequence of the hot pepper provides insights into the evolution of pungency in *Capsicum* species. *Nature Genet.* 46: 270–278.

<https://doi.org/10.1038/ng.2877>.

Google Scholar: [Author Only](#) [Title Only](#) [Author and Title](#)

Kitajima, T.S., Kawashima, S.A., and Watanabe, Y. (2004). The conserved kinetochore protein shugoshin protects centromeric cohesion during meiosis. *Nature* 427: 510-517. <https://doi.org/10.1038/nature02312>.

Google Scholar: [Author Only](#) [Title Only](#) [Author and Title](#)

Kobayashi, K., Suzuki, T., Iwata, E., Nakamichi, N., Suzuki, T., Chen, P., Ohtani, M., Ishida, T., Hosoya, H., Müller, S., et al. (2015). Transcriptional repression by MYB3R proteins regulates plant organ growth. *EMBO J.* 34: 1992–2007.

<https://doi.org/10.15252/embj.201490899>.

Google Scholar: [Author Only](#) [Title Only](#) [Author and Title](#)

Kraft, K.H., Brown, C.H., Nabhan, G.P., Luedeling, E., Ruiz, Jd.J.L., d'Eeckenbrugge, G.C., Hijmans, R.J., and Gepts, P. (2014). Multiple lines of evidence for the origin of domesticated chili pepper, *Capsicum annuum*, in Mexico. *Proc. Natl. Acad. Sci. USA* 111: 6165–6170. <https://doi.org/10.1073/pnas.1308933111>.

Google Scholar: [Author Only](#) [Title Only](#) [Author and Title](#)

Launholt, D., Merkle, T., Houben, A., Schulz, A., and Grasser, K.D. (2006). Arabidopsis chromatin-associated HGMA and HGMB use different nuclear targeting signals and display highly dynamic localization within the nucleus. *Plant Cell* 18: 2904–2918.

<https://doi.org/10.1105/tpc.106.047274>.

Google Scholar: [Author Only](#) [Title Only](#) [Author and Title](#)

Lee, T.A., Wetering, S.W.V., and Brusslan, J.A. (2013). Stromal protein degradation is incomplete in *Arabidopsis thaliana* autophagy mutants undergoing natural senescence. *BMC Res. Notes* 6: 17. <https://doi.org/10.1186/1756-0500-6-17>.

Google Scholar: [Author Only](#) [Title Only](#) [Author and Title](#)

Li, Yh., Zhao, Sc., Ma, Jx., Li, D., Yan, L., Li, J., Qi, Xt., Guo, Xs., Zhang, L., He, Wm., et al. (2013). Molecular footprints of domestication and improvement in soybean revealed by whole genome re-sequencing. *BMC Genomics* 14: 579. <https://doi.org/10.1186/1471-2164-14-579>.

Google Scholar: [Author Only](#) [Title Only](#) [Author and Title](#)

Liu, T., Tang, S., Zhu, S., Tang, Q., and Zheng, X. (2014). Transcriptome comparison reveals the patterns of selection in domesticated and wild ramie (*Boehmeria nivea* L. Gaud). *Plant Mol. Biol.* 86: 85–92. <https://doi.org/10.1007/s11103-014-0214-9>.

Google Scholar: [Author Only](#) [Title Only](#) [Author and Title](#)

Liu W, Chen L, Zhang S, Hu F, Wang Z, Lyu J, Wang B, Xiang H, Zhao R, Tian Z, et al. (2019) Decrease of gene expression diversity during domestication of animals and plants. *BMC Evol. Biol.* 19, 19. <https://doi.org/10.1186/s12862-018-1340-9>.

Google Scholar: [Author Only](#) [Title Only](#) [Author and Title](#)

Lippman, Z., and Tanksley, S.D. (2001). Dissecting the genetic pathway to extreme fruit size in tomato using a cross between the small-fruited wild species *Lycopersicon pimpinellifolium* and *L. esculentum* var. Giant Heirloom. *Genetics* 158: 413–422.

Google Scholar: [Author Only](#) [Title Only](#) [Author and Title](#)

McClung de Tapia, E. (1992). The origins of agriculture in mesoamerica and central america. The origins of agriculture: An international perspective. In Watson, P.J., and Cowan, C.W. (Eds.). Washington, D.C., Smithsonian Institution Press. Pp. 143–171.



Google Scholar: [Author Only](#) [Title Only](#) [Author and Title](#)

McGuinness, B.E., Hirota, T., Kudo, N.R., Peters, J-M., and Nasmyth, K. (2005). Shugoshin prevents dissociation of cohesin from centromeres during mitosis in vertebrate cells. *PLoS Biol.* 3: e86. <https://doi.org/10.1371/journal.pbio.0030086>.

Google Scholar: [Author Only](#) [Title Only](#) [Author and Title](#)

Martínez-López, L.A., Ochoa-Alejo, N., and Martínez, O. (2014). Dynamics of the chili pepper transcriptome during fruit development. *BMC Genomics* 15: 143. <https://doi.org/10.1186/1471-2164-15-143>.

Google Scholar: [Author Only](#) [Title Only](#) [Author and Title](#)

Mizushima, N., and Komatsu, M. (2011). Autophagy: renovation of cells and tissues. *Cell* 147: 728–741. <https://doi.org/10.1016/j.cell.2011.10.026>.

Google Scholar: [Author Only](#) [Title Only](#) [Author and Title](#)

Monson, M.S., Cardona, C J., Coulombe, R.A., and Reed, K.M. (2016). Hepatic transcriptome responses of domesticated and wild Turkey embryos to aflatoxin B<sub>1</sub>. *Toxins (Basel)* 8: 1–22. <https://doi.org/10.3390/toxins8010016>.

Google Scholar: [Author Only](#) [Title Only](#) [Author and Title](#)

Müller, N.A., Wijnen, C.L., Srinivasan, A., Ryngajillo, M., Ofner, I., Lin, T., Ranjan, A., West, D., Maloof, J.N., Sinha, N.R., et al. (2016). Domestication selected for deceleration of the circadian clock in cultivated tomato. *Nature Genet.* 48: 89–93. <https://doi.org/10.1038/ng.3447>.

Google Scholar: [Author Only](#) [Title Only](#) [Author and Title](#)

Nashima, K., Shimizu, T., Nishitani, C., Yamamoto, T., Takahashi, H., Nakazono, M., Itai, A., Isuzugawa, K., Hanada, T., Takashina, T., et al. (2013). Microarray analysis of gene expression patterns during fruit development in European pear (*Pyrus communis*). *Sci. Hortic.* 164: 466–473. <https://doi.org/10.1016/j.scienta.2013.09.054>.

Google Scholar: [Author Only](#) [Title Only](#) [Author and Title](#)

Ogawa, D., Ishikawa, K., Nunomura, O., and Mii, M. (2010). Correlation between fruit characters and degree of polysomaty in fruit tissues of *Capsicum*. *J. Jap. Soc. Hortic. Sci.* 79: 168–173. <https://doi.org/10.2503/jjshs1.79.168>.

Google Scholar: [Author Only](#) [Title Only](#) [Author and Title](#)

Ogawa, D., Ishikawa, K., and Mii, M. (2012). Difference in the polysomaty degree during fruit development among plants with different ploidy levels produced by artificial chromosome doubling of a pepper (*Capsicum annuum*) cultivar 'Shishitou No. 562'. *Sci. Hortic.* 134: 121–126. <https://doi.org/10.1016/j.scienta.2011.11.015>.

Google Scholar: [Author Only](#) [Title Only](#) [Author and Title](#)

Paran, I., and Van Der Knaap, E. (2007). Genetic and molecular regulation of fruit and plant domestication traits in tomato and pepper. *J. Exp. Bot.* 58: 3841–3852. <https://doi.org/10.1093/jxb/erm257>.

Google Scholar: [Author Only](#) [Title Only](#) [Author and Title](#)

Perry, L., Dickau, R., Zarrillo, S., Holst, I., Pearsall, D.M., Piperno, D.R., Berman, M.J., Cooke, R.G., Rademaker, K., Ranere, A.J., et al. (2007). Starch fossils and the domestication and dispersal of chili peppers (*Capsicum* spp. L.) in the Americas. *Science* 315: 986–988. <https://doi.org/10.1126/science.1136914>.

Google Scholar: [Author Only](#) [Title Only](#) [Author and Title](#)

Petrovská, B., Jeřábková, H., Kohoutová, L., Cenklová, V., Pochylová, Ž., Gelová, Z., Kočárová, G., Váchova, L., Kurejová, M., Tomašíková, E., et al. (2013). Overexpressed TPX2 causes ectopic formation of microtubular arrays in the nuclei of acentrosomal plant cells. *J. Exp. Bot.* 64: 4575–4587. <https://doi.org/10.1093/jxb/ert271>.

Google Scholar: [Author Only](#) [Title Only](#) [Author and Title](#)

Pickersgill, B. (1971). Relationships between weedy and cultivated forms in some species of chili peppers (genus *Capsicum*). *Evolution* 25: 683–691.

Google Scholar: [Author Only](#) [Title Only](#) [Author and Title](#)

Pickersgill, B. (2007). Domestication of plants in the Americas: insights from Mendelian and molecular genetics. *Ann. Bot.* 100: 925–940. <https://doi.org/10.1093/aob/mcm193>.

Google Scholar: [Author Only](#) [Title Only](#) [Author and Title](#)

Pickersgill, B. (2016). Chile peppers (*Capsicum* spp.). In *Ethnobotany of Mexico: interactions of people and plants in Mesoamerica*. Lira, R., Casas, A., Blancas, J. (Eds.). New York: Springer. Pp. 417–437.

Google Scholar: [Author Only](#) [Title Only](#) [Author and Title](#)

Pignocchi, C., Minns, G.E., Nesi, N., Koumproglou, R., Kitsios, G., Benning, C., Lloyd, C., Doonan, J.H., and Hills, M. J. (2009). ENDOSPERM DEFECTIVE1 is a novel microtubule-associated protein essential for seed development in *Arabidopsis*. *Plant Cell* 21: 90–105. <https://doi.org/10.1105/tpc.108.061812>.

Google Scholar: [Author Only](#) [Title Only](#) [Author and Title](#)

Pollinger, J.P., Bustamante, C.D., Fledel-Alon, A., Schmutz, S., Gray, M.M., and Wayne, R.K. (2005) Selective sweep mapping of genes with large phenotypic effects. *Genome Res.* 15: 1809–1819. <https://doi.org/10.1101/gr.4374505>.

Google Scholar: [Author Only](#) [Title Only](#) [Author and Title](#)

Qin, C., Yu, C., Shen, Y., Fang, X., Chen, L., Min, J., Cheng, J., Zhao, S., Xu, M., Luo, Y., et al. (2014). Whole-genome sequencing of

**cultivated and wild peppers provides insights into Capsicum domestication and specialization. Proc. Natl. Acad. Sci. USA 111: 5135–5140. <https://doi.org/10.1073/pnas.1400975111>.**

Google Scholar: [Author Only Title Only Author and Title](#)

**R Core Team (2013) R: A language and environment for statistical computing. R Foundation for Statistical Computing, Vienna, Austria. URL <http://www.r-project.org>.**

Google Scholar: [Author Only Title Only Author and Title](#)

**Razifard, H., Ramos, A., Della Valle, A.L., Bodary, C., Goetz, E., Manser, E.J., Li, X., Zhang, L., Visa, S., Tieman, D., van der Knaap, E. and Caicedo A.L. (2020). Genomic evidence for complex domestication history of the cultivated tomato in latin america. Mol. Biol. Evol. 37: 1118–1132. <https://doi.org/10.1093/molbev/msz297>.**

Google Scholar: [Author Only Title Only Author and Title](#)

**Rong, J., Lammers, Y., Strasburg, J.L., Schidlo, N.S., Ariyurek, Y., De Jong, T.J., Klinkhamer, P.G., Smulders, M.J., and Vrieling, K. (2014). New insights into domestication of carrot from root transcriptome analyses. BMC Genomics 15: 895. <https://doi.org/10.1186/1471-2164-15-895>.**

Google Scholar: [Author Only Title Only Author and Title](#)

**Ross-Ibarra, J., Morrell, P.L., and Gaut, B.S. (2007). Plant domestication, a unique opportunity to identify the genetic basis of adaptation. Proc. Natl. Acad. Sci. USA 104: 8641–8648. <https://doi.org/10.1073/pnas.0700643104>.**

Google Scholar: [Author Only Title Only Author and Title](#)

**Rothhammer, S., Seichter, D., Förster, M., and Medugorac, I. (2013). A genome-wide scan for signatures of differential artificial selection in ten cattle breeds. BMC Genomics 14: 908. <https://doi.org/10.1186/1471-2164-14-908>.**

Google Scholar: [Author Only Title Only Author and Title](#)

**Santaguida, S., and Musacchio, A. (2009). The life and miracles of kinetochores. EMBO J. 28: 2511–2531. <https://doi.org/10.1038/emboj.2009.173>.**

Google Scholar: [Author Only Title Only Author and Title](#)

**Sauvage, C., Rau, A., Aichholz, C., Chadoeuf, J., Sarah, G., Ruiz, M., Santoni, S., Causse, M., David, J., and Glémin, S. (2017). Domestication rewired gene expression and nucleotide diversity patterns in tomato. Plant J. 91: 631–645. <https://doi.org/10.1111/tj.13592>.**

Google Scholar: [Author Only Title Only Author and Title](#)

**Singh, J., Zhao, J., and Vallejos, C.E. (2018). Differential transcriptome patterns associated with early seedling development in a wild and a domesticated common bean (*Phaseolus vulgaris* L.) accession. Plant Sci. 274: 153–162. <https://doi.org/10.1016/j.plantsci.2018.05.024>.**

Google Scholar: [Author Only Title Only Author and Title](#)

**Spies, D., and Ciaudo, C. (2015). Dynamics in transcriptomics: advancements in RNA-seq time course and downstream analysis. Comput. Struct. Biotechnol. J. 13: 469–477. <https://doi.org/10.1016/j.csbj.2015.08.004>.**

Google Scholar: [Author Only Title Only Author and Title](#)

**Sun, B., Zhu, Z., Chen, C., Chen, G., Cao, B., Chen, Ch., and Lei, J. (2018). Jasmonate-inducible R2R3-MYB transcription factor regulates capsaicinoid biosynthesis and stamen development in Capsicum. J. Agric. Food Chem. 67: 10891-10903. <https://doi.org/10.1021/acs.jafc.9b04978>.**

Google Scholar: [Author Only Title Only Author and Title](#)

**Steiner, A., Rybak, K., Altmann, M., McFarlane, H.E., Klaeger, S., Nguyen, N., Facher, E., Ivakov, A., Wanner, G., Kuster, B. and others (2016). Cell cycle-regulated PLEIADÉ/At MAP 65-3 links membrane and microtubule dynamics during plant cytokinesis. Plant J. 88: 531–541. <https://doi.org/10.1111/tj.13275>.**

Google Scholar: [Author Only Title Only Author and Title](#)

**Studer, A., Zhao, Q., Ross-Ibarra, J., and Doebley, J. (2011). Identification of a functional transposon insertion in the maize domestication gene *tb1*. Nature Genet. 43: 1160. <https://doi.org/10.1038/ng.942>.**

Google Scholar: [Author Only Title Only Author and Title](#)

**Swain, P. S., Elowitz, M. B., and Siggia, E. D. (2002). Intrinsic and extrinsic contributions to stochasticity in gene expression. Proc. Natl. Acad. Sci. USA 99: 12795–12800. <https://doi.org/10.1073/pnas.162041399>.**

Google Scholar: [Author Only Title Only Author and Title](#)

**Tanaka, Y., Nakashima, F., Kirii, E., Goto, T., Yoshida, Y., and Yasuba, Ki. (2017). Difference in capsaicinoid biosynthesis gene expression in the pericarp reveals elevation of capsaicinoid contents in chili peppers (*Capsicum chinense*). Plant Cell Rep. 36: 267–279. <https://doi.org/10.1007/s00299-016-2078-8>.**

Google Scholar: [Author Only Title Only Author and Title](#)

**Taitano, N., Bernau, V., Jardón-Barbolla, L., Leckie, B., Mazourek, M., Mercer K., McHale L., Michel A., Baumler D., Kantar and E. van der Knaap (2019). Genome-wide genotyping of a novel Mexican chile pepper collection illuminates the history of landrace differentiation after *Capsicum annum* L. domestication. Evol. Applications, 12: 78–92. <https://doi.org/10.1111/eva.12651>.**

Google Scholar: [Author Only Title Only Author and Title](#)

**Tian, F., Stevens, N.M., and Buckler, E.S. (2009). Tracking footprints of maize domestication and evidence for a massive selective**

sweep on chromosome 10. *Proc. Natl. Acad. Sci. USA* 106: 9979–9986. <https://doi.org/10.1073/pnas.0901122106>.

Google Scholar: [Author Only](#) [Title Only](#) [Author and Title](#)

Wightman, R., Chomicki, G., Kumar, M., Carr, P., and Turner, S.R. (2013). SPIRAL2 determines plant microtubule organization by modulating microtubule severing. *Curr. Biol.* 23: 1902–1907. <https://doi.org/10.1016/j.cub.2013.07.061>.

Google Scholar: [Author Only](#) [Title Only](#) [Author and Title](#)

Wu, S., Zhang, B., Keyhaninejad, N., Rodríguez, G.R., Kim, H.J., Chakrabarti, M., Illa-Berenguer, E., Taitano, N.K., Gonzalo, M.J., Díaz, A., Yupeng, P., Courtney, P., Leisner, D., Halterman, Buell, C.R., Weng, Y., Jansky, S.H., van Eck, H., Willemsen, J., Monforte, A.J., Meulia, T. and van der Knaap E. (2018) A common genetic mechanism underlies morphological diversity in fruits and other plant organs. *Nature Comm.* 9: 1–12. <https://doi.org/10.1038/s41467-018-07216-8>.

Google Scholar: [Author Only](#) [Title Only](#) [Author and Title](#)

Wu, Z., Liu W., Jin, X., Ji, H., Wang, H., Glusman, G., Robinson M, Liu L, Ruan J, and Gao S (2019) NormExpression: an R package to normalize gene expression data using evaluated methods. *Frontiers Genet.* 10: 400. <https://doi.org/10.3389/fgene.2019.00400>.

Google Scholar: [Author Only](#) [Title Only](#) [Author and Title](#)

Vanneste, S., Coppens, F., Lee, E., Donner, T.J., Xie, Z, Van Isterdael, G, Dhondt, S., De Winter, F., De Rybel, B., Vuylsteke, M., et al. (2011). Developmental regulation of CYCA2s contributes to tissue-specific proliferation in Arabidopsis. *EMBO J.* 30: 3430–3441. <https://doi.org/10.1038/emboj.2011.240>.

Google Scholar: [Author Only](#) [Title Only](#) [Author and Title](#)

Voelckel, C., Borevitz, J.O., Kramer, E.M., and Hodges, S.A. (2010). Within and between whorls: comparative transcriptional profiling of *Aquilegia* and *Arabidopsis*. *PLoS One* 5: e9735.

Google Scholar: [Author Only](#) [Title Only](#) [Author and Title](#)

Vos, J.W., Pieuchot, L., Evrard, J.L., Janski, N., Bergdoll, M., de Ronde, D., Perez, L.H., Sardon, T., Vernos, I., and Schmit, A.C. (2008). The plant TPX2 protein regulates prospindle assembly before nuclear envelope breakdown. *Plant Cell* 20: 2783–2797. <https://doi.org/10.1105/tpc.107.056796>.

Google Scholar: [Author Only](#) [Title Only](#) [Author and Title](#)

Yao, M., Wakamatsu, Y., Itoh, T.J., Shoji, T., and Hashimoto, T. (2008). Arabidopsis SPIRAL2 promotes unin-errupted microtubule growth by suppressing the pause state of microtubule dynamics. *J. Cell Sci.* 121: 2372–2381. <https://doi.org/10.1242/jcs.030221>.

Google Scholar: [Author Only](#) [Title Only](#) [Author and Title](#)

Zeder, M.A. (2015). Core questions in domestication research. *Proc. Natl. Acad. Sci. USA* 112: 3191–3198. <https://doi.org/10.1073/pnas.1501711112>.

Google Scholar: [Author Only](#) [Title Only](#) [Author and Title](#)

Zhu, Z., Sun, B., Cai, W., Zhou, X., Mao, Y., Chen, C., Wei, J., Cao, B., Chen, C., Chen, G., and others (2019). Natural variations in the MYB transcription factor MYB31 determine the evolution of extremely pungent peppers. *New Phytol.* 223: 922-938. <https://doi.org/10.1111/nph.15853>.

Google Scholar: [Author Only](#) [Title Only](#) [Author and Title](#)